Development of Proximity-Induced Bio-Barcode Assay for the Electrochemical Detection of a Cancer Protein Biomarker

Sarah Traynor (B.Sc.)

School of Biomedical Engineering

Submitted in partial fulfillment of the requirements for the degree of

Master of Applied Science

Faculty of Engineering, McMaster University

Hamilton, Ontario

Abstract

There is a tremendous need for biosensing systems that can be operated at the point-of-care for disease screening and diagnostics and health monitoring. In spite of this, systems that offer the required analytical sensitivity and specificity in clinical samples, *and* are truly simple to operate using a sample-in-answer-out approach remain elusive. To address this challenge, the development and optimization of an electrochemical bio-barcode assay (e-biobarcode assay) that integrates biorecognition with signal transduction using molecular (DNA/protein) machines and signal readout using nanostructured electrodes is presented within this thesis. The e-biobarcode assay eliminates multi-step processing and uses a single step for analysis following sample collection into the reagent tube. Using this assay, a clinically-relevant performance for the analysis of prostate specific antigen (PSA) in undiluted and unprocessed human plasma: a log-linear range of 1 ng mL^{-1} – 200 ng mL^{-1} and a LOD of 0.385 ng mL^{-1} was achieved. The simplicity of the e-biobarcode assay offers a realistic solution for biomarker analysis at the point-of-care.

Table of Contents

List of Figures

List of Schemes

List of Tables

List of Abbreviations

Ab_1	Antibody One (capture antibody)
Ab_2	Antibody Two (signalling antibody)
ALP	Alkaline Phosphatase
BPH	Benign Prostatic Hyperplasia
BSA	Bovine Serum Albumin
C_{dl}	Double-Layer Capacitance
CA	Chronoamperometry
CASPE-MFD	Commercially Available Screen-printed Electrode-Based Microfluidic Device
β-CD	β-Cycextrin
CNT	Carbon Nanotube
CV	Cyclic Voltammetry
DNA	Deoxyribonucleic Acid
DPV	Differential Pulse Voltammetry
DRE	Digital Rectal Exam
dsDNA	Double Stranded Deoxyribonucleic Acid
E_i	Initial Potential
E_f	Final Potential
E_r	Reduction Potential
EIS	Electrochemical Impedance Spectroscopy
ELISA	Enzyme Linked Immunosorbent Assay
FC	Fragment Crystallizable
Fc	Ferrocene
GCE	Glassy Carbon Electrode
GO	Graphene Oxide
GQD-AuNR	Graphene Quantum Dot Gold Nanorod
HRP	Horse Radish Peroxidase

HQ	Hydroquinone
IgG	Immunoglobulin G
IL-6	Interleukin-6
LOD	Limit-of-detection
LSV	Linear Sweep Voltammetry
MB	Methylene Blue
MCH	Mercaptohexanol
MGCE	Magnetic Glassy Carbon Electrode
MNP	Magnetic Nanoparticle
MPBA	4-Mercaptophenylboronic Acid
NP	Nanoparticle
PAMAM	Polyamidiamine
PAP	Prostatic Acid Phosphatase
paPSA	Proteolytically Active PSA
PBM	Polymethylene Blue
PCa	Prostate Cancer
PL-4	Platelet Factor-4
PLLA	Poly-L-lactide
POC	Point-of-care
Poly-A	Poly-adenine
PSA	Prostate Specific Antigen
PSMA	Prostate Specific Membrane Antigen
R_{ct}	Charge Transfer Resistance
R_s	Electrolyte Resistance
RCA	Rolling Circle Amplification
rGO	Reduced Graphene Oxide
RNA	Ribonucleic Acid
RSD	Relative Standard Deviation

SAM	Self-assembled Monolayer
SCE	Standard Calomel Electrode
SELEX	Systematic Evolution of Ligands by EXponential Enrichment
SBR	Signal-to-blank Ratio
ssDNA	Single Stranded Deoxyribonucleic Acid
SWV	Square-wave Voltammetry
TCEP	Tris(2-carboxyethyl)phosphine
TWJ	Three-way Junction
VEGF	Vascular Endothelial Growth Factor
Z_w	Warburg Impedance

Acknowledgments

First and foremost, I would graciously like to thank my supervisor Dr. Leyla Soleymani for her guidance, support and encouragement for the past two years. Without her motivation, insight and knowledge, everything I have achieved in my Master's studies would not be possible.

I would also like to thank Dr. Feng Li not only for all his help and support throughout the duration of this project, but for the past four years.

Thank you to Alex Guan for helping me with many trouble-shooting experiments and encouraging me throughout the past two years.

I owe a great deal to the past and present members of the Soleymani group who have supported me everyday. The times we have spent together, inside and outside of the lab, will be some of my most cherished memories from the past two years. Thank you for all the fun we had together, I could not have asked for better people to work with. Additionally, thank you to Richa Pandey who not only contributed so much to my research and answered all my *many* questions, but also always provided me with a good laugh.

Lastly, I want to thank all my family and friends who have always provided constant support and encouragement. To my husband Matt Guest, you inspire me every day and have been my biggest supporter from the start. Thank you for always believing in me and pushing me to be the best I can.

Chapter 1: Introduction

1.1 Background

1.1.1 Background on Point-of-care Biosensors

A sought-after form of clinical technology is one that enables diagnosis and monitoring of disease at the patient point of care (POC), performed in a non-invasive manner with a rapid turnaround time.[1] The discovery of disease biomarkers has opened the door to the development of such technology through the emergence of biosensing platforms. Biosensors use biomolecular recognition to generate a detectable signal through binding of a specific molecular target, resulting in quantification.[2] The most notable advantages of biosensing over traditional diagnostic methods such as polymerase chain reaction or cell culture, s the ability to rapidly analyze a small volume sample, the low cost of fabrication and compatibility with miniaturization, rendering it an acceptable technology for integration into portable handheld POC devices.[3]

The need for early detection and continual monitoring has been the driving force for the development of biosensing technology and increasing the demand for POC biosensors.[4] Early disease diagnosis is essential for increasing likelihood of survival, creating an effective treatment plan and can be facilitated with devices capable of rapid sample analysis in a sample-in-answer-out format. In addition, such devices would enable decentralized continual monitoring both pre- and post-treatment, minimizing hospital visits by potentially at-risk patients.[5] The ease of use and portability of POC biosensors combined with the decreased priced of manufacturing compared to conventional laboratory equipment offers a viable solution to reaching communities with limited resources and insufficient healthcare infrastructure.[6]

Putting a low-cost, simple to use, miniaturized diagnostic tool with rapid turnaround time into the hands of physicians, volunteers and patients around the world has the potential to not only save many lives, but also increase patient comfort during stressful periods.[3]

1.1.2 Challenges

While the need for POC diagnostic tools is well understood, the benefits are well defined, and there have been many reports claiming ultra-sensitive biosensing achievements, commercially available devices remain elusive.[4] Currently, the POC device market with regards to disease management is dominated primarily by the glucose meter.[7] The reasoning for the discrepancy between the high number of reported biosensors and the number of commercially available devices is attributed to the lack of truly simple tests.[8] A simple test is defined by features such as ability to directly use unprocessed specimens, requiring only basic reagent manipulation (i.e. mix reagent A with reagent B), needs no operator intervention for analysis, does not require specialized or technical training, yields a result that is easy to read and does not require further calculations, and performs comparably to already existing methods.[8] Of these requirements, designing a biosensor that 1. achieves sensitivity akin to classic methods 2. can perform unhindered by the matrix effect and 3. does so rapidly with a simple assay design , seem to be the most difficult to achieve simultaneously.[9]

Achieving sensitivity with biosensing platforms that is comparable to or more superior than standard diagnosis methods has been extensively reported in literature, however it is critical that sensitivity is evaluated in clinically-relevant samples.[10] The most significant bottleneck of biosensing devices is sample preparation prior to analysis. This step ultimately negates benefits of

using a rapid detection system, thus a successful POC device must be able to perform in unprocessed biological samples.[4] Detection of small biological molecules can become challenging in clinically relevant samples due to the complexity of the solution. Blood, urine, plasma and serum are all commonly sampled for disease diagnosis and can negatively impact detection sensitivity.[11] These fluids are comprised of many cells, molecules and proteins that may non-specifically adsorb onto the transducing surface, inhibiting signal transduction or target capture. Additionally, urine has an acidic pH that can denature sensitive assay reagents such as nucleic acid or proteins, effecting the biosensors readings.[10] Preventing non-specific adsorption using surface blocking methods is essential for practical use in a complex matrix and circumventing the limitation that sample processing imposes.[4]

The challenge of achieving these limits in clinically relevant samples is further increased when the number of wash and reaction steps are restricted. Reagent addition and separation steps introduce a source of error, variation and increases total readout time, reducing the practicality of the detection scheme.[12] Minimizing these steps by developing no-wash biosensors not only makes the detection scheme more accessible to untrained users but also facilitates integration into POC testing.[13]

Reagent stability also presents a problem in commercializing a biosensing device for clinical decision making. The biomolecules such as proteins or nucleic acid that are used for detection typically require refrigerated storage due to thermally instability.[14] Realizing a device suitable for use in remote areas must comply with long-term stability at room temperature or potentially elevated temperatures, eliminating the need for cold chain transportation.[15]

Overcoming the limitations presented must be done using cost-effective solutions as the market for POC devices heavily relies on the affordability of the equipment.[16] Much research has been focused on increasing sensitivity, forgoing the cost criteria. Reagent, signal transduction and housing costs must be minimized in order to develop POC biosensors that can be used by a variety of users with different economic status.[17] Demonstrating a detection scheme that utilizes cost-effective reagents and transduction method while achieving high sensitivity in a simplistic manner is expected to aid in realizing a practical design for integrating into handheld devices and help meet the demand for POC biosensors.[4]

1.1.3 Motivation

The motivation of this thesis is to overcome some of the shortcomings that have prohibited biosensors from being translated from the research lab to the market. These shortcomings, for the most part, center around integration of a sensitive and specific assay into a handheld device for analyzing clinical samples. Circumventing multi-step sample processing, sequential reagent addition, or non-specific interactions will aid in realizing a realistic tool for clinical analysis at the POC.

Our goal was to develop a one-step protein detection assay and integrate it with an electrochemical readout method for sensitive detection. We focused on addressing

1. Eliminating multiple reaction and wash steps typical of immunoassays
2. Compatibility with miniaturized devices
3. Enhancing sensitivity without amplification or separation elements
4. Preventing non-specific adsorption in unprocessed clinical samples

Protein concentrations are widely affected in diseases and are secreted throughout the body making them excellent biomarker candidates and a focus of biosensing.[18,19] The development of no-wash assays focuses on reducing reaction and wash steps in order to make protein biosensing assays more compatible with POC devices. They are centralized around simple mixing of sample solution with signal generating probes in solution, taking advantage of 3-dimensional diffusion of the target molecule and signaling probes.[13]

Bio-barcode assays, which translate the capture of a protein target into the release of a DNA barcode, have been one of the leading assays in the development of simple no-wash assays.[20] These assays not only enable solution-based target capture but the translation from protein to DNA facilitates well-defined nucleic acid amplification methods such as PCR for increasing sensitivity.[21] The major drawback of bio-barcode assays is the need for enzymes and/or nanoparticles (NPs) for amplification and magnetic beads for separation, contradicting the purposed benefits of one-step detection. The demonstrated success of bio-barcode assays has inspired us to develop an assay based on this design, however, we aimed to further improve it by eliminating the need for amplification or separation elements. Eliminating amplification elements such as enzymes from the detection scheme can enhance stability and reproducibility, aligning it to closer meet POC device criteria.[22]

The signal transduction method is the main defining feature of a biosensor and must be carefully selected to obtain the desired sensitivity.[23] Many techniques such as fluorescence[24], luminescence[25], electrochemistry[26] and surface enhance Raman scattering[27] have been used to successfully transduce binding interactions into quantifiable signals, typically performed by measuring a change occurring at a surface. Of these techniques, electrochemistry has proven to be one of the most advantageous signal transduction methods for the development of POC biosensors,

as exemplified by the wide success of the handheld glucose sensor.[28] Electrochemical biosensors are rapid, sensitive, inexpensive, robust, easy to use and compatible with miniaturization, satisfying most criteria for commercially available POC products.[22] For these reasons we chose to integrate our bio-barcode assay for sensitive protein detection with electrochemical readout. This integration is made simple using the bio-barcode assay since the protein capture can occur in solution and the resulting DNA barcode can be captured on an electrode surface. Electrochemical DNA biosensors rely on hybridization of a single stranded target with an immobilized capture probe and is made extremely simple with well-defined immobilization techniques and easy probe sequence modification.[29] Modifying the released bio-barcode with a redox active molecule allows for us to detect the presence of the surrogate target on an electrode by probing with electrochemical techniques. The simple design of this electrochemical bio-barcode assay will allow for sample-in-answer-out protein biomarker analysis, coinciding with POC device requirements.

While eliminating amplification elements and decreasing number of washing steps enhances stability and turnaround time it can also decrease sensitivity.[30] To circumvent this, alternative methods of increasing the assay's sensitivity will be used. Surface modification resulting in 3-dimensional (3D) transducing surfaces has been shown to be extremely effective at increasing detection sensitivity of bioassays by allowing for the deposition of an increased number of capture probes with optimal spacing.[31] Nanostructured surfaces can be fabricated using simple, reliable and fast electrodeposition techniques making it a much more viable option for increasing sensitivity than amplification elements.[32] The important role of nano-structuring in biosensing will be demonstrated using gold electrodes engineered with 3D surface structures to enhance sensitivity of the one-step, amplification-free electrochemical bio-barcode assay.

As previously discussed, one of the major issues with developing POC biosensors is the inability to perform in complex matrices, usually due to non-specific adsorption. As a result, there have been many antifouling reagents developed using molecules such as poly(ethylene glycol) (PEG) to minimize adsorption of interfering molecules onto the surface of biosensors.[33] Due to the auto-oxidization of PEG several other molecules have been used for preventing non-specific adsorption including biological reagents such as milk proteins and serum albumins with bovine serum albumin (BSA) being the most common.[34] They work by adhering to the sensing surface in a controlled manner, decreasing the area for other larger interfering elements to adsorb. For our biosensor, we wanted to introduce a relatively inexpensive and simple method of preventing non-specific adsorption that would not increase steric hindrance at the electrode surface or inhibit electron transfer. We chose to exploit the affinity between the DNA base adenine and gold[35] by using a poly-adenine (poly-A) sequence for surface blocking. The small size of the molecule will not interfere with target capture and DNA does not significantly impact electron transfer.[36]

Ultimately, the goal of this work is to demonstrate simple, sensitive and rapid protein detection in a clinically relevant sample using an assay that is designed to be compatible with POC integration. This will be accomplished by combining all discussed features (bio-barcode assay, electrochemical readout, nanostructured electrode surface and poly-A) to construct a sample-in-answer-out biosensing platform that addresses limitations of current assay designs. The performance of the developed assay will be evaluated using one of the most validated cancer protein biomarkers, prostate specific antigen (PSA).

1.2 Objectives

The primary objective of this research is to design a sample-in-answer-out assay capable of detecting a relevant protein biomarker at a clinically relevant level, in a complex matrix. All objectives have been specifically chosen to coincide with viable translation of the detection assay into a handheld device.

Specific objectives of this research are summarized below:

1. Design a one-pot assay for protein capture and signal transduction
2. Develop material engineering solutions for improving sensitivity
3. Develop strategies for reducing non-specific adsorption
4. Demonstrate practical clinical use focusing on sensitivity and selectivity

1.3 Thesis Outline

The remainder of this thesis is arranged as follows:

Chapter 2 provides a literature review of electrochemical biosensors used for the detection of prostate specific antigen over the passed five years.

Chapter 3 focuses on the development and optimization of critical aspects within the purposed electrochemical bio-barcode biosensors design. Probe density, target hybridization time, assay intermediate preparation and concentrations, reaction time, surface blocking and dilution factor of the biological sample were all investigated using a model streptavidin/biotin system. The

importance of each parameter is thoroughly discussed and the optimal condition for each is reached within this chapter.

Chapter 4 focuses on validating the optimized assay conditions using a model cancer protein target, prostate specific antigen. A limit-of-detection is found for a baseline system using prostate specific antigen and planar gold electrodes and further material engineering is performed using nanostructuring to increase the sensitivity. The practicality of the sensor is then demonstrated by successfully detecting prostate specific antigen in unprocessed human plasma.

Chapter 5 focuses on the conclusions of this work providing a summary of the key findings, contributions to the field and potential future work.

Chapter 2: Literature Review on Electrochemical PSA Detection

2.1 Preface

The focus of this chapter will be introducing biomarkers and how they can be used to identify lethal disease, specifically focusing on the relationship between prostate specific antigen (PSA) and prostate cancer (PCa). The importance of handheld devices for clinical application, and how biosensing in combination with electrochemical methods is aiding in the production of such devices will be discussed. An overview will be given on PSA biosensors, followed by in-depth review highlighting electrochemical PSA biosensors that have shown outstanding performance in clinically relevant samples over the past five years. These sensors will be divided into the mechanism of the assay scheme and compared across relevant metrics of clinical biosensors.

Multiple authors have contributed to this chapter, as it has been published as a literature review under the title "Recent advances in electrochemical detection of prostate specific antigen (PSA) in clinically-relevant samples" in the sensors section of the Journal of The Electrochemical Society. Sarah Traynor independently wrote the introduction to electrochemical biosensors, introduction to electrochemical PSA detection, indirect detection assays and conclusion, and contributed to ideas, writing, editing and gathering of information for all other sections. Dr. Richa Pandey wrote the sandwich assays section, contributed to the detection mechanism section and made scheme 2.1, Roderick Maclachlan wrote the direct detection assays section and Dr. Amin Hosseini wrote the electrochemical readout methods for PSA detection section and made figure 2.1. Dr. Tohid Didar, Dr. Feng Li and Dr. Leyla Soleymani contributed to the design and writing of the review.

This thesis is centered around the development of an electrochemical biosensor capable of detecting a cancer protein biomarker at clinically relevant levels. For this work, PSA was employed as a model protein target due to the high level of validation, as well as the significant clinical impact that coincides with the introduction of a POC device. An intensive background on electrochemical PSA sensors that have been presented within the last five years, focusing on three broadly categorized assay designs: sandwich assays, direct detection assays and indirect detection assays is given. This review has been done to demonstrate how the performance and design of the sensor covered in this work compares and differs from what currently exists.

2.2 Introduction to Electrochemical PSA Detection

Early diagnosis and surveillance of cancer allows for improved prognosis, increased survival rates, and a better quality of life for patients. This has fueled research in the discovery of early-stage cancer biomarkers, as well as in the development of new and improved technologies for ultra-sensitive biomarker analysis.[37] Biomarkers are measurable biologically-relevant indicators, which are expressed in either increased or suppressed levels due to the presence of a disease.[38] The fluctuation of biomolecular markers such as proteins and nucleic acids from normal physiological levels found in healthy humans is used for the diagnosis, prognosis and monitoring of diseases such as cancer, and has formed the foundation for developing clinical diagnostic tests.[39]

Prostate cancer (PCa) is one of the most life-threatening diseases for men over the age of 50 with the lethality being ascribed to the lack of symptoms that are expressed in early stages.[40] Consequently, tremendous efforts have gone into the discovery of biomarkers associated with PCa, and technology for their use in clinical applications. Prostatic acid phosphatase (PAP) was one of

the first biomarkers used for the diagnosis and staging of (PCa), but due to the difficulty in accurately quantifying the localized production of the isoenzyme to the prostate, investigators spent years trying to find a more reliable diagnostic reagent.[41] In 1979 Wang and colleagues isolated and purified a 33-kD glycoprotein that was distinct from PAP, but was also highly specific to prostate cells, termed prostate specific antigen (PSA).[42] A subsequent study found that PSA could be detected in human serum, proving that in addition to being cell-type specific, it is released into circulation enabling minimally-invasive analysis.[43] Shortly after, it was concluded that the concentration of serum PSA coincided with prostatic tumor progression and could be used for diagnosis, staging and monitoring the disease after treatment.[44] PSA was also identified in healthy males; however, a level above the threshold concentration of 4 ng mL^{-1} has been recognized as an indication of PCa.[45] Although PSA is one of the most validated biomarkers for clinical decision making in regards to PCa, it is not currently used for PCa screening due to the controversies raised in the literature regarding the specificity of PSA. Increased levels of PSA is also associated with benign prostatic hyperplasia (BPH), leading to false positive PCa diagnosis and unnecessary invasive biopsies, demonstrating the lack of specificity required for a screening biomarker.[46] Despite this, PSA blood tests are commonly used in monitoring cancer progression in patients receiving treatment and for early diagnosis in combination with a digital rectal exam (DRE). Given that frequent PSA analysis is performed to monitor the efficacy of treatments in cancer patients (in the form of PSA velocity or doubling time measurement)[47], there is a need for point-of-care tests with facile sample collection, easy operation, and rapid sample to answer times, similar to the home glucose test, for disease monitoring.[48]

Tremendous research efforts have been focused on the POC detection of proteins, and particularly PSA, using biosensors.[49] Electrochemical biosensors have been central in the

development of handheld bioanalytical systems as they combine sensitivity, specificity, and multiplexing with scalable and cost-effective manufacturing.[50] Due to their promise in creating market translatable technologies, this review is focused on electrochemical biosensors for the detection of PSA. PSA detection using optical methods – fluorescence[51], colorimetric[52], surface plasmon resonance[53], and surface enhanced Raman spectroscopy[54]– have been discussed elsewhere. Several articles have been published on the electrochemical detection of PSA in the last five years with multiple reviews focusing on a particular electrode material[55,56], biorecognition element[57], or signal transduction mechanism for PSA detection. The rest of this chapter will focus on categorizing electrochemical PSA detection platforms based on their operating mechanisms, and solely include assays that have been validated with clinical samples or using complex biological matrices over the past five years. This chapter is meant to highlight the advantages and disadvantages of various biosensing mechanisms used for PSA detection, demonstrating the importance of choosing the right assay for the particular application case.

2.3 Electrochemical Readout Methods for PSA Detection

Electrochemical methods rely on charge transfer and electrochemical reactions occurring at the electrode/electrolyte interface for signal generation.[58] A typical electrochemical sensor consists of a working (sensing), counter, and reference electrode.[59] The desired electrochemical reactions take place at the surface of the working electrode while the counter electrode creates a conduction path within the electrolyte, leading to a current flow between the working and counter electrodes. Typically, working and counter electrodes are made of conductive and chemically stable materials such as gold, platinum, carbon, and silicon.[60] A reference electrode is employed to control the applied potential on the working electrode. The most frequently used reference

electrodes are saturated calomel electrode (SCE) and Ag/AgCl electrode, due to their steady and distinct reference potentials.[61,62] The most common electrochemical techniques employed in PSA sensing for point-of-care platforms include chronoamperometry (CA),[62,63] cyclic voltammetry (CV),[64,65] linear sweep voltammetry (LSV),[66] differential pulse voltammetry (DPV),[67] square-wave voltammetry (SWV),[68] and electrochemical impedance spectroscopy (EIS).[65,69] In this section, we briefly describe these methods.

In CA, a potential step is applied to the sensing electrode and the current response of the system is measured as a function of time (Figure 2.1a).[58] Typically, the initial potential (E_i) is chosen so that redox reactions are minimized, whereas, the final potential (E_f) results to fast surface reaction kinetics and the generation of a diffusion-limited current.[70] It is difficult to sense the existence of multiple target analytes using CA, which has led to the wide-spread use of voltammetric techniques in biosensing. In LSV (Figure 2.1b), the applied voltage is linearly scanned from E_i to E_f with a constant scan rate (voltage ramp), measuring the generated electrochemical current. When the working electrode potential approaches the reduction potential (E_r), the cathodic current increases. As the applied potential increases, the concentration of the electroactive species on the working electrode surface decays. Due to the generation of a concentration gradient, the flux of the species towards the electrode increases and thus the current grows. As the scanning continues and the potential passes E_r, the flux reaches its maximum point and then drops due to exhaustion of the analytes at the electrode surface, resulting in a peaked i-v curve.

If the direction of the voltage sweep is reversed (Figure 2.1c), the reduced species become re-oxidized at the electrode surface generating an anodic current.[71] CV has an extensive application in electrochemical sensing. Valuable data regarding redox potentials and reaction rates of the

electroactive species and their interactions can be collected from CV curves.[58] However compared with other voltammertric techniques, they suffer from lower analytical sensitivity due to the presence of a non-Faradaic background current.

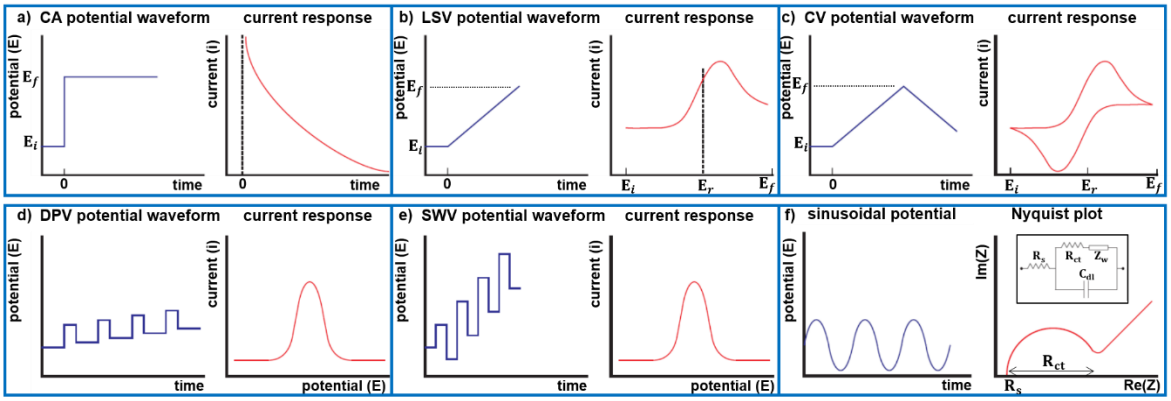

Figure 2.1. Electrochemical methods: a) CA step potential and current response as a function of time; b) LSV potential ramp and resulting i-v curve; c) CV potential sweep and resulting CV curve; d) DPV potential waveform and current response; e) SWV potential waveform and current response; f) Applied sinusoidal potential, corresponding Nyquist plot, and EIS equivalent electrical circuit (inset).

DPV and SWV are two classes of voltammetric techniques that increase analytical sensitivity by removing the background capacitive signal.[71] DPV applies a sequence of voltage pulses of fixed amplitude that are overlapped on a potential ramp (Figure 2.1d).[71] The current measurement is performed at two specific points on each pulse, the first just before application of the pulse and the second at the end of the pulse. The reason for choosing these sampling points is to allow for the non-Faradaic current component to decay. For each pulse, the first current measurement is subtracted from the second and plotted against the base potential. The obtained peak current is directly proportional to the concentration of the electroactive analytes on the surface of the working electrode. SWV is another form of pulse voltammetry in which a symmetrical square-wave potential with a defined amplitude is overlaid on a staircase potential with a fixed step height, where the leading pulse of the square wave concurs with the staircase step (Figure 2.1e). The net current is calculated by subtracting the reverse current (anodic) from the forward

current (cathodic) and the current peak is centered on the redox voltage. Similar to DPV, the obtained peak current is directly proportional to the quantity of the electroactive species. SWV possesses many advantages including high sensitivity, elimination of background currents, and rapid response time.[72]

EIS is a highly sensitive label-free technique which can be used to detect a single biomolecule on the surface of a sensing electrode.[73,74] It is based on the application of a small sinusoidal voltage (Figure 2.1f) to the working electrode and measuring the complex impedance at the electrode/electrolyte interface over an appropriate frequency range.[75] The obtained impedance spectrum is then fitted with an equivalent electrical circuit model composed of resistors and capacitors, providing an insight of the electrode/electrolyte interface. The corresponding circuit model of a three-electrode electrochemical cell is shown in Figure 2.1f-inset, where R_s is the resistance of the electrolyte; R_{ct} represents the charge transfer resistance caused by redox reaction of electroactive species with the working electrode; Z_w is known as Warburg impedance caused by the diffusion process of reactants and C_{dl} represents the double-layer capacitance at the working electrode/electrolyte interface.[76,77] The measured equivalent impedance is described using the Nyquist plot (Figure 2.1f), where the real part of the obtained impedance is plotted on the X-axis and the imaginary part is plotted on the Y-axis. At high frequencies, the plot is illustrated by a semi-circle with R_{ct} representing its diameter. At low frequencies, where ion diffusion dominates, the plot is basically a straight line with a slope of 45°.[78] Changes in the impedance spectra are caused by the specific interactions of target proteins with bioreceptors on the surface of the working electrodes.[79] EIS-based biosensors are well-known for their high sensitivity and specificity, rapid sample-to-response time, and their capability for integration with microfluidic

devices. However, the drawback of using such a sensitive technique includes the interference from non-specific adsorption onto the electrode surface.[77,80]

2.4 Detection Mechanisms

Electrochemical biosensors for PSA detection can be broadly categorized based on their approaches for translating biorecognition events into electrochemical signals. These are schematically illustrated in Scheme 2.1 and described below.

1. Sandwich assays: In these assays, the target analyte is sandwiched between two biorecognition elements, typically antibodies for capture and subsequent signal transduction. The biorecognition event is translated into an electrochemical signal by labeling one of the biorecognition elements with enzymes or nanoparticles (NPs) as described later.
2. Direct detection assays: These assays typically use an immobilized biorecognition element for analyte capture and generate a change in electrochemical signal based on a single binding event with PSA.
3. Indirect detection assays: These assays rely on the capture of PSA by biorecognition elements such as aptamers or DNA/protein complexes. Upon target capture, dynamic biorecognition systems undergo structural changes that can be programmed to release or generate an additional detectable element that results in an electrochemical signal change.

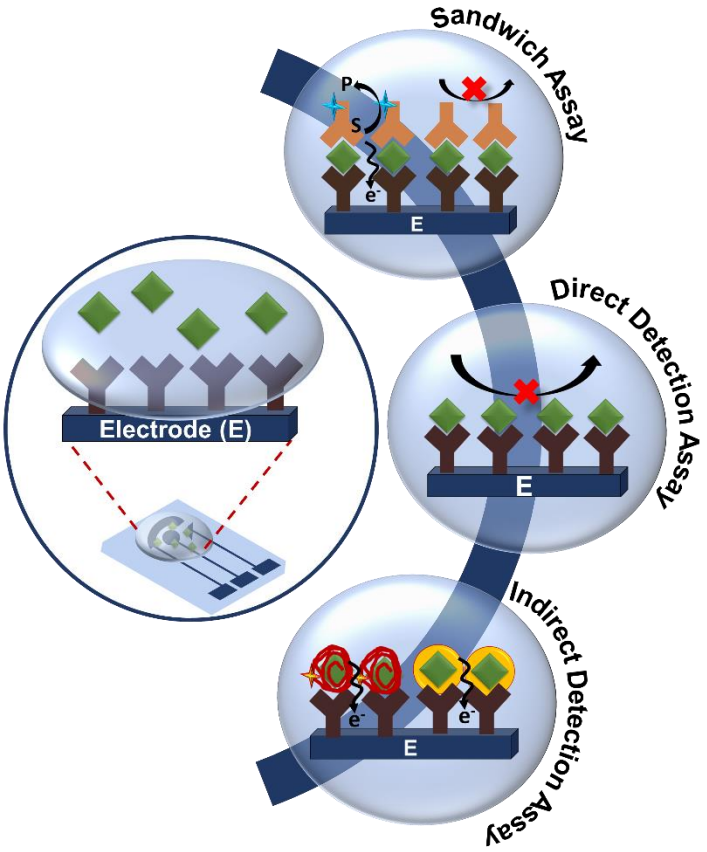

Scheme 2.1. Schematic representation of an electrochemical chip and the detection mechanisms involved in PSA detection: Sandwich Assay, Direct Detection Assay and Indirect Detection Assay.

2.4.1 Sandwich Assays

Enzyme linked immunosorbent assay (ELISA) is a commonly used sandwich assay for protein analysis and is typically programmed to transduce an optical signal change.[81] Electrochemical analogues of ELISA use biorecognition and target labeling steps similar to those used in ELISA; but employ voltammetry or amperometry to generate an electrochemical signal. This method relies on sandwiching PSA between two highly specific biorecognition elements such as antibodies. Typically, one antibody (Ab_1) is designated for the capture of the target while a second antibody (Ab_2) is used for signal generation or amplification. The first interaction usually occurs between an immobilized Ab_1 and the PSA molecule, followed by binding of Ab_2 to the

Ab_1-PSA complex. Ab_2 can be labelled with either an enzyme or a redox molecule to achieve an electrochemical signal upon successful capture of the target protein. Antibodies are used in most sandwich assays as biorecognition elements but there are alternatives such as aptamers and nanobodies, which are also discussed in this section.

In electrochemical sandwich assays, the redox properties of the enzyme tagged Ab_2 is commonly used for signal transduction. In this approach, Ab_2 is directly tagged with enzymes such as horse radish peroxidase (HRP), alkaline phosphatase (ALP), glucoamylase, β-galactosidase or glucose oxidase, which catalyze the reduction of their respective substrates in the presence or absence of a mediator.[70] HRP is a widely used enzyme in electrochemical sandwich assays that catalyzes the reduction of H_2O_2 in the presence of hydroquinone (HQ).[70] Chen et al. developed commercially available screen-printed electrode-based microfluidic devices (CASPE-MFDs) to demonstrate the detection and quantification of PSA in human serum samples.[82] In this assay, magnetic beads conjugated with Ab_1 were immobilized on the gold screen printed electrodes. Following PSA capture on the magnetic beads, HRP/Ab_2 was introduced to the electrode using microfluidics. Magnetic beads were used to increase the surface density of Ab_1 on the electrode surface and to enhance the capture of target PSA. The redox current was generated by the enzymatic and electrochemical reaction between HRP and HQ respectively using both CA and SWV. Using these devices, a linear range of 0.001-10 ng mL^{-1} and a limit-of-detection (LOD) of 0.84 pg mL^{-1} were obtained for detecting PSA in serum. HRP is the most commonly used enzyme in electrochemical sandwich assays due to its stability and fast reaction kinetics. However, it produces a background signal in the absence of the analyte due to the electrochemical activity of its H_2O_2 substrate. Additionally, HRP relies on the use of mediators for signal generation. ALP has been used to overcome the background and mediator limitations of HRP. For example, Zani

et al. demonstrated a magnetic bead-based assay that used mouse IgG-Ab_1 for PSA capture and ALP tagged anti-mouse FcC IgG for signal transduction.[83] ALP catalyzes the conversion of α-naphthyl phosphate to α-naphthol. Oxidation of α-naphthol at the electrode surfaces generates an amperometric signal (Figure 2.2a). This sensor demonstrated a linear range of 1–80 ng mL^{-1}, and a LOD of 2 ng mL^{-1} in human serum samples. While enzyme-based sandwich assays are highly specific to PSA, they have limitations due to the intrinsic instability of enzymes.[84] These assays also require multiple aggressive washing steps to alleviate non-specific binding that may lead to false negative or false positive results.

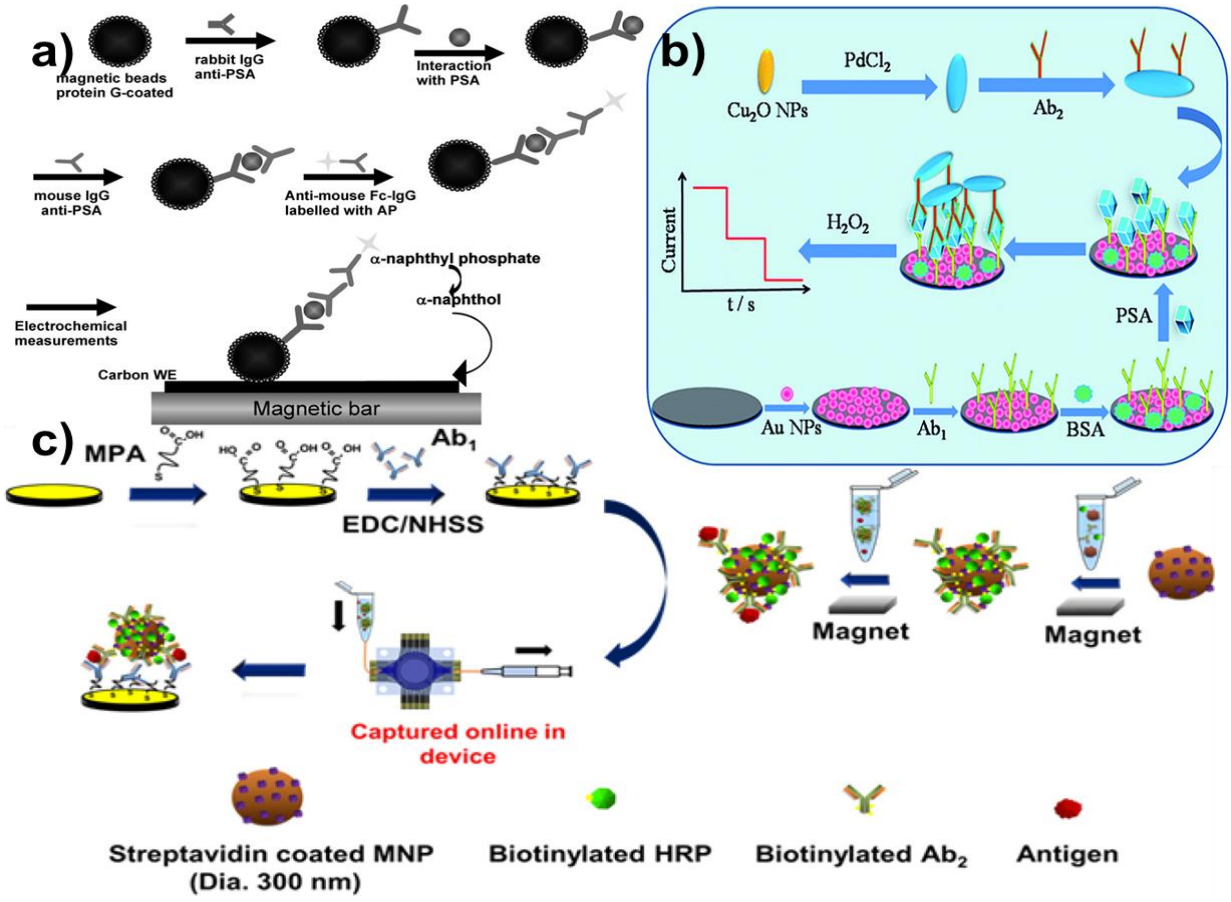

Figure 2.2. Sandwich assays: a) Magnetic bead based assay for PSA detection using ALP (Reprinted from (Zani et.al; 2010)[83] with permission from Electroanalysis); b) Pd@CuO NP based detection of PSA (Reprinted from (Chu et.al;2016)[85] with permission from Royal Chemistry Society); c) Multiplexed detection of PSA using magnetic NPs (Reprinted from (Tang et.al; 2016)[86] with permission from American Chemical Society).

To further enhance assay sensitivity and LOD, NPs can be used as labels. NPs may serve as enzyme alternatives for directly catalyzing redox reactions, or they can function as scaffolds for increasing the loading density of enzymes or antibodies. Incorporation of NPs offers ease of labeling, tunable physical and chemical properties, and large surface-to-volume ratio. The increase in available surface area enables enhanced loading of enzymes for better signal amplification and allows for increasing the quantity of Ab_1 for increasing capture efficiency.[87,88] Nanomaterials such as NPs[89,90], nanoclusters[91], nanosheets[92], or cargo releasing nanocarriers[93,94] have been used in electrochemical sandwich assays. Chu et al. chose biocompatible Pd@CuO NPs for enhanced catalysis towards the reduction of H_2O_2 (Figure 2.2b). [85] They constructed a sandwich assay based on the Ab_1-PSA-Ab_2-Pd@CuO architecture, with a linear range of 10^{-5} - 10^{2} ng mL^{-1}, and a LOD of 0.002 pg mL^{-1}. This sensor showed a recovery rate of 99.2%-101.2% in human serum for PSA, which is a measure of signal preservation associated with a known amount of PSA quantified using the sensor in a biological solution that contains material that may interfere with signal generation. Feng et al. constructed a sandwich assay with Ab_1-PSA-Ab_2- PtCu@rGO/g-C_3N_4.[95] In this study, bimetallic Pt-Cu NPs were integrated with 2D rGO-gC_3N_4 to improve electrical charge transfer and activity for the reduction of H_2O_2. This assay demonstrated a linear range of 50 fg mL^{-1}-40 ng mL^{-1}, a LOD of 16.6 fg mL^{-1}, and a recovery rate of 99.7% - 101.0% for PSA detection in human serum. Tang et al. demonstrated that integrating magnetic NPs (MNPs) labelled with Ab_2 and HRP into a high-throughput microfluidic array aided in sensitive, rapid and parallel detection of PSA and three other prostate cancer protein biomarkers (Figure 2.2c).[96] The device consisted of a thirty two-electrode sensor-array, with eight electrodes dedicated to detecting each analyte. Antibodies for PSA, prostate specific membrane antigen (PSMA), interleukin-6 (IL-6) and platelet factor-4 (PF-4) were immobilized onto each of the eight-electrode sensing patches. The capture of each

protein target was performed off-chip and in serum using MNPs labelled with four different antibodies. Following analyte capture by the respective antibodies, MNPs were loaded into the sensor by a syringe and captured by a ring-shaped magnet. A HQ/H_2O_2 solution was then loaded for signal generation using DPV (Figure. 2.2c). A LOD of 0.05-2 pg mL^{-1} and a dynamic range of sub pg mL^{-1} - above 1 ng mL^{-1} were achieved. The clinical relevance of the device was demonstrated by analyzing seven patient samples and comparing device performance against ELISA. The results were well-correlated with ELISA demonstrating a relative standard deviation (RSD) of ±3-10%. The use of NPs in sandwich assays provides a promising avenue for enhancing analytical performance of biosensors. In spite of this, the development of NPs that combine chemical stability, biocompatibility and highly efficient catalysis remains a challenge.

In addition to antibodies, aptamers and nanobodies have been used for the recognition of PSA in electrochemical detection platforms. The use of these biorecognition elements is envisioned to solve the challenges related to the low stability, high non-specific adsorption, and chemical functionalization of antibodies.[97] Nanobodies are clones of the various domains of an antibody; however, they do not include the fragment crystallizable (FC) regions, making them smaller and more resistant to non-specific interactions compared to antibodies.[97] They can be raised against PSA *in vivo* and used for capture and detection antibodies.[98] Using this adaption to the universal sandwich assay, Liu et al. were able to reach a LOD of 0.08 ng mL^{-1} with a linear range of 0.1 – 100 ng mL^{-1} and 90-100% recovery in three spiked human serum samples.[98] This sensor was challenged with 17 patient samples, and an excellent correlation was found between this assay and a commercially available analyzer based on photometry (Roche Cobas).

Aptamers are single-stranded DNA or RNA molecules that have very high affinity and specificity to non-nucleic acids targets, such as proteins, small molecules, or whole cells. Because

aptamers are selected *in vitro* and can be mass produced through chemical synthesis, they have emerged as promising antibody-alternatives in sandwich assays.[99] Aptamers are first identified through Systematic Evolution of Ligands by EXponential enrichment (SELEX) that involves isolation from synthetic DNA libraries *in vitro*.[100] Savory et al. were the first to identify an aptamer for PSA by applying a genetic algorithm to aptamer sequences that were selected through the SELEX process.[101] Aptamer-based sandwich assays build on the same operating principles as those based on antibodies. However, since the size of aptamers are significantly smaller than antibodies, the detection aptamers are typically conjugated to small redox molecules – instead of enzymes – for directly generating an electrochemical signal. This modification was demonstrated by Meng and colleagues who replaced the detection antibody with a PSA-specific aptamer labelled with ferrocene (Fc).[102] In the presence of the target, an Ab_1/PSA/Apt_2-Fc sandwich was formed, and the electrochemical response of Fc was recorded using DPV. This assay displayed a linear detection range of 0.05 – 100 ng mL^{-1} with a LOD of 0.017 ng mL^{-1} and a human serum recovery rate of 96.8-101.4%. Chen et. al demonstrated the innovative use of nucleic acids within a sandwich assay by utilizing DNA tetrahedron as a scaffold for the immobilization of Ab_1, and used HRP-tagged Ab_2/Au for signal transduction.[62] The DNA tetrahedron did not interact directly with the target; however they enhanced the assay sensitivity due to the increased nano-spacing for the antibody to efficiently capture PSA and Ab_2 compared to double stranded DNA molecular linkers. A LOD of 1 pg mL^{-1} was obtained for a linear range up to 0.02 ng mL^{-1}. The analysis of PSA in patient samples was successfully validated using the standard chemiluminescence methods.

Conventional sandwich assays have proven to be reliable and powerful tools for electrochemical PSA analysis over the past 25 years.[103] These assays have demonstrated a LOD as low as 1.25 fg mL^{-1} and have resulted in dynamic ranges as wide as 10 fg mL^{-1} – 100 ng mL^{-1}.

The customizability of these assays provides an excellent quantitative analysis platform that can be applied to a wide variety of protein biomarkers. While sandwich assays are considered one of the most successful strategies for detecting PSA, the multiple operational steps and washing procedures used in these assays hinder their reproducibility and limits their applicability for POC analysis. Hence, there is an urgent need for developing single-step and label-free assays for PSA analysis, which will be discussed in the next section.

2.4.2 Direct Detection Assays

Contrary to sandwich assays, direct detection assays require a single biorecognition molecule and binding event for detecting the target analytes. Elimination of the second binding event reduces assay complexity and reagent amounts, increases assay speed, decreases false positive signals associated with non-specific interactions of the detection antibody with the transducer, and allows for *in situ* analysis.[104] In a typical design, the recognition elements, antibodies and aptamers, are immobilized onto the electrode surface and specific binding of PSA is measured. The complex that is formed through the binding of the biorecognition molecule and PSA creates an inert layer that alters the flux of electrons or redox species to the electrode surface.[78,79] These effects can be measured through impedance-based, voltammetric or amperometric techniques, most commonly EIS, DPV or CA.

Impedance-based techniques have found great success for direct sensing of PSA since protein capture at the electrode surface directly influences the double layer capacitance and charge transfer resistance of the interface.[105] EIS is typically used for direct PSA analysis, where models based on the Randles circuit are used to extract the resistive and capacitive parameters.[106] PSA capture at the electrode hinders the ability of redox species to reach the electroactive surface, which

increases the charge transfer resistance and decreases the double layer capacitance.[107] Using this direct detection strategy with anti-PSA capture antibodies and bovine serum albumin (BSA) used as a blocking agent (Figure 2.3a), a LOD of 0.06 ng mL^{-1} with a recovery rate in a range of 91% – 106% in human serum was acheived.[108] A major challenge with this technique is that non-specifically adsorbed molecules, in addition to specific PSA capture, can influence the measured signal. To circumvent this issue, surface blockers such as carbo-free, gelatin, ethanolamine hydrochloride and BSA have been used following surface functionalization with capture antibodies or inside target solutions for reducing non-specific adsorption.[109]

Aptamers have also been used in similar electrochemical setups to detect PSA using EIS. Contrary to antibody recognition, upon binding to the target, the aptamers typically undergo a structural change that gives rise to a signal change. As a result of the structural changes that aptamers undergo, both decrease[110] and increase[111] in the R_{ct} have been reported, depending on the mechanism that is used to detect PSA. In one mechanism, target capture results in a blocking layer that impedes the ability of redox species to interact with the electrode surface. The performance of aptamers and antibodies in direct PSA detection using such mechanism was compared on graphene quantum dot gold nanorod (GQDs-AuNR) modified screen-printed electrodes. Through the use of EIS, LODs of 0.14 ng mL^{-1} and 0.42 ng mL^{-1} (with linear ranges of 0.1–12 ng mL^{-1} and 0.4 –12 ng mL^{-1}) were achieved with aptamers and antibodies respectively, demonstrating an enhanced LOD with aptamers.[112] The second mechanism arises from the inherent negative charge of aptamers. In this case, when PSA molecules bind to aptamers on the surface of the electrode, a decrease in the charge transfer resistance is seen. This reduction in charge transfer resistance is

either related to the PSA architecture exposing more positive charges when bonded to the aptamer or due to the screening of the charges of the aptamer by the protein (Figure 2.3b).

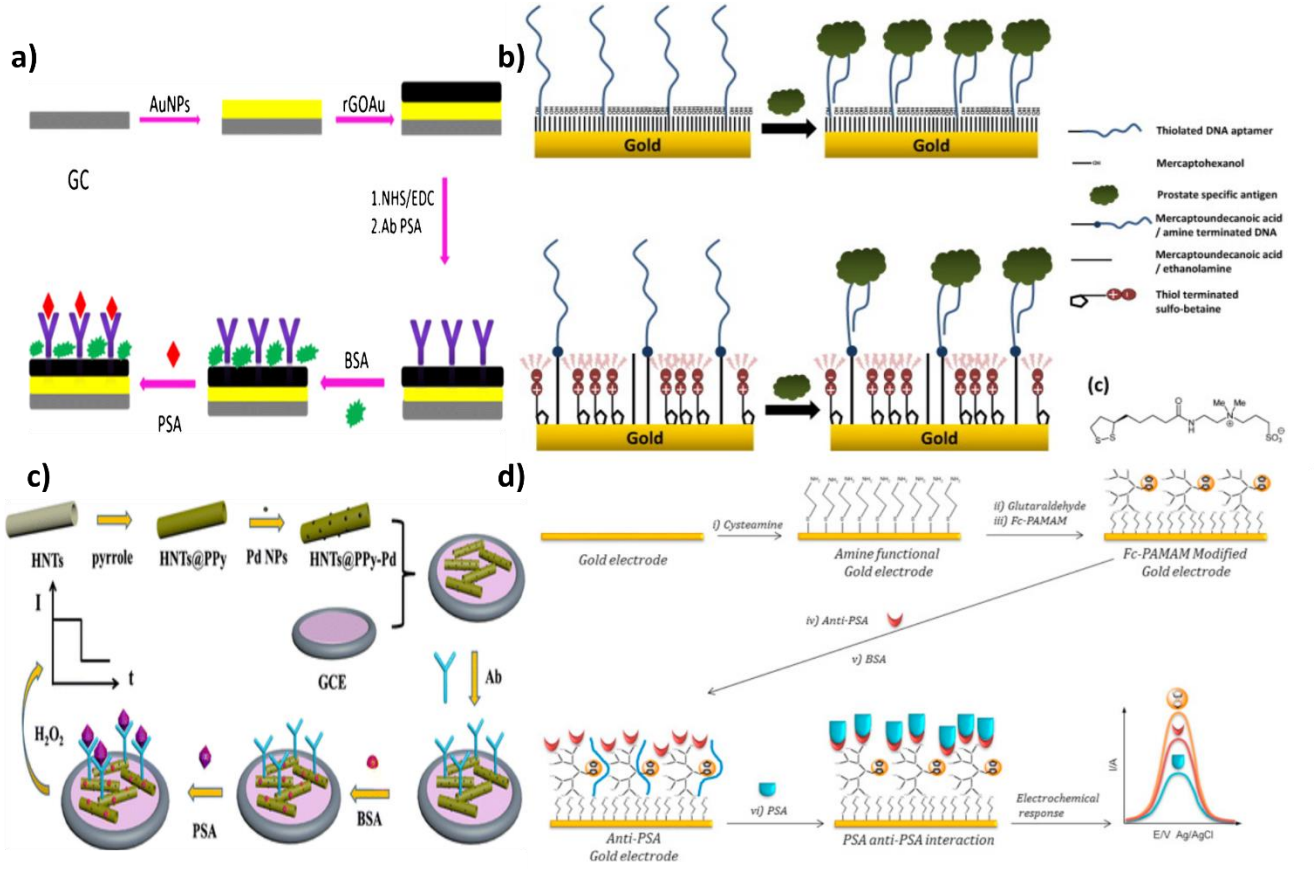

Figure 2.3. Direct detection assays: a) EIS based PSA immunoassay using reduced GO decorated with AuNPs, functionalized with PSA-specific antibody, and blocked using BSA (Reprinted from (Assari et al; 2019)[108] *with permission from Microchimica Acta.); b) EIS-based PSA aptasensor Au electrodes (Reprinted from (Jolly et al; 2015)*[110] *with permission from Elsevier); c) Amperometric-based PSA immunosensor on polypyrrole coated halloysite nanotubes decorated with PdNPs (Reprinted from (Li et al; 2017)*[113] *with permission from Springer); d) Voltammetric-based PSA immunosensor on Au electrodes (Reprinted from (Cevik et al; 2016)*[114] *with permission from Elsevier).*

In either case, this reduces the electrostatic barrier for the transport of ferro/ferricyanide anions towards the electrode surface.[110] Using this mechanism, PSA concentrations lower than 1 ng mL^{-1} in a linear range of 0.5 – 1000 ng mL^{-1} were measured. The measurement of a decrease in R_{ct} compared to the increase observed in the first mechanism is important for distinguishing between specific target capture and non-specific adsorption. In the first mechanism, both non-

specific adsorption and selective target capture result in an increase in R_{ct}; however in the second mechanism, target binding results in a decrease in the R_{ct} and non-specific adsorption results in an increase in the R_{ct}.

EIS has been extensively shown to register subtle changes corresponding to specific protein binding, but practicality of the technique for clinical PSA sensing is questioned. As briefly discussed earlier, non-specific interactions of biomolecules in complex samples poses a high risk for obtaining a false positive result, however EIS has also been demonstrated to be extremely environmentally sensitive in the absence of interfering biomolecules.[115] Extreme sensitivity to electrode contamination, buffer incubation and multiple scans may be overcome by introducing multiple control experiments performed in parallel, however these additional requirements impede on the desired simplicity of a clinical biosensor. For this reason, voltammetric and amperometric techniques have also been applied for the direct sensing of PSA. In these assays, protein capture reduces the flux of redox species to the electrode surface and decreases the electrochemical current, resulting in signal-off biosensors.[116–123] These assays are operationally simple and have led to the development of sensors with a low LOD and a wide dynamic range. One example is an immunosensor fabricated by Li et al. (Figure 2.3c) that consists of halloysite nanotubes with a polypyrrole shell functionalized with antibodies and deposited on a glassy carbon electrode (Ab/HNTs@PPy-Pd/GCE).[113] In this assay, PSA binding decreases the signal obtained from the reduction of H_2O_2, leading to a LOD of 0.03 pg mL^{-1} and a linear dynamic range of 0.0001 - 25 ng mL^{-1}. This assay demonstrated successful PSA detection in human serum with a recovery rate of 100.8% - 103.2%. Another approach to direct detection of PSA using voltammetry involves incorporating redox-active moieties directly onto the electroactive surface and relying on the inhibition of efficient electron transfer caused by the formation of an insulating layer through

accumulation of target protein on the surface. This configuration produces a signal-off sensor where the change in signal is dictated by steric hindrance caused by surface capture of PSA.[124–129] Çevik et al. constructed a direct detection platform using Fc-cored polyamidiamine dendrimers (Fc-PAMAM) deposited on a gold electrode (Figure 2.3d).[114] Anti-PSA antibodies were immobilized onto the electrode surface and a change in the electrochemical response of the redox core upon binding of PSA could be measured using DPV. A clinically relevant linear range of 0.01-100 ng mL^{-1} was reported and a detection limit of 0.001 ng mL^{-1} was calculated. Zhang et al. used a similar strategy of incorporating a redox active moiety onto the electrode surface, but instead of relying on the formation of an insulating layer, PSA was quantified by the dissociation of the insulating layer. An aptamer-streptavidin-DNA complex was reversibly immobilized onto a hemin-graphene/palladium NP/GCE.[130] Binding of PSA to the complex prompted a dissociation event from the surface due to weak coordination chemistry used for immobilization. The result was exposed hemin at the surface and an increase in the hemin oxidation peak, detected using DPV. The linear range was found to be 0.025 - 205 ng mL^{-1} with a LOD of 8 pg mL^{-1}. Signal recoveries ranging from 95.0-100.3% were found in three spiked human serum samples.

Novel catalysts are being increasingly used in direct detection assays to increase the binding-induced signal changes. AuNP functionalized CuO_2@CeO_2 core shell particles have been used in such assays for harboring the capture antibodies.[131] The synergistic effects of the two metal oxides with the metal and the architecture of the composite increases electron transfer efficiency and reaction efficiency towards the reduction of H_2O_2 for a one step Ab-PSA interaction. This immunosensor demonstrates a linear detection range of 0.1 pg mL^{-1} - 100 ng mL^{-1} and a LOD of 0.03 pg mL^{-1}. A study of different concentrations of PSA in human serum demonstrated a recovery rate ranging from 98.3% - 100.2%.

While steric hindrance has proven to be useful in developing assays for the direct detection of PSA, other approaches using signal reporters have been used to translate a single binding event to a measurable signal. One strategy involves incorporating redox molecules directly into the biorecognition elements, where analyte capture causes a structural change, which results in a change in the position or accumulation of the redox molecules relative to the electrode surface. Such assays have been developed using methylene blue (MB) as the redox molecule and PSA aptamer as the biorecognition element by taking advantage of the intrinsic binding properties between MB and DNA. Free MB in solution can interact specifically to exposed guanidine bases in single stranded DNA (ssDNA) or intercalate into double stranded DNA[132] and can be detected using voltammetric methods[133]. Both signal-on[134] and signal-off[135,136] aptasensors have been developed using MB/DNA interactions by immobilizing a PSA aptamer onto an electrode surface and monitoring an increase or decrease in current. Another method of employing a MB-based aptasensor is through direct conjugation of MB to one end of an immobilized PSA aptamer. The structural change of the aptamer caused by PSA binding leads to a change in electrochemical signal that can be detected by voltammetry. Sattarahmady et al. constructed a PSA sensor by immobilizing a MB modified aptamer sequence onto a nanostructured gold electrode and measured the reduction of MB using DPV.[137] Aptamer folding caused by specific recognition of PSA resulted in a decreased distance between MB and gold, achieving more efficient electron transfer. This signal-on sensor demonstrated a linear range of 0.125-128 ng mL^{-1}, a LOD of 50 pg mL^{-1}, and successful performance in multiple human serum samples. Structure switching aptamers have also been used with metal NPs as the signal reporter rather than MB. Zhao et al. reported a PSA biosensor that relied on the structural change of a Ag/CdO NP labelled aptamer to cause a decrease in the electrochemical signal by dissociation from the electrode surface.[138] Aptamer

functionalized Ag/CdO NPs were assembled onto GO/Fe_3O_4 nanosheets, which could then magnetically adsorb onto the surface of a magnetic GCE (MGCE). A large DPV signal could be generated in the absence of PSA, but upon biorecognition, dissociation of the NPs caused by the reversible association of aptamer with the nanosheet resulted in a decrease in the generated signal. The linear range of the biosensor was found to be 50 pg mL^{-1} – 50 ng mL^{-1} and the LOD was calculated to be 28 pg mL^{-1}. The recovery of PSA in four human serum samples were in the 97.3 – 103.4% range, demonstrating the potential for practical use. The use of the MGCE contributed to simple and automated assembly of the electroactive components onto the electrode surface while the Ag core of the NP allowed for enhanced electron transfer. The combined components of this sensor attributed to the wide, clinically relevant linear range, low LOD and ease of fabrication. The structure-switching capabilities of aptamers and their conjugation with small redox molecules enables the development of direct signal-on biosensors, which has been challenging to develop using antibodies.

Direct detection assays reduce the amount of analytes and washing steps that are required in sandwich assays and decrease the complexity of PSA analysis. Additionally, these assays can be used for monitoring analytes *in situ*.[113,139] The shortcoming of these assays is that non-specific adsorption of materials onto the sensing surface often produces a signal that is difficult to decouple from the signal generated through target binding.[78]

2.4.3 Indirect Detection Assays

While there is value in the simplicity of direct detection assays and the versatility of sandwich assays, “indirect” assay designs not belonging to these categories have been developed to increase the sensitivity of biosensors, diminish the need for expensive reagents, and to enable

multiplexing. As with sandwich and direct detection assays, indirect detection assays rely on the specific biorecognition of PSA using antibodies or aptamers. However, this single binding event does not result in a detectable signal. Instead they rely on additional interactions, such as DNA strand displacement[140], to either release a surrogate target, or indirectly induce a reaction that generates an electrochemical signal correlating to PSA concentration. Typically, the signal generated by these assays is transduced using voltammetric techniques.

Through the indirect detection mechanisms, it is possible to introduce functional components for signal enhancement and target recycling for signal amplification. Non-enzymatic target recycling was reported by Zhao et al. where a series of DNA strand displacement reactions initiated by PSA capture led to the capture of a dual reporter DNA immobilized metal-polymer.[141] PSA aptamers were immobilized onto magnetic beads along with a partially complementary DNA strand that could be released upon biorecognition of PSA (Figure 2.4a). The release of the partially complementary strand could hybridize with hairpin DNA that was immobilized onto a GCE/AuNP electrode. This hybridization event exposed a toehold region, through which a catalytic DNA segment could displace the partially complementary DNA strand while maintaining the open form of the immobilized hairpin DNA. This open form left a region of the immobilized hairpin DNA that was complementary to the reporter probe DNA unprotected and available for hybridization. The reporter probe DNA was conjugated with Au/Pt-polymethylene blue (PBM) composites that when bound to the hairpin DNA through complementary base pairing with the reporter probe generated a large current signal. The release of the partially complementary strand could further open other hairpin DNA molecules, demonstrating surrogate target recycling. SWV was used to measure the electrochemical signal and H_2O_2 was used to catalyze the redox reaction of the PBM reporter, further enhancing the signal. An ultra-low LOD and wide linear range were reported as

10 fg mL^{-1} and 2.3 fg mL^{-1}- 100 ng mL^{-1}, respectively. This sensor proved its clinical applicability with successful recovery rates of 98.8-103% in two human serum samples, and acceptable relative error when compared to chemiluminescence immunoassays. Enzymatic amplification has also been performed, utilizing rolling circle amplification (RCA), to generate long DNA sequences that could associate with CuNPs.[142] This assay involved two recognition elements, an immobilized antibody and an aptamer/RCA primer loaded AuNP. A sandwich structure could be formed between the loaded AuNPs and antibodies in the presence of PSA, triggering the generation of RCA products. The generated products specifically interacted with CuNPs that could be subsequently dissociated and measured using differential pulse stripping voltammetry on an gold electrode. The cascade of signal amplification processes resulted in a linear range of 0.5 – 500 fg mL^{-1} and a LOD of 0.02 fg mL^{-1}. The sample analysis performed in human serum was compared to results obtained using an electrochemiluminescence immunoassays and a relative deviation of less than 8% was reported. Miao et al. constructed an ultrasensitive signal-off sensor driven by target-triggered dissociation, measured by LSV.[66] They utilized DNA origami as a molecular scaffold, PSA aptamers as recognition elements, AgNPs as signal reporters and an exonuclease as a signal amplification component (Figure 2.4b). The PSA aptamer sequence was designed with an NH_2 terminus for the attachment of AgNPs. Immobilization of the unlabeled aptamer to the electrode surface was done via complementary base pairing with a sequence in the DNA scaffold. Upon recognition of PSA, the conformational change in PSA aptamer resulted in its dissociation from the complementary strand. Signal transduction was done through the addition of AgNPs onto the sensor after introducing the sample. In the absence of the target, a large signal was obtained using LSV; however, in the presence of PSA, the lack of the amino-terminated aptamer resulted in a reduced signal. Prior to the addition of AgNPs, exonuclease was introduced to free captured

PSA by degrading the aptamer, allowing for target recycling and enhanced sensitivity. A LOD of 0.11 pg mL^{-1} was achieved with a linear range of 1 pg mL^{-1} - 160 ng mL^{-1}. The performance of the device was challenged in six undiluted human serum samples and was compared to the results obtained through an immunoradiometric assay. The RSD ranged from 1.73-6.08% showing acceptable agreeance between the two detection methods.

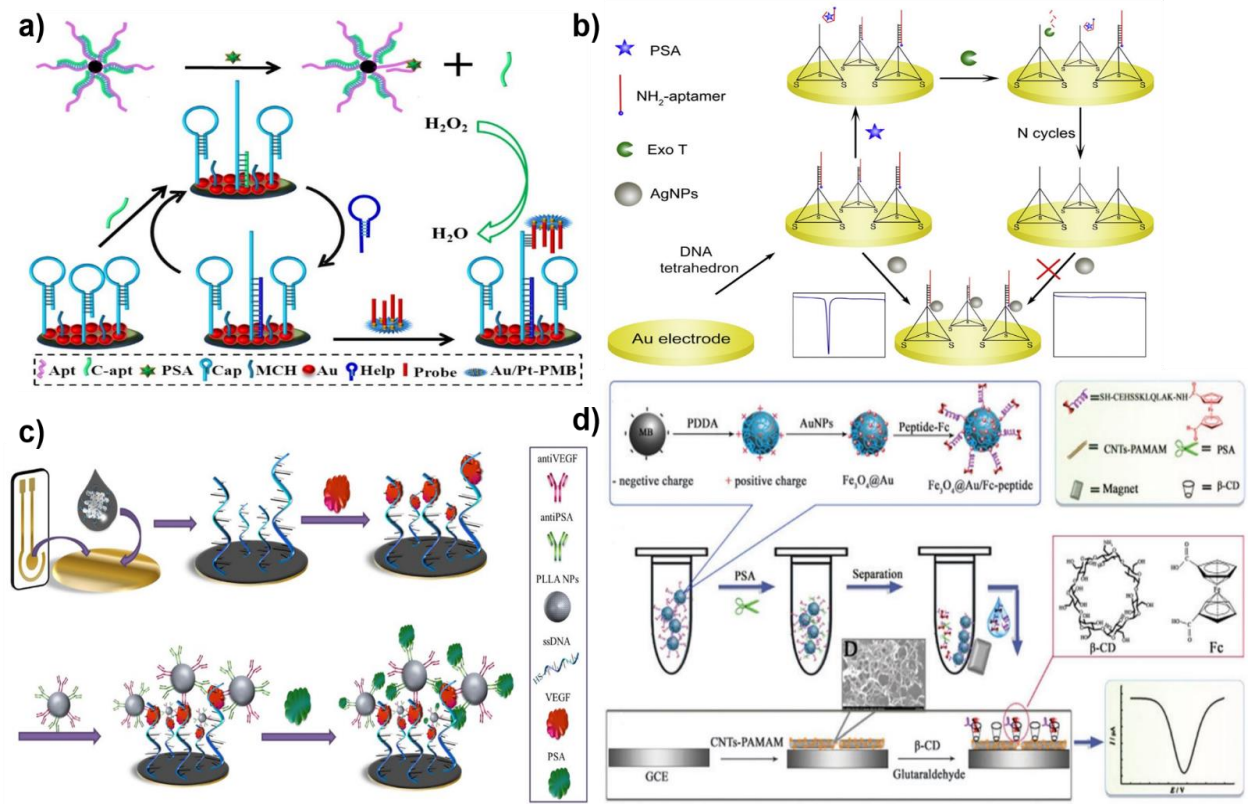

Figure 2.4. Indirect detection assays: a) Enzyme-free target recycling based assay for the detection of PSA using dual metal PMB (Reprinted from (Zhao et al;2018)[141] with permission from Elsevier); b)Target-triggered dissociation based assay for PSA detection with enzyme assisted amplification (Reprinted from (Miao et al;2018)[66] with permission from Elsevier); c) Simultaneous detection of PSA and VEGF using ssDNA modified GO and PLLA (Reprinted from (Pan et al;2016)[143] with permission from Elsevier); d) Enzymatic peptide cleavage based assay for the detection of PSA using host-guest interaction of Fc and β-CD (Reprinted from (Xie et al;2015)[144] with permission from the Royal Society of Chemistry).

Many assays have reported great success not only because of the use of target recycling for amplification but also because of the use of other signal generation strategies, such as metal NPs. Xia et al.[145] was able to demonstrate how metal NPs can be used to greatly amplify the electrochemical signal without the use of enzymes or other target recycling tactics. Using an

aptamer as a biorecognition element, PSA could be captured at the electrode surface and subsequent reactions could be performed to exploit the saccharide groups of the glycoprotein upon immobilization. The PSA-aptamer complex was decorated with 4-mercaptophenylboronic acid (MPBA) that induced *in situ* network formation of AgNPs. The solid-state Ag/AgCl reaction from the AgNP network could be measured using LSV and a linear range of 0.5-200 pg mL^{-1} was obtained, as well as a LOD of 0.2 pg mL^{-1}. When challenged with clinical samples, acceptable RSDs were achieved, validating the clinical performance of the sensor. In this assay, signal generation is achieved by the aggregation of AgNPs onto protein saccharides; therefore, it can be easily applied to the detection of other relevant glycoproteins.

Non-metallic NPs have also been used in the indirect detection of PSA. An assay designed by Pan et al. was able to simultaneously detect PSA and vascular endothelial growth factor (VEGF), a non-specific tumor protein biomarker, by incorporating poly-L-lactide (PLLA) NPs for delivering the target capture elements and amplifying the electrochemical signal (Figure 2.4c).[143] The detection was based on the increase of steric hindrance and the resultant decrease in electron flow from $[Fe(CN)_6]^{3-/4-}$ to the electrode in response to target binding. A solution of ssDNA and GO was incubated on an Au electrode to manufacture a sensing platform capable of capturing VEGF through association with the specifically chosen ssDNA sequence. After incubation of the electrode with the first target protein, PLLA NPs labelled with both anti-PSA and anti-VEGF were introduced and specifically interacted with the VEGF-ssDNA complex on the electrode surface. Decrease in electrochemical signal corresponding to this binding event was recorded using DPV. PSA could then bind to the PLLA NP-VEGF-ssDNA, further reducing the electrochemical signal. Linear ranges of 0.05 – 100 ng mL^{-1} and 1 – 100 ng mL^{-1} for VEGF and PSA were obtained, respectively. The LOD for both proteins were the lower limit of the linear ranges.

Antibodies and aptamers are common biomolecules used to detect protein targets such as PSA, but recently peptides are being used as biorecognition elements within indirect assays.[146] Peptide sequences incorporated into PSA detection assays are not used to capture or immobilize the protein, but rather exploit the proteolytic activity of PSA to induce an electrochemical signal. One approach employs an enzymatically cleavable peptide sequence that upon interaction with proteolytically active PSA (paPSA) results in a cleavage of the portion of peptide responsible for generating a detectable signal by binding to metal NPs.[147] Decrease in electrochemical signal can be directly correlated to the concentration of paPSA, generating a signal-off sensor. Conversely, the enzymatic cleavage can increase the signal magnitude by reducing steric hindrance on the electrode surface.[148] In this design, the cleavable peptide sequence immobilized on the surface was chemically conjugated to BSA, enhancing surface blockage and decreasing electron transfer with the redox active electrolyte. Exposure of the electrode surface as a result of peptide cleavage by paPSA increases the electrochemical signal, presenting a signal-on method for paPSA detection. A different approach uses the cleaved peptide as a surrogate target molecule for the detection of paPSA. Xie and colleagues demonstrated this by taking advantage of both the enzymatic properties of PSA and the host-guest interaction between Fc and β-cycextrin (β-CD) to create a sensor capable of reaching a LOD of 0.78 pg mL^{-1} (Figure 2.4d).[144] Two recognition elements were immobilized in this work; a peptide sequence with a PSA cleavage site labelled with a Fc molecule onto an Fe_3O_4@Au magnetic bead and β-CD onto multi-walled CNT-PAMAM on a GCE. The peptide sequence acted as a surrogate target as it could be cleaved from the magnetic bead in the presence of paPSA and captured by the β-CD on the CNT PAMAM electrode surface. The peptide cleavage was transduced into an electrochemical signal using DPV and Fc as a redox probe. The increasing concentration of electroactive peptides on the surface corresponded directly to the concentration

of PSA through a linear range of 0.001 ng mL^{-1} – 30 ng mL^{-1}. Recovery of paPSA in human serum was between 101.2 – 106.3%. The detection of a specific isoform of PSA could be viewed as a limitation, however, paPSA has been demonstrated to be involved in PCa metastasis rendering it a suitable protein biomarker for determining the aggression level.[149] In addition, the low cost, ease of synthesis, and stability of peptides make them excellent substitutes for antibodies in immunoassays.

The increased sophistication of indirect detection assays through incorporation of multiple biorecognition elements, NPs, redox labels or other biomolecular processes has led to PSA biosensors with increased sensitivity and selectivity and has provided a basis for multi-target analysis. Although the increased complexity of these assays results in a parallel increase in the number of washing steps and the amount of reagents; they have demonstrated ultralow and clinically-relevant LODs ranging from 1 ng mL^{-1} down to 0.020 fg mL^{-1}.

2.5 Conclusion

In recent years, there has been tremendous research efforts towards improving the sensitivity, specificity and LOD of PSA detection using electrochemical methods for clinical decision making. Based on the operating principles, we can categorize the electrochemical detection of PSA into the conventional sandwich assay, direct capture assay, and the indirect detection assay. The sandwich assays are the electrochemical analogues of ELISA, which is commonly used in biological research and clinical analysis. Although sandwich assays are widely researched; these rely on multiple steps and a large amount of reagents. An alternative to this is the direct approach where a single capture event leads to signal generation by using the concepts of EIS and voltammetry. Indirect detection assays are another alternative to sandwich assays, in

which PSA binding results in the release of a functional target, which can be captured for electrochemical signal transduction. This approach typically comes at a cost of increased complexity, with the advantage of increased sensitivity and selectivity. Although sandwich and direct detection assays have demonstrated clinically-relevant performance, the indirect detection assays shine in demonstrating a record performance: an assay of this type successfully detects as low as 0.11 fg mL^{-1} of PSA with a wide linear range of 1 fg mL^{-1} - 100 ng mL^{-1}.[148] Despite ultra-sensitivity in detecting levels of PSA within the clinical realm, challenges exist when attempting to commercialize indirect biosensors with the main obstacles being reagent stability and the increased cost of reagents and materials.

Chapter 3: Optimization of a Bio-barcode Assay for Electrochemical Protein Detection

3.1 Preface

The focus of this chapter will be on optimizing reaction conditions in order to achieve the most efficient and successful protein detection. The importance of each condition will be discussed and results from varying conditions will be examined. Probe density, target hybridization time, reagent concentrations, reaction time, surface blocking and dilution factor of the biological sample were all investigated using a model streptavidin/biotin system to develop the most optimal system for protein detection.

Sarah Traynor was the only author to contribute to this section.

3.2 Introduction

This thesis is centered around the development of an electrochemical detection scheme to be applied towards the detection of a protein cancer biomarker. To accomplish this, a bio-barcode assay integrated with electrochemical readout will be utilized to develop a simple biosensing platform with minimal reaction and wash steps and the applicability of the assay will be demonstrated using PSA. Bio-barcode assays have demonstrated uniquely exceptional performance in achieving ultra-sensitive protein detection (attomolar concentration) while maintaining a simplistic design.[150,151] To eliminate the need for amplification and separation elements, the assay will use the formation of a proximity-induced three way junction (TWJ) in response to the target protein to release the bio-barcode.[152] Capture of the protein target and release of the bio-barcode will be performed in solution and then transferred to an electrode for electrochemical detection. The released bio-barcode will be labelled with a methylene blue (MB)

molecule and captured by a double stranded (ds) DNA probe immobilized on the electrode surface, enabling signal generation via the reduction of methylene blue using SWV. The assay contains three important intermediates – the biorecognition motifs TB and B*C which are DNA strands conjugated to a biorecognition element, the MB labelled bio-barcode containing duplex T*C*:CR* and the ds capture probe CP:D1.

The assay design is presented in Scheme 3.1 and occurs as follows:

1. Capture of the protein target will occur in solution through bio-recognition elements conjugated onto DNA strands TB and B*C.
2. Recognition of a single protein target by both TB and B*C will result in the formation of a DNA/protein complex.
3. The resulting complex can bind a toehold region of the MB-labelled bio-barcode containing duplex (T*C*:CR*), initiating a strand displacement reaction that releases the MB-labelled barcode (CR*). The result is the formation of a three-way junction and a free single stranded labelled barcode.
4. The single stranded MB-labelled barcode can participate in an on-chip strand displacement reaction, displacing D1 from the CP:D1 capture duplex.
5. Square-wave voltammetry can be used to determine whether the MB-labelled barcode has hybridized with the capture probe via the reduction of MB at the gold electrode surface.

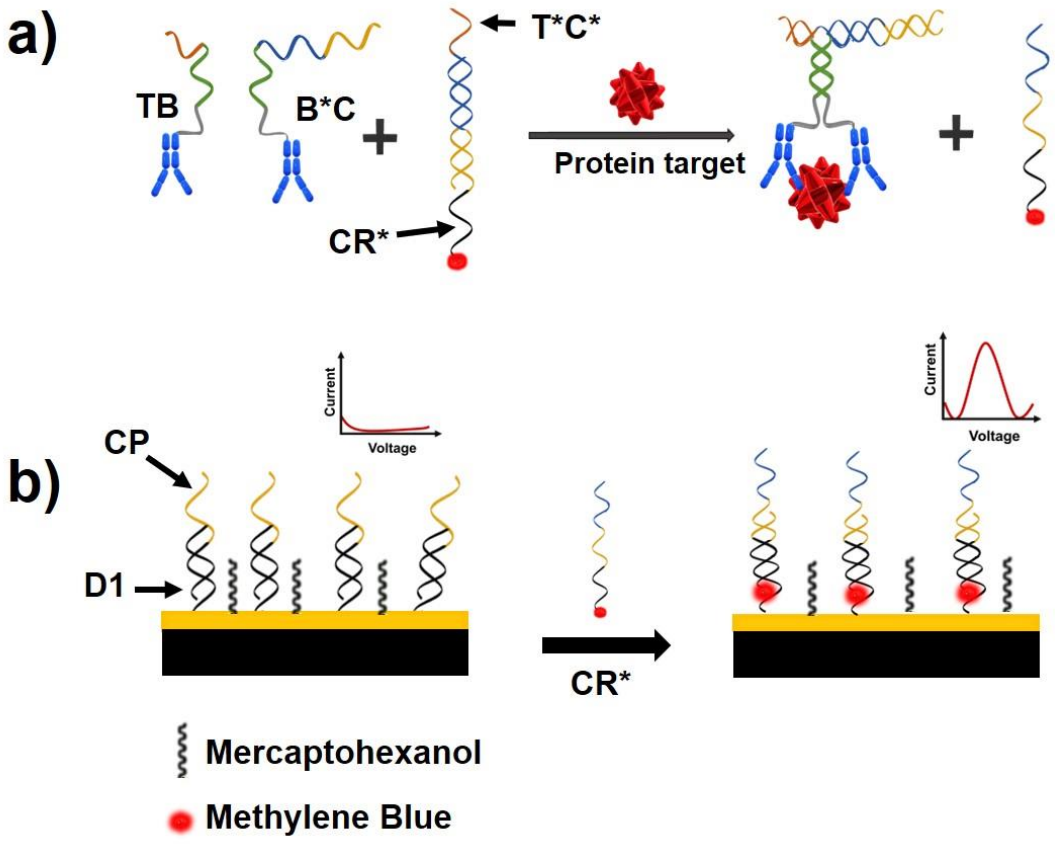

*Scheme 3.1. Schematic of electrochemical bio-barcode assay. a) assay components in solution. TB and B*C recognize a protein target and form three-way junction with T*C* releasing MB-labelled CR*. b) On-chip hybridization of the released bio-barcode. The electrode is pre-modified with capture probe CP:D1 and mercaptohexanol. When CR* is released in assay it can hybridize with CP, releasing the D1 strand, resulting in an increase of electrochemical signal.*

Bio-barcode sensing platforms, like the one presented here, are compositions of many assay components and bio-recognition elements, forming a sensitive detection platform capable of quantifying ultra-low levels of a molecular analyte.[153] To ensure that the system performs in a specific and reliable manner we should work to reduce the signal changes that may be caused by inefficient capture of target or surrogate target, inefficient strand displacement within the assay or interference from non-target molecules. Accomplishing this can be done by optimizing working parameters for ideal performance. The whole detection scheme is performed in two environments:

protein capture and release of the bio-barcode is done in solution followed by capture of the bio-barcode on a surface. This results in two areas of optimizations, one affecting the efficiency of events occurring in solution and one affecting events at the electrode surface. For solution protein capture and release of the bio-barcode, optimizations should be focused on the preparation of assay intermediates, as well as the concentration of the intermediates. In addition, the incubation period of this protein capture step should be investigated. To ensure the capture of the labelled bio-barcode on the surface occurs in an efficient manner, probe spacing, target hybridization time, surface blocking and sample preparation should be optimized.

In this chapter, optimizations to the proposed biosensor using a developed baseline system with biotin as the biorecognition element and streptavidin as the protein target will be discussed. The optimizations include determining the probe density required to obtain the highest signal by investigating both probe concentration and deposition time, experiments performed to achieve the highest signal-to-blank ratio (SBR) by examining concentration of assay components and ratios, and exploring poly-A as a surface blocker. In addition, conditions required for successful PSA detection in a relevant biological sample will be investigated by determining signal loss in different levels of dilution of human plasma. The result of optimizing this biosensing platform will be demonstrated in chapter 4 when the analytical ability of the sensor is challenged.

3.3 Experimental

3.3.1 Studying the Effect of Probe Density on the Generated Electrochemical Signal

The sensing electrode was prepared following the procedure outlined in section 4.3.5 and probe DNA was annealed following the procedure outline in section 4.3.4. After annealing, probe DNA was reduced for 2 hours at a final concentration of 1, 0.5 and 0.25 µM using TCEP in

deposition buffer at a ratio of 1:50 (probe:TCEP). Following reduction, 3 µL each probe concentration was placed on an electrode and left for 2 hours in a humidity chamber in the dark. After 2 hours the electrode was washed in washing buffer to remove any non-specifically bound DNA and a CV scan was performed from 0 – 0.5 V in 2 mM $[Fe(CN)_6]^{4-/3-}$ to ensure immobilization. A MCH backfill was done using 100 mM MCH for 20 minutes, followed by another CV scan in 2 mM $[Fe(CN)_6]^{4-/3-}$ to ensure both removal of non-specifically adsorbed probe, and aligning of specifically adsorbed probe, with washing between each step. Once the sensing surface was prepared, 3 µL of 0.3 µM of CR* was put onto the electrode and the electrode was incubated in a humidity chamber for 30 minutes at 37°C. The electrode was then washed in washing buffer to remove non-specifically adsorbed target and SWV was performed from 0 – (-0.5) V in washing buffer. This was repeated for probe deposition times of 4, 8, 16 and 24 hours.

3.3.2 Studying the Effect of Hybridization Time on the Generated Electrochemical Signal

The sensing surface was prepared following the procedure outlined in section 4.3.5 with 0.5 µM probe for 16 hours. After qualitative scans, 3 µL of 50 nM CR* was placed on the electrode surface and was incubated at 37°C for 5 minutes. The electrode was washed in washing buffer and SWV was performed from 0 – (-0.5) V in washing buffer. This was repeated for incubation periods of 15, 30, 45, 60 and 120 minutes.

3.3.3 Studying the Effect of the Ratio of the T*C* Strand to the CR* Strand During Annealing for Preparation of Bio-barcode Containing Duplex on the Signal-to-blank Ratio

In order to produce a 1:1 ratio of T*C*:CR*, 10 µL of 100 µM CR* was mixed with 10 µL of 100 µM T*C* and 30 µL of annealing buffer. For a 1.1:1 ratio, 10 µL of 100 µM CR* was mixed with 11 µL of 100 µM T*C* and 29 µL of annealing buffer. For a 1.2:1 ratio, 10 µL of 100

µM CR* was mixed with 12 µL of 100 µM T*C* and 28 µL of annealing buffer. Each mixture was heated to 90°C for 5 minutes and then the solution was brought to 25°C incrementally over 30 minutes.

3.3.4 Studying the Effect of the Concentration of Assay Intermediates on the Signal-to-blank Ratio

The sensing electrode was prepared following the procedure outlined in section 4.3.5. For optimization of the assay intermediates, the full e-biobarcode assay was performed with varying concentrations of T*C*:CR* and biorecognition probes TB and B*C. TB and B*C were mixed with T*C*:CR* and streptavidin in reaction buffer so that the final desired concentrations of TB, B*C and T*C*:CR* were reached and the final concentration of streptavidin was 10 nM. A blank solution was also prepared by adding reaction buffer in place of streptavidin. A 3 µL drop of solution was deposited on to the prepared electrodes and incubated at 37°C for 45 minutes in a humidity chamber. The electrodes were then washed in washing buffer and SWV was performed from 0 – (-0.5) V in washing buffer.

3.3.5 Studying the Effect of introducing a Protein Capture Reaction Step at 37°C on the Signal-to-blank Ratio

The sensing electrode was prepared following the procedure outlined in section 4.3.5. For protein detection with a reaction period, 10 µL of 100 nM streptavidin was mixed with 10 µL of 250 nM TB, 10 µL of 250 nM B*C, 10 µL of 200 nM T*C*:CR* and 60 µL of reaction buffer. The mixture was incubated in an Eppendorf tube for 30 minutes at 37°C. After incubation 3 µL of the mixture was deposited onto the prepared electrode and incubated in a humidity chamber for 45 minutes. The electrodes were then washed in washing buffer and SWV was performed from 0 – (-0.5) V in washing buffer. For protein detection without a reaction period, 10 µL of 250 nM TB

and B*C were mixed with 10 µL of 100 nM streptavidin, 10 µL of 200 nM T*C*:CR* and 60 µL of reaction buffer. A 3 µL drop of the mixture was immediately deposited onto the prepared electrode and incubated in a humidity chamber for 45 minutes. The electrodes were then washed in washing buffer and SWV was performed from 0 – (-0.5) V in washing buffer.

3.3.6 Studying the Effect of Poly A as a Surface Blocker on the Generated Electrochemical Signal

The sensing electrode was prepared following the procedure outlined in section 4.3.5. For protein detection using poly-A as a surface blocker 10 µL of 100 nM streptavidin was mixed with 10 µL of 250 nM TB, 10 µL of 250 nM B*C, 10 µL of 200 nM T*C*:CR* and 60 µL of reaction buffer. The mixture was incubated in an Eppendorf tube for 30 minutes at 37°C. During this incubation period, 3 µL of 1 µM poly-A was deposited onto the prepared electrode and left at room temperature for 30 minutes. After 30 minutes the drop was removed using a KimWipe and 3 µL of the reaction mixture was deposited onto the electrode. The electrode was incubated in a humidity chamber at 37°C for 30 minutes. The electrodes were then washed in washing buffer and SWV was performed from 0 – (-0.5) V in washing buffer.

3.3.7 Studying the Effect of Human Plasma Dilution on the Total Electrochemical Signal Loss

The sensing electrode was prepared following the procedure outlined in section 4.3.5. Human plasma was diluted 2x, 4x, 6x and 8x using reaction buffer. 5 µL of 100 µM stock solution CR* was mixed with 95 µL of undiluted human plasma. CR* was further diluted to 20 nM using the undiluted human plasma. A 3 µL solution of plasma spiked with 20 nM CR* was deposited onto the prepared electrode and incubated at 37°C for 45 minutes in a humidity chamber. The

electrodes were then washed in washing buffer and SWV was performed from 0 – (-0.5) V in washing buffer. This was repeated for 2x, 4x, 6x and 8x diluted plasma.

3.4 Results and Discussion

3.4.1 Studying the Effect of Probe Density on the Generated Electrochemical Signal

A typical electrochemical biosensor will have a biomolecule immobilized onto the surface of the electrode acting as a biorecognition probe. Many classes of biomolecules have been employed as molecular recognition probes, but one of the most well-understood is DNA.[154] DNA is an excellent probe candidate since synthetic DNA is relatively inexpensive, stable and the target can easily be selected through manipulated of the capture probe sequence. One of the most common methods of immobilization of DNA onto an electrode surface is through the formation of a self-assembled monolayer (SAM).[155] DNA can readily be modified to contain moieties that either have specific affinities for certain metals or can form covalent bonds with other chemical compounds. The thiol-gold interaction is one that has been heavily investigated and has been extensively used for immobilization of thiolated DNA onto a gold electrode. Under typical conditions, immobilization can be initiated by depositing a drop of thiolated DNA onto a clean gold electrode or submerging an electrode into the solution. Adsorption of thiolated DNA onto gold is believed to happen in a step-wise manner; first the bases of the DNA adsorb non-specifically onto the gold, followed by a rearrangement that leads to the thiol-gold bond.[156] The flexibility of the probe can cause folding of the DNA resulting in probe laying adjacent to the electrode surface, requiring another agent for probe alignment and removal of non-specifically adsorbed probe. MCH, a 6-carbon chain with a thiol group at one end and a hydroxyl group at the

other, has been extensively used for this purpose.[157] The thiol group competes with the adsorbed DNA bases for gold, removing any non-specifically bound DNA, resulting in a SAM with a hydroxyl group protruding into the solution. This slightly negative hydroxyl group aligns parallel to the DNA and is thought to repel the negatively charged DNA, generating more order within the molecular probe layer. This stiff layer can now more efficiently hybridize a complementary DNA target due to the decreased steric hindrance caused by surface immobilization.

For this detection scheme, a partial DNA duplex was used as the capture probe and immobilized onto the surface of the gold electrode via this SAM process. MCH was used in excess for removal of non-specifically adsorbed probe and for aligning the probe DNA. The process of depositing and aligning the probe was qualitatively monitored using cyclic voltammetry (CV) (Chapter 4 Appendix, Figure 4.7). Deposition of the ds probe results in the formation of negatively charged layer at the surface of the electrode. A reversible redox-active species such as $[Fe(CN)_6]^{4-/3-}$ can be used to determine if probe has been successfully deposited onto the electrode surface by comparing a post-deposition scan to a pre-deposition scan. When a potential in the range of 0 – 0.5 V (against Ag/AgCl) is reversibly applied to a gold electrode in a $[Fe(CN)_6]^{4-/3-}$ solution, characteristic oxidation and reduction peaks can be recorded. Upon addition of the negatively charged DNA $[Fe(CN)_6]^{4-/3-}$ is repelled from the surface resulting in attenuation of these characteristic peaks. After MCH is added and only the specifically adsorbed DNA remains, some recovery of the peaks can be observed.

Probe density is an integral factor affecting the efficiency of a DNA biosensor that is influenced by many components.[158] Spacing of probes on a surface directly correlates to target capture efficiency and must be optimized in order to achieve the best performance. There is an ideal probe density that must be reached, one that results in the most capture possible but also

achieves the least amount of steric hindrance. Steric hindrance is especially important when investigating DNA biosensors as accumulation of too much charge from the immobilized probe can inhibit efficient hybridization or strand replacement reactions necessary for target capture (Scheme 3.2). Probe concentration, deposition time and formation of an aligning SAM all contribute to the probe density and must be investigated.

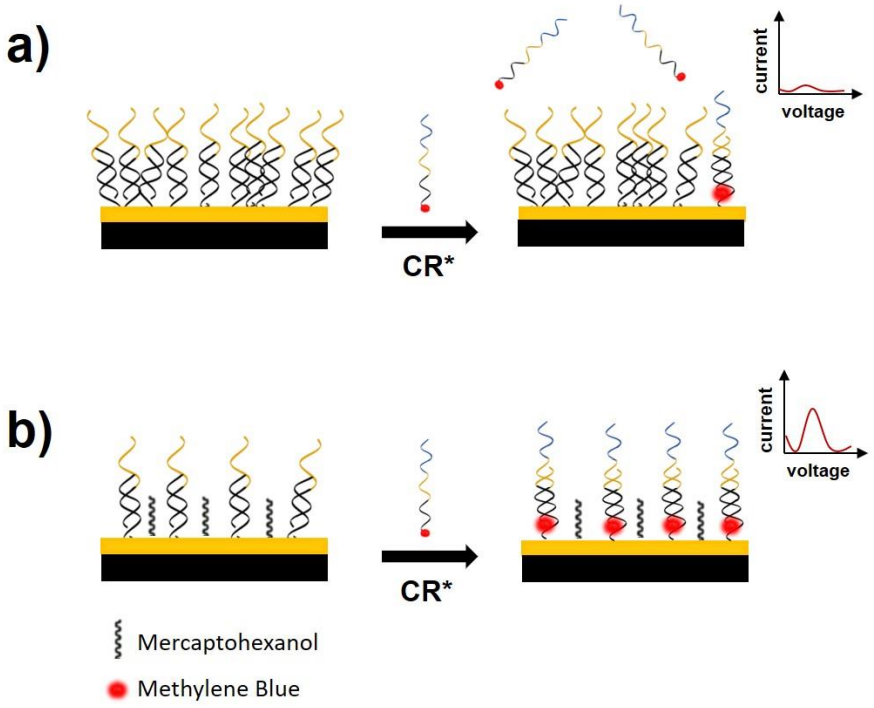

Scheme 3.2. Schematic demonstrating the effect of molecular crowding. a) Probe density is high preventing strand displacement to occur, caused by increase steric hindrance resulting in a low electrochemical signal. b) Probe density is optimized resulting in adequate spacing required for strand displacement. The electrochemical generated from the same amount of target as (a) has increased due to less steric hindrance.

In order to optimize probe density, probe concentration and deposition time was first studied using a simple assay that involves capture of a MB-labelled single strand of DNA (CR*) by an immobilized double stranded (ds) probe (CP:D1). Figure 3.1 shows the results of this

optimization step, done by comparing the signals that were obtained using 0.3 µM of CR* using 1 µM, 0.5 µM and 0.25 µM of probe for a series of increasing deposition times. Since at all concentrations of probe 16 hours resulted in the highest signal, 16 hours was chosen as the optimal deposition time, and because 0.5 µM of probe correlated to the overall highest signal, this was chosen as the optimal probe concentration. When the probe concentration was at the higher limit of 1 µM, signal magnitude was low for all deposition times, likely attributed to crowding of the electrode leading to the repulsion of the incoming negatively charged MB-labelled reporter. When the probe concentration was at the lower limit of 0.25 µM the signal magnitude was also low, likely due to the lack of probe.

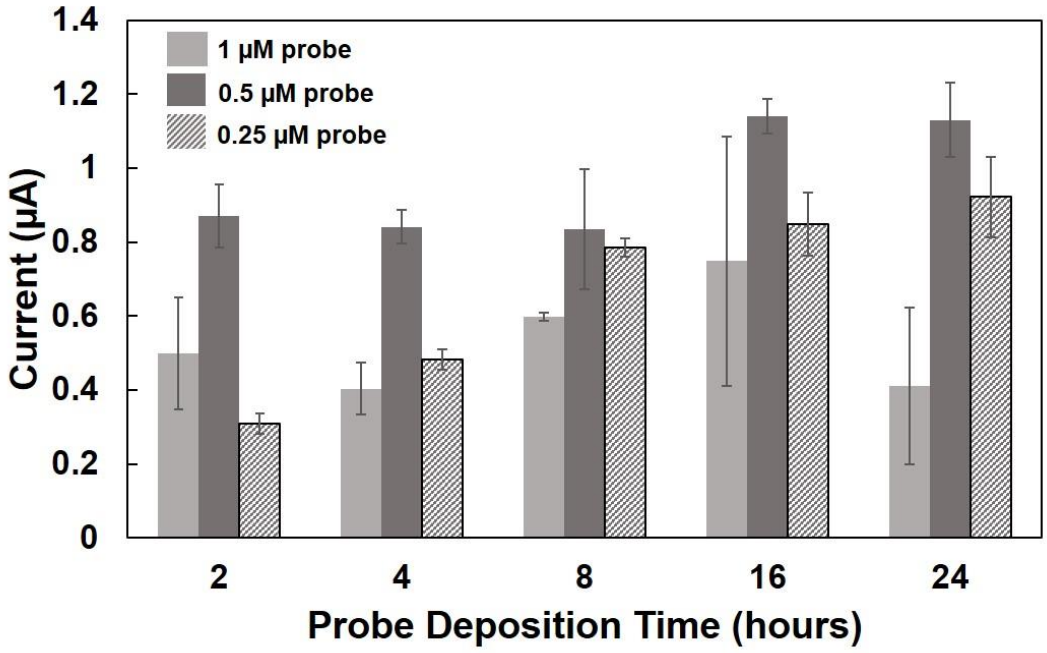

Figure 3.1. Effect of probe concentration and deposition time on the generated electrochemical signal obtained using 300 nM CR. The error bars represent the standard deviation from the mean. Each bar represents average data obtained from the same sample measured using at least 2 electrodes.*

3.4.2 Studying the Effect of Target Hybridization Time on the Generated Electrochemical Signal

A practical sensing device must be one that produces results in a rapid but reasonable time period, making hybridization time an important parameter. The kinetics of DNA strand displacement reactions are known to be very fast in solution but due to diffusion limiting steps and unfavorable conditions, slower at an interface.[159] Hybridization time was investigated for this sensor by immobilizing the ds probe and monitoring the generated signal from 50 nM CR* at different hybridization times (Scheme 3.3).

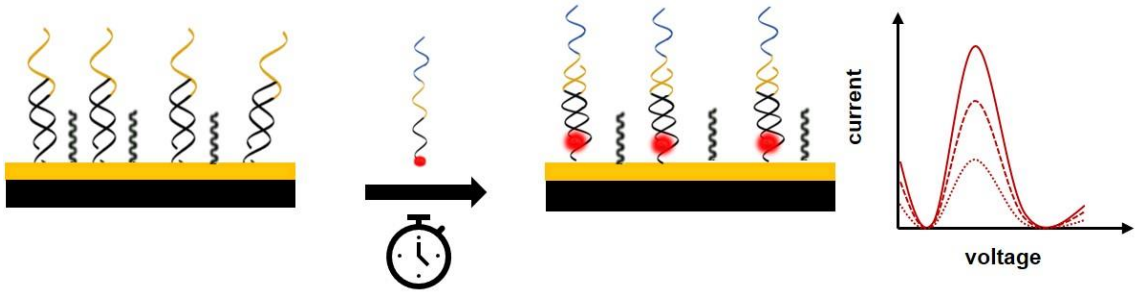

Scheme 3.3. Schematic of simplified assay used to determine the optimal target hybridization time. The single stranded target CR is incubated on an electrode prepared with capture probe CP:D1. Varying times will yield different electrochemical signal due to the number of target molecules that are captured.*

Figure 3.2 shows the results of this experiment where increasing signal peaks until 60 minutes can be seen. After 60 minutes, the signal decreased likely due to reverse reactions by the displaced D1 strand. In order to obtain optimal performance, a large signal generated in a short amount of time is quintessential. Since there was not a large difference between the signal obtained at 45 minutes and 60 minutes, a hybridization time of 45 minutes was used for all following experiments.

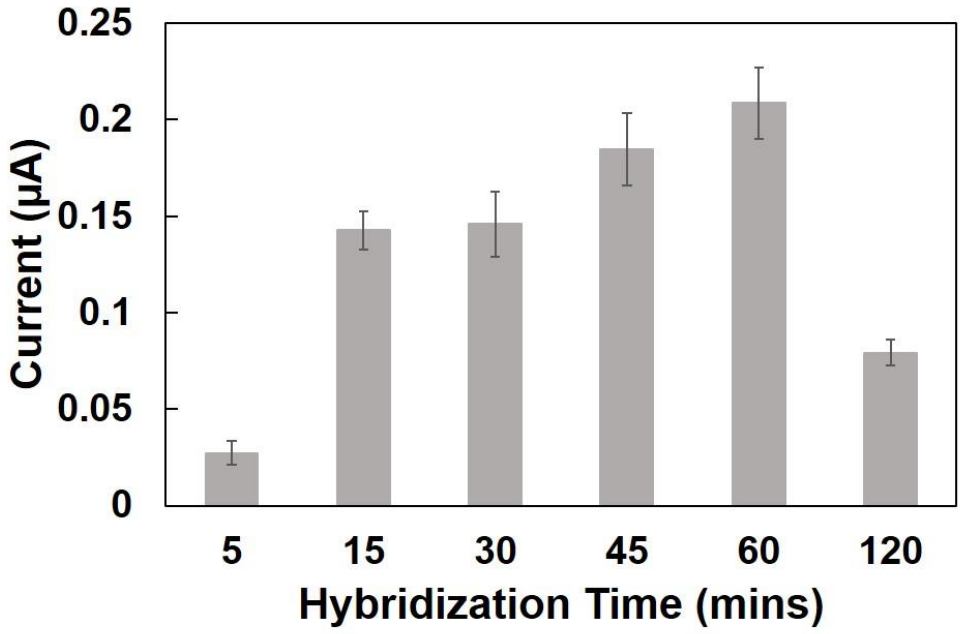

Figure 3.2. The peak electrochemical current in response to varying target hybridization times using 50 nM CR as the target. The error bars represent the standard deviation from the mean. Each bar represents average data obtained from the same sample measured using at least 2 electrodes.*

3.4.3 Studying the Effect of the Ratio of the T*C* Strand to the CR* Strand During Annealing for Preparation of Bio-barcode Containing Duplex on the Signal-to-blank Ratio

Decreasing background signal is crucial in obtaining a high SBR and pushing the LOD of a sensor to the lowest limit. In this designed assay, a partial duplex T*C*:CR* which contained the reporting strand CR* was in the assay mixture and could possibly contribute to a background signal if not properly hybridized. To make sure that the background was minimized, the ratio at which the duplex was annealed at was optimized. Annealing in the presence of excess T*C* results in a higher likelihood that all CR* is consumed but may also contribute to a lower generated signal. T*C* has complimentary regions to TB and B*C that could consume these strands, taking away from their participation in the reaction. For this reason, different ratios of 1:1, 1.1:1 and 1.2:1

T*C*:CR* were tested to see which produced the highest signal with the lowest background (Figure 3.3).

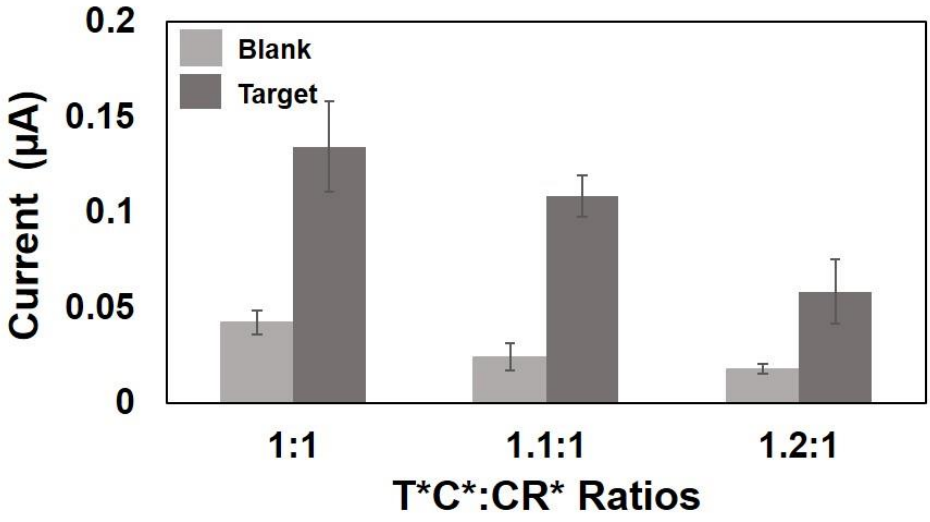

*Figure 3.3. Comparison of peak electrochemical current generated using varying annealing ratios for the preparation of assay intermediate duplex T*C*:CR* using 1 nM of TCcomp as the target. The error bars represent the standard deviation from the mean. Each bar represents average data obtained from the same sample measured using at least 3 electrodes.*

This was investigated using another simplified assay where the prepared sensor was challenged with a reaction mixture that contained 10 nM of T*C*:CR* at different ratios and a strand that was complementary to T*C* (TCcomp) at 1 nM, to mimic the formation of the TWJ and the release of the MB-labelled reporting barcode. The electrochemical signals that were obtained can be seen in Figure 3.3. In order to assess which ratio produced the best results the SBR was compared between each of the duplex ratio conditions. A ratio of 1:1 produced the largest signal and the largest background, while a ratio of 1.2:1 produced the lowest signal and lowest background, achieving SBRs that were 3.2 and 3.4 respectively. Conversely, a ratio of 1.1:1 produced a large signal while maintaining a low background, affording a SBR of 4.5. A ratio of

1.1:1 was used to prepare the T*C*:CR* duplex for all further parameter optimizations and investigation of the proposed sensor.

3.4.4 Studying the Effect of the Concentration of Assay Intermediates on the Signal-to-blank Ratio

Optimizations of the system have consisted of challenging the sensing electrode with a simplified version of the bio-barcode assay and have been focused on the release and on-chip capture of the MB-labelled bio-barcode. These aspects are fundamental within the assay and must be finely tuned before moving onto the more complex full protein capture assay. Since CR* release and on-chip hybridization conditions have been successfully optimized, further parameters of the e-biobarcode assay were investigated to ensure protein capture results in efficient release of CR*. Considerations of the full protein capture assay included intermediate strand concentrations, reaction temperature and reaction time. For the following optimization experiments, streptavidin was used as the protein target with biotin as the biorecognition element conjugated to both TB and B*C. The binding between this protein and small molecule is fast, almost irreversible and very well understood, making it an excellent biorecognition reaction to use as a model system for protein capture.[160]

The background signal produced from the MB-labelled reporter containing duplex (T*C*:CR*) was previously examined by comparing SBR produced from varying annealing ratios, but in the full e-biobarcode assay there are additional factors that can contribute to the background signal. The full assay contains two biorecognition motifs (TB and B*C) that must only hybridize in the presence of a protein target, driven by proximity as a result of binding the same protein target. This hybridization event between TB and B*C leads to the formation of a TWJ,

releasing CR*. Spontaneous formation of the unstable duplex may form between TB and B*C at higher concentrations without binding of the target protein, resulting in the formation of the TWJ and consequently the displacement of CR*, yielding a false positive signal. In order to prevent this, the concentration of the intermediates which include the biorecognition motifs (TB and B*C), and the MB-labelled reporter containing duplex (T*C*:CR*) was investigated (Scheme 3.4).

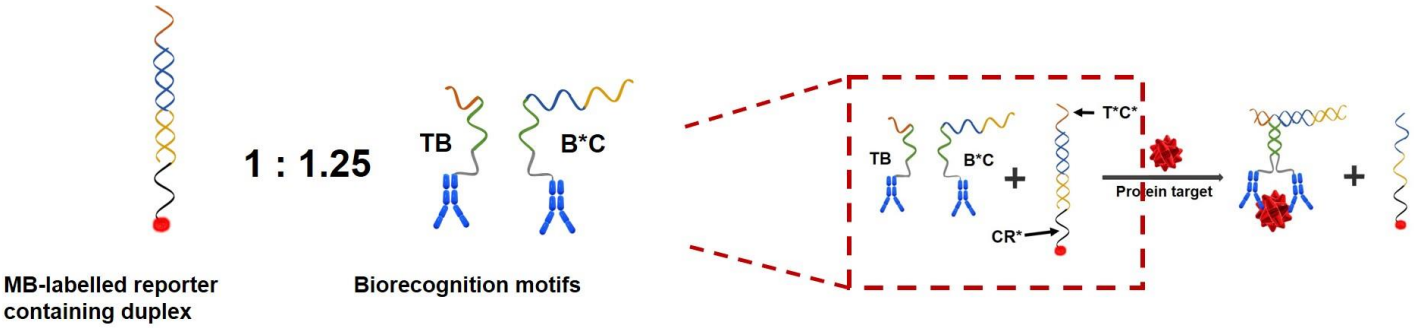

Scheme 3.4. Schematic demonstrating the intermediates that were optimized. The ratio of 1 duplex to 1.25 of each biorecognition motif is kept constant. The concentrations of each are varied through this experiment and used to detect a protein target.

The ratio of T*C*:CR* to TB and B*C had been previously optimized at 1:1.25, however the concentrations required needed to be determined. Concentrations of 1 nM : 1.25 nM, 10 nM : 12.5 nM, 20 nM : 25 nM, 60 nM : 75 nM and 100 nM : 125 nM were used to detect streptavidin at a concentration of 10 nM and the SBR was compared between each condition (Figure 3.4). A concentration ratio of 20 nM : 25 nM yielded the best results in terms of the largest SBR of 4.0. As the concentration of the intermediates increased to 60 nM : 75 nM and 100 nM : 125 nM, the signal produced increased, as did the blank signal resulting in SBRs that were 2.6 and 2.7, respectively. As the intermediate concentrations decreased below 20 nM : 25 nM, the blank signal decreased but the target signal also decreased, again resulting in a lower SBRs. Intermediate concentrations of 1 nM : 1.25 nM had a SBR of 3.3 while concentrations of 10 nM : 12.5 nM had

a SBR of 3.6. Achieving great sensitivity with a biosensor is heavily attributed to the SBR, therefore the intermediate concertation which produced the highest, 20 nM : 25 nM, was chosen for continued investigation of the proposed detection system.

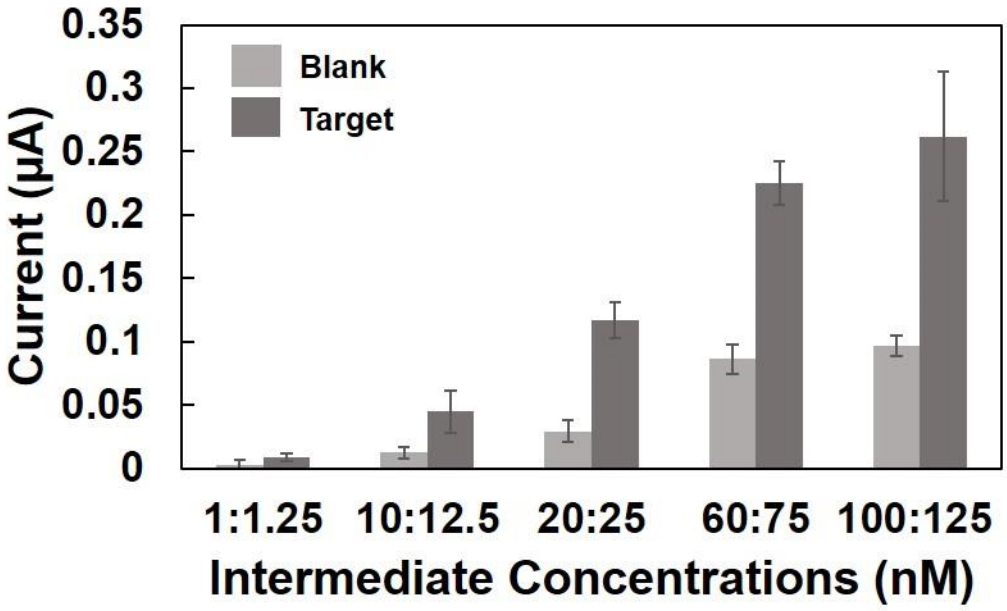

*Figure 3.4. Peak electrochemical current generated using the e-biobarcode assay with varying concentrations of assay intermediates. The concentration ratios on the x-axis represent the concentration of T*C*:CR* to TB* / BC* in nM respectively. These signals were obtained using 10 nM streptavidin in reaction buffer as the protein target. The error bars represent the standard deviation from the mean. Each bar represents average data obtained from the same sample measured using at least 3 electrodes.*

3.4.5 Studying the Effect of Introducing a Protein Capture Reaction Step at 37°C on the Signal-to-blank Ratio

An important consideration that influenced the design of this sensing platform was minimizing the number of wash and reaction steps in order to demonstrate sample-in-answer-out protein detection. A large limitation of many detection systems is the sequential addition of each component onto the sensing surface leading to many reaction and wash steps. To circumvent this, protein recognition with TB and B*C, and the release of MB-labelled CR* was done in the same

solution followed by on-chip hybridization that required a single deposition step. Timing of this intermediate protein capture step was optimized in order to maximize the amount of protein capture, and thus released CR*, while minimizing time requirements to maintain practicality. Incorporating a reaction step was investigated by comparing the generated electrochemical signal obtained when the sample and all intermediates were mixed and immediately placed on electrode for hybridization with the signal obtained when 30 minutes was allotted for the reaction of TB, B*C and streptavidin before adding T*C*:CR* and depositing onto the electrode. This reaction period was done at 37°C in order to increase the kinetics of the strand displacement reactions. Upon the introduction of a reaction step done for 30 minutes at 37°C, the SBR increased from the previous 4.0 to 4.3. While this was not a significant increase in the SBR, the increase that can be seen in the peak signal obtained from the 10 nM streptavidin target was encouraging enough to continue with the addition of this step (Figure 3.5). The extremely rapid interaction that occurs between streptavidin and biotin is likely the cause of the small change in the SBR obtained from increasing the reaction time and temperature, however, the goal of the sensor is application towards detection of PSA. The interaction between anti-PSA and PSA is not as efficient as the biotin-streptavidin interaction, likely making this additional reaction period extremely important for demonstrating sensitive PSA detection. For these reasons, a 30-minute reaction time at 37°C was continually used for the optimizations to follow.

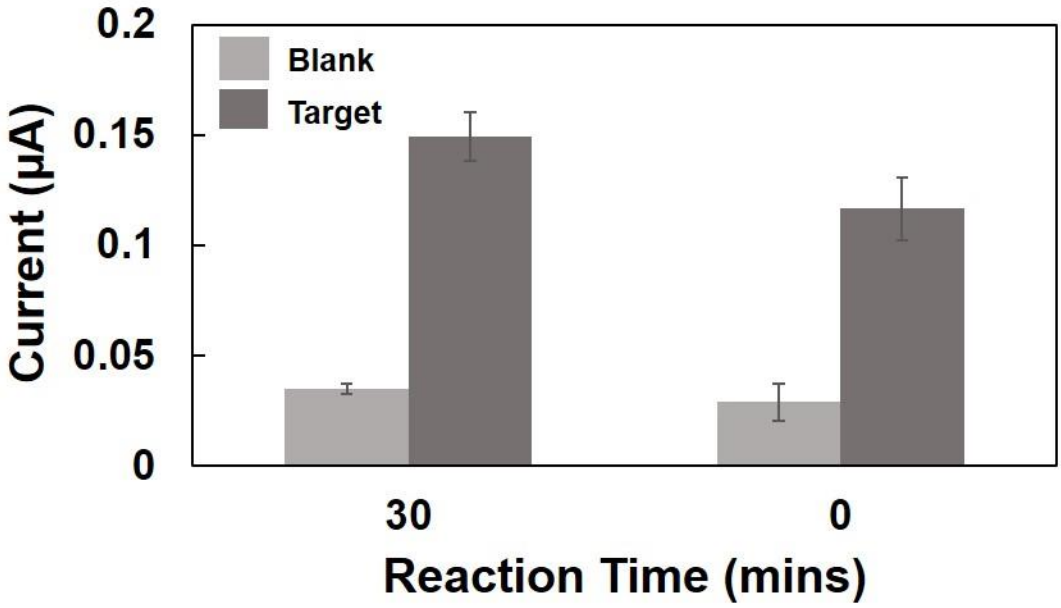

Figure 3.5. Peak electrochemical current generated using the e-biobarcode assay in response to 10 nM streptavidin in reaction buffer with and without a 30-minute reaction step performed at 37℃. The error bars represent the standard deviation from the mean. Each bar represents average data obtained from the same sample measured using at least 3 electrodes.

3.4.6 Studying the Effect of Poly A as a Surface Blocker on the Generated Electrochemical Signal

When investigating the full protein capture assay, minimizing the blank signal was also approached from another perspective. Biomolecules are known to non-specifically adsorb onto electrode surfaces, interfering in the peak current that is obtained.[161] This interference from biomolecules can occur in one of two ways; either the non-specific adsorption causes an increase in blank signal through the adsorption of the reporting molecule due to the affinity between the nucleotides and the surface[162], or it can cause a decrease in overall signal by formation of an insulating layer that prevents target diffusion or electron transfer.[163] In buffer, it is hypothesized that the non-specific adsorption interferes with the peak current following the former mechanism, while in a complex matrix, such as human plasma, with many interfering proteins and small

molecules, the latter is more prominent. In either case, it is extremely important to explore a method of preventing non-specific adsorption on the electrode in order to obtain the most efficient biosensor possible. The effect of a surface blocker was investigated using a 20-mer poly-A sequence, which worked to prevent non-specific adsorption through strong interactions with gold owing to NH_2-gold bonding.[35] It is believed that the small biomolecule adsorbs onto bare gold, causing the surface to have a slight negative charge, preventing the adsorption of other biomolecules. Poly-A was introduced into the reaction by depositing it onto the electrode for 30 minutes, prior to deposition of the reaction mixture, in excess to assume complete coverage of exposed gold (Scheme 3.5).

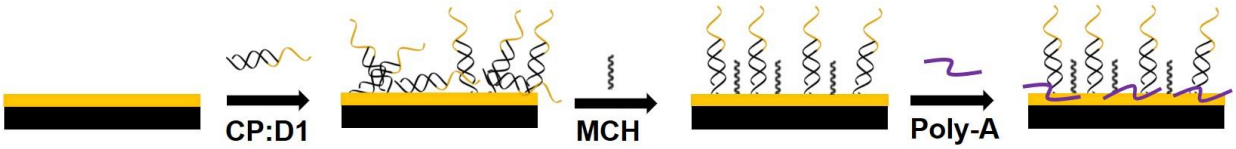

Scheme 3.5. Schematic demonstrating each step of preparing the sensing electrode with poly-A as a surface blocker. The capture probe CP:D1 is deposited followed by a MCH backfill for probe aligning and removal of non-specifically adsorbed probe. Poly-A is then deposited prior to use to block any exposed gold.

The detection results using 10 nM streptavidin with and without 1 µM poly-A can be seen in Figure 3.6. In buffer, poly-A slightly reduced the blank signal and increased the target signal obtained minimally. However, these results indicate that a more prominent effect will likely be seen when performing protein detection in a more complex sample matrix.

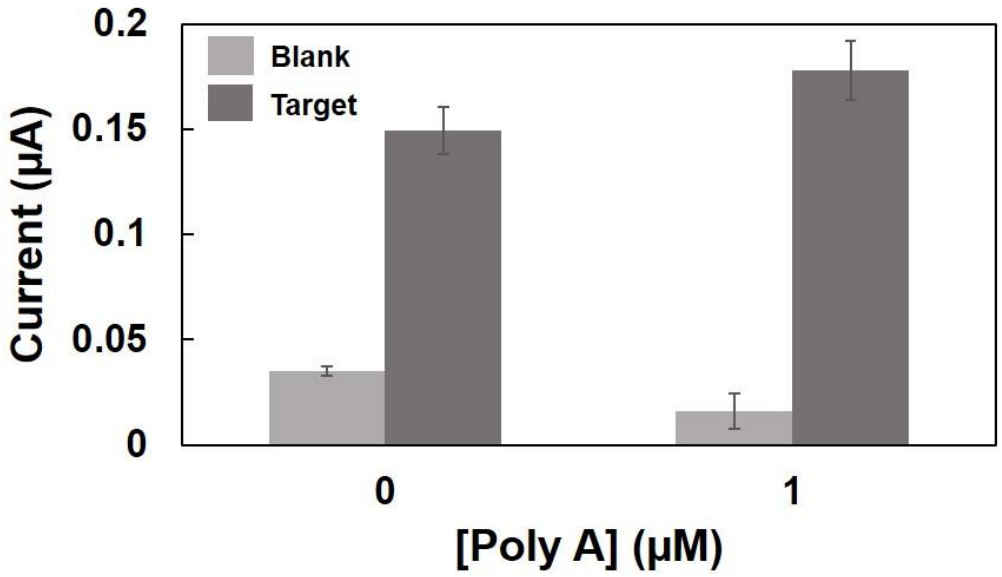

Figure 3.6. Comparison of the peak electrochemical current that is generated using the e-biobarcode assay in response to 10 nM streptavidin in reaction buffer with and without 1 μM poly-A for surface blocking. The error bars represent the standard deviation from the mean. Each bar represents average data obtained from the same sample measured using at least 3 electrodes.

3.4.7 Studying the Effect of Human Plasma Dilution on the Total Electrochemical Signal Loss

Demonstrating practicality of a detection system requires performance in a complex clinical sample such as human blood, plasma, serum or urine. Knowing that the e-biobarcode assay was going to be applied to the detection of PSA, the practicality was investigated by optimizing the design for use in human plasma. Many assays reach ultra-low sensitivities in clinical samples but commonly require dilution steps to prevent interference. As stated previously, it is believed that the adsorption of molecules in complex samples creates an insulating layer on the electrode surface that inhibits signal generation and to circumvent this poly-A was employed as a surface blocker. The usefulness of this surface blocked was challenged by investigating if, or how much, dilution of human plasma was required to obtain a signal from CR*. CR* was suspended in human plasma that had been diluted 2x, 4x, x, 8x and undiluted at a concentration of 20 nM and the

obtained signal was recorded (Figure 3.7). While the signal magnitude does decrease as expected, there is not a significant difference between undiluted and diluted plasma. Since performance in undiluted plasma would translate to no sample preparation, and the generated current was not greatly influenced, undiluted plasma was chosen for experiments to demonstrate practicality.

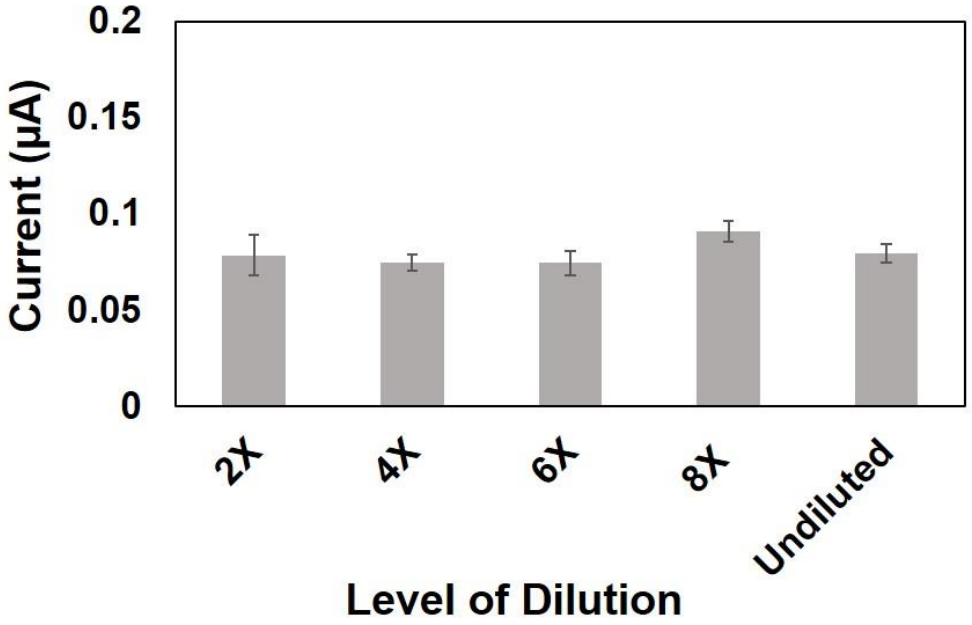

Figure 3.7. Comparison of the peak electrochemical current generated from 20 nM CR in human plasma that has been diluted at varying levels. The error bars represent the standard deviation from the mean. Each bar represents average data obtained from the same sample measured using at least 3 electrodes.*

3.5 Conclusion

In this chapter, optimizations were done towards the development of a protein biosensor using streptavidin/biotin binding as a model system. The optimizations that were performed in this chapter are going to be applied in the next chapter for evaluating the analytical ability and practicality of the sensor towards a real cancer protein biomarker. The conditions that were optimized include probe density, hybridization time, preparation conditions for assay

intermediates, concentration of assay intermediates, the effect of an incubated reaction step, surface blocking with poly-A, and sample processing.

Probe density is one of the most critical factors affecting efficient capture of the release bio-barcode at the electrode surface. The effect of probe density was studied by depositing three different concentrations of capture probe (0.25 µM, 0.5 µM and 1 µM) on the electrode surface all for varying deposition times (2, 4, 8, 16 and 24 hours). The effect of the varying conditions was evaluated by measuring the current generated from the MB-labelled bio-barcode (CR*) hybridizing with the immobilized capture probe using SWV. For this study 300 nM of CR* was used as the target concentration. The results showed an overall increase in generated current for the increasing deposition times, until 16 hours where the current plateaued. The results also showed that a concentration of 0.5 µM of probe produced the highest currents at all deposition times. The optimal condition was found to be depositing 0.5 µM of probe for 16 hours. The increasing generation of current over the increasing time periods to a plateau was expected as the electrode should eventually reach saturation. At this point, the amount of probe on the surface should be enough to ensure capture but not crowd the electrode resulting in steric hindrance.[158] We expected that the highest probe concentration would result in the crowding effect, and that the lowest probe concentration may not be sufficient for generating a large electrochemical signal.

In addition to probe density, we investigated how increasing the hybridization time of the released bio-barcode effected electrochemical signal generation. This study was performed by detecting 50 nM of the MB-labelled bio-barcode (CR*) on the electrode surface after depositing the target solution on the sensing electrode and varying incubation times (5, 15, 30, 45, 60 and 120 minutes). The resulting trend was an increase of electrochemical signal corresponding to increasing incubation times until 120 minutes where the signal significantly decreased (over 50%).

The increasing trend observed until 60 minutes was expected as an increasing incubation time allows more CR* to hybridize with capture probe, however the significant decrease in signal at 120 minutes was not expected. We hypothesize that since the capture of the bio-barcode was dependant on a strand displacement reaction with the ds capture probe, the excess of time may have permitted the reverse reaction to occur, displacing CR*. The optimal time chosen for target hybridization was 45 minutes since a sufficient electrochemical signal was measured and the difference in signal between 45 and 60 minutes was not large enough to justify the additional time.

Within the detection assay there were two main components – the biorecognition motifs TB and B*C, and the bio-barcode containing duplex T*C*:CR*. Preparing the bio-barcode duplex required annealing T*C* with CR* so that there was no free CR*, which had the MB label, in the assay solution. To ensure that a small blank signal was obtained when there was no protein target in the sample (thus increasing the SBR) the ratio at which T*C* was annealed to CR* was investigated. This was done by varying the ratio of the T*C* strand to the CR* during the annealing process. Annealing conditions were kept constant while the ratios varied from 1:1, 1.1:1 and 1.2:1 T*C*:CR*. The effect of the annealing ratio was studied using one "target" solution containing 20 nM of T*C*:CR* and 1 nM of a strand complementary to T*C* (TCcomp), and one "blank" solution containing 20 nM of T*C*:CR*. The electrochemical signal that was generated for both the target and blank solution was measured on separate electrodes using SWV and the SBR was calculated. The trend that was observed was a decrease in both the target and blank signal for the increasing amount of T*C* compared to CR* and the largest SBR of 4.5 was calculated for an annealing ratio of 1.1:1. This trend was expected as excess T*C* will ensure that all CR* is consumed, decreasing the blank signal. However, once all the CR* has been hybridized the

remaining T*C* can hybridize TCcomp. This reaction with excess T*C* will result in TCcomp consumption without the release of CR*, resulting in lower target signals.

The concentration of assay intermediates was optimized to ensure that the release of CR* was only caused by binding of the protein target by the biorecognition motifs and not by spontaneous formation of the TWJ. Spontaneous formation can happen if the concentration of the assay components is too high, leading to an increased blank signal. The effect of assay intermediate concentration was studied by varying the concentration of both the bio-barcode containing duplex T*C*:CR* and the biorecognition motifs TB and B*C and calculating the SBR using 10 nM of streptavidin as the protein target. The ratio of the bio-barcode containing duplex to the recognition motifs was kept constant at 1:1.25 (T*C*:CR* : TB/B*C) but the concentration of the components was varied (1 : 1.25 nM, 10 : 12.5 nM, 20 : 25 nM, 60 : 75 nM and 100 : 125 nM). As expected, an increase in current generated using a target solution correlated directly to an increase in intermediate concentrations, as did the blank solution. The optimal concentration was found to be 20 nM T*C* and 25 nM TB/B*C as it produced the highest SBR of 4.0.

Optimizing protein capture in solution was achieved by investigating the results of a reaction incubation period. To do this, sample solution that contained 10 nM of streptavidin was added to the assay intermediates and incubated at 37°C for 30 minutes. After the incubation, the solution was deposited on to the electrode surface and the electrochemical signal generated was measured. The SBR was compared between two tests, one done with the additional reaction step and one performed without. The introduction of the reaction step increased the SBR, however less than we expected (increase from 4.0 to 4.3). The information that was gathered from this experiment indicated that the reaction step enhanced protein capture but did not impact the blank solution. The binding of streptavidin to biotin is extremely rapid and we hypothesized that while

this interaction was not greatly enhanced during this step, a less efficient interaction could be. In addition, the little impact it had on the blank indicated that when using a less efficient protein capture method (antibody/antigen) for PSA detection this step would be useful for increasing the SBR.

On-chip hybridization was also optimized by studying the ability of poly-A to act as a surface blocker. The effect of poly-A was investigated by performing protein capture in solution and then transferring the solution to both electrodes prepared with 1 µM of poly-A on the surface and without poly-A on the surface. The current generated from 10 nM of streptavidin in buffer was measured and compared between the two conditions. The electrode with poly-A on the surface showed a slight decrease in blank signal and a slight increase in target signal compared to the electrode with no surface blocker. It is expected that when working with a more complex matrix such as a biological sample 1 µM of poly-A could be used as an effective surface blocker.

Protein rich biological fluid such as plasma is notorious for causing electrochemical signal loss. To ensure that our sensor would be able to perform in a clinically-relevant fluid we first optimized the level of dilution that would need to be done to the biological sample. This was performed using human plasma diluted 2, 4, 6, and 8 times, as well as an undiluted sample. The effect that interfering molecules had on MB-labelled bio-barcode capture and electrochemical signal generation was investigated by spiking 20 nM of CR* into the human plasma at the varying levels of dilution and measuring the current generated. As expected, the generated current was less than previously observed in buffer however, it did not significantly vary for all dilution levels, including the undiluted sample. This result was surprising but demonstrated that if protein capture in solution lead to the release of the bio-barcode, the assay could be performed in unprocessed and undiluted human plasma.

Chapter 4: Bio-barcode Assay for the Electrochemical Detection of PSA

4.1 Preface

The focus of this chapter is to demonstrate the successful performance of the designed bio-barcode assay towards electrochemical detection of a protein cancer biomarker. A brief introduction on electrochemical protein biomarker detection will be reiterated, and an insight into the enhanced performance of bio-barcode assays will be given. The analytical ability of the designed sensor will be covered focusing on PSA detection both in buffer and undiluted human plasma. The practicality and specificity of the proposed sensor will be discussed and performance metrics such as LOD will be highlighted.

Multiple authors have contributed to this work as it has been prepared for publication under the title "Dynamic bio-barcode assay enables electrochemical detection of a cancer protein biomarker in undiluted human plasma using a sample-in-answer-out approach" in Angewandte Chemie International Edition. Sarah Traynor performed all electrochemical experiments and wrote the article. Both Sarah Traynor and Alex Guan performed fluorescence experiments, and Alex Guan contributed to writing. Richa Pandey contributed to editing and made scheme 4.1.

4.2 Introduction

Sensitive and accurate protein analysis is critical to disease diagnostics, monitoring, and management.[164] The existing laboratory-scale instruments for protein analysis do not allow for frequent screening and monitoring of patients at primary healthcare settings, patient bedsides, or home settings mainly due to their high cost and complex operating protocols for non-technical users.[3] To develop a point-of-care (POC) protein analyzer, major research efforts are targeted

toward developing sensitive and specific biosensors that parallel the handheld glucose monitor in terms of ease-of-operation, response time, and operating and equipment cost.[165]

Electrochemical readout is ideally-suited for POC protein biosensing because it offers high detection sensitivity with rapid readout and is compatible with low-cost and miniaturized readout circuitry.[166] However, most electrochemical protein biosensors fail to operate in a sample-in-answer-out (SIAO) manner, especially when they are challenged with *unprocessed* clinical samples.[167] This difficulty stems from the dependence of these assays on multiple steps involving washes, target labeling, and the addition of reagents to process the sample and amplify and transduce a signal.[168,169]

Programmable *DNA-based* assays – target-responsive structure switching assays (DNAzymes and apatamer),[170] proximity-dependent surface hybridization assays[171–173] proximity ligation assays (PLA),[174] and nucleic acid programmable protein arrays (NAPPA)[175] – have been used to integrate protein capture with built-in signal transduction to eliminate the need for multi-step processing.[20] Among these methods, bio-barcode assays that generate a nucleic acid barcode in response to protein recognition hold great promise for simplifying protein analysis.[21] In spite of this, the common employment of loaded nanoparticles (NPs)[176] or enzymes[177] for amplifying the nucleic acid reporter, makes single-step operation using these assays challenging.

Combining the simplicity of a bio-barcode assay with the sensitivity of electrochemical readout offers tremendous potential for developing sensitive and specific, yet simple POC biosensors. Bio-barcode assays can be programmed to perform specific protein capture in solution, followed by the release of a short and fast-diffusing DNA barcode, thus eliminating the mass transport and steric hindrance issues encountered in surface-based protein biosensors.[178]

Additionally, since these assays have a built-in mechanism for releasing signal transducing probes, they can eliminate the need for the manual addition of reagents.[151]

With the vision of creating a SIAO electrochemical bio-barcode assay (e-biobarcode assay) for analysing clinical samples, we integrated: (1) a proximity-induced bio-barcode assay, designed for electrochemical signal transduction using one-pot operation[152], with (2) electrochemical readout using three dimensional nanostructured electrodes, optimized for enhanced sensitivity,[31,32] and (3) a surface coating of poly adenine (poly-A), used for reducing non-specific adsorption and biofouling (Scheme 4.1). The unique combination of these components enabled us to perform protein analysis in undiluted human plasma samples in a SIAO manner without the need for sample processing.

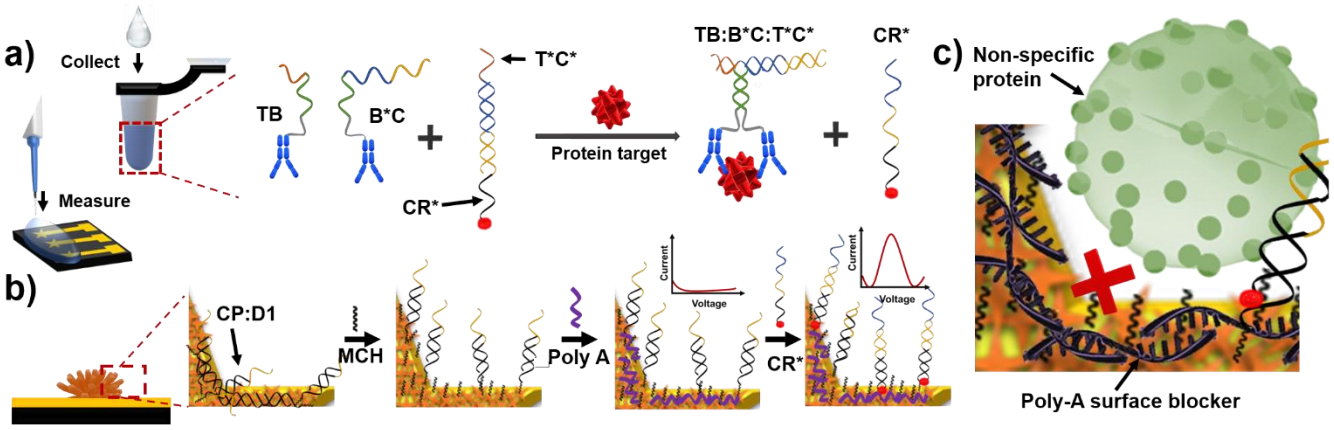

*Scheme 4.1 Schematic illustration of the operating principles and the components of the bio-barcdoe assay a) The sample is introduced into the assay vial (collect) and a drop of the sample/reagent mix (measure) is taken and placed on the electrochemical chip for measurement. Inside the assay vial, the antibody-modified DNA motifs TB and B*C bind the same protein target, inducing hybridization at a short complementary region (green region) initiating the formation of a three way junction with the exposed region of T*C*, releasing redox-labelled CR* from the T*C*:CR* duplex through toehold mediated strand displacement. b) on-chip hybridization of the redox-labelled bio-barcode: thiol binding immobilizes a partially complementary double-stranded capture probe CP:D1, followed by the addition of MCH for probe alignment and surface blocking. The released barcode displaces D1 from the CP:D1 immobilized duplex via toehold mediated strand displacement bringing the redox tag near the electrode surface, inducing an electrochemical signal. c) prevention of non-specific adsorption using poly-A as a surface blocker: after immobilization of CP:D1 and MCH, poly-A is deposited and adsorbed through adenine-gold interactions, preventing non-specific adsorption of biomolecules such as proteins found in clinical samples.*

4.3 Experimental

4.3.1 Materials

Magnesium chloride ($MgCl_2$, ≥99.0%), sodium chloride (NaCl, ≥99.0%), phosphate buffer solution (1.0M, pH 7.4), 6-mercapto-1-hexanol (MCH, 99%), tris(2-carboxyethyl)phosphine hydrochloride (TCEP), potassium hexacyanoferrate(II) trihydrate ($[Fe(CN)_6]^{4-/3-}$, ≥99.95%), gold(III) chloride solution ($HAuCl_4$, 99.99%), 100X tris-EDTA (TE, pH 7.4), 10X tris borate-ETDA (TBE, pH 8.3), Tween 20, bovine serum albumin (BSA), streptavidin from *Streptomyces avidinii*, biotin, prostate-specific antigen from human semen (PSA), glial fibrillary acidic protein from human brain (GFAP), were purchased from Sigma-Aldrich (Oakville, Canada). Biotinylated human kallikrein 3/PSA polyclonal antibody (goat IgG) and biotinylated normal goat IgG control was purchased from R&D Systems (Minneapolis, MN). SYBR gold nucleic acid gel stain, DNA gel loading dye (6X), acrylamide solution (40%), ammonium persulfate (APS), 10X sterile phosphate buffer saline (PBS, pH 7.4) and tetramethylethylenediamine (TEMED) were purchased from Thermo Fisher Scientific (Mississauga, Canada). Sulfuric acid (H_2SO_4, 98%) and 2-propanol (99.5%) were purchased from Caledon Laboratories (Georgetown, Canada). Ethanol was purchased from Commercial Alcohols (Brampton, Canada). Hydrochloric acid (37% w/w) was purchased from LabChem (Zelienople, PA). Human plasma was donated by the Canadian Plasma Resources (Saskatoon, Canada). All reagents were of analytical grade and were used without further purification. Milli-Q grade ultrapure water (18.2 MΩ·cm) was used to prepare all solutions and for all washing steps. Methylene blue modified sequences were purchased from Biosearch Technologies (Novato, CA) and purified by dual high-performance liquid chromatography (HPLC). All other DNA samples were purchased from Integrated DNA Technologies (Coralville, IA) and purified by HPLC.

4.3.2. DNA sequences

Table 1. All DNA sequences used within thesis written from 5' – 3'.

Sequence Name	Sequence 5' – 3'
TB	*Biotin*-TTTTTTTTTTTTTTTGTGAGGTTCGTGTGATG
B*C	AAGCGTGTATCCCATGTGTCCCTCACTTTTTTTTTTTTTTT-*biotin*
T*C*	CATCACACGGACACATGGGATACACGCTT
CR*	*MB*-TCTTCCAATCAGTCTCTCAAGCGTGTATCCCATGTGTC
D1	TCTTCCAATCAGTCTCTCAA
CP	TACACGCTTGAGAGACTGATTGGAAGA-*SH*
Poly-a	AAAAAAAAAAAAAAAAAAAAA
FAM-CP	TACACGCTTGAGAGACTGATTGGAAGA-*FAM*
IOWA Black-D1	*IOWA Black*-TCTTCCAATCAGTCTCTCAA
TCcomp	GTAGTGTGCCTGTGTACCCTATGTGCGAA

4.3.3. Duplex preparation for the bio-barcode assay

The barcode containing duplex T*C*:CR* was prepared at a final concentration of 10 µM by mixing 10 µL of T*C* and 12 µL of CR*, each at an initial concentration of 50 µM, in 28 µL of annealing buffer (1x TE, 10 mM $MgCl_2$, 0.05% Tween20). The mixture was heated to 90°C for 5 minutes and then the solution was brought to 25°C inclemently over 30 minutes. The fluorescent capture beacon was prepared at a final concentration of 10 µM by mixing 10 µL of FAM labelled CP with 15 µL of IOWA Black labelled D1, each at an initial concentration of 50 µM in 25 µL of annealing buffer. The mixture was heated to 90°C for 5 minutes and then the solution was brought to 25°C incrementally over 30 minutes. The same procedure was followed for the thiolated capture probe used for all electrochemical detection; 10 µL of CP was mixed with 15 µL D1, each at an initial concentration of 50 µM, in 25 µL annealing buffer. The mixture was heated to 90°C for 5 minutes and then the solution was brought to 25°C incrementally over 30 minutes.

4.3.4. Recognition probe preparation

DNA probes for detection of PSA were prepared following a previously published protocol.[152] Briefly, 25 uµL of 2.5 µM TB or B*C was mixed with 25 µL of 3 µM streptavidin (both diluted in 1X PBS containing 0.01% BSA) and incubated at 37°C for 30 minutes, followed by 30 minutes at 25°C. 50 µL of biotinylated anti-PSA prepared in 1X PBS was added to the mixture and incubated for 1 hour at 25°C followed by 2 hours at 4°C. The recognition probes were then diluted with 150 µL of biotin solution (1X TE, 1 mM biotin, 0.01% BSA) to 250 nM and left at 4°C overnight.

4.3.5. Preparation of the sensing surface

Pre-stressed polystyrene substrates (Graphix Shrink Film, Maple Heights, OH) were cleaned with ethanol, DI water, and then dried with air. Following the solvent cleaning step, a vinyl mask (BDF Graphics, Toronto, Canada) was put on the PS substrate and the electrode design was cut into the mask using a CraftRobo Pro (Graphtec, Tokyo, Japan). The mask was then removed from the portion of the working electrode space and gold was sputtered onto the surface using a Torr (DC/RF). The gold sputtered electrodes were then prepared for probe deposition by first electrochemically cleaning by running reversible CV scans in 0.5 M H_2SO_4 from 0 – 1.6 V at a scan rate of 0.1 V/s until the reduction peak was stable (Chapter 4 Appendix, Figure 4.6). The electrodes were then held at a high potential of 1 V For 10 seconds, followed by a low potential of -1 V for 10 seconds. The pre-annealed thiol modified probe (CP:D1) was reduced at a final concentration of 500 nM using a 50 mM TCEP solution in deposition buffer (25 mM phosphate buffer solution, 25 mM NaCl, 100 mM $MgCl_2$) for 2 hours in the dark at room temperature. After reduction, 3 µL of reduced probe solution was dropped on the surface of the clean working

electrode and left in the dark at room temperature for 16 hours. Non-specifically adsorbed probe was then washed using washing buffer (25 mM phosphate buffer solution, 25 mM NaCl) and a CV scan was performed from 0 – 0.5 V in 2 mM $[Fe(CN)_6]^{4-/3-}$ to ensure immobilization (Chapter 4 Appendix, Figure 4.7). A MCH backfill was done using 100 mM MCH for 20 minutes, followed by another CV scan in 2 mM $[Fe(CN)_6]^{4-/3-}$ to ensure both removal of non-specifically adsorbed probe, and aligning of specifically adsorbed probe, with washing between each step. 3 µL of 1 µM poly-A was deposited onto the surface of the electrode for 30 minutes at room temperature. The drop was removed using a KimWipe, but the electrode was not washed. The electrode was then ready for electrochemical detection experiments. All electrochemical experiments were carried out on a CHI 420b with a three-electrode set-up with a gold electrode as the working, a Ag/AgCl as the reference and a platinum wire as the counter.

4.3.6. Fluorescence validation assay

For verification that a signal could be induced through recognition of the released bio-barcode, 10 µL of 100 nM streptavidin was mixed with 10 µL of 250 nM TB, 10 µL of 250 nM of B*C, 10 µL of 200 nM T*C*:CR* and 60 µL reaction buffer (1X PBS, 10 mM $MgCl_2$, 0.05% Tween 20) and incubated at 37°C for 30 minutes. A blank solution was prepared by adding 10 µL of buffer in place of streptavidin. After incubation an 81 µL volume was put into a well of a 96-well plate. A 9 µL solution of the FAM/IOWA Black labelled CP:D1 capture beacon was added to the well and fluorescence was immediately measured every minute for 60 minutes. All experiments were done in duplicates.

4.3.7. Verification of complex DNA structure formation using native PAGE

All sequences were prepared at a concentration of 1 µM with reaction buffer. For target analysis, a reaction mixture containing 1.25 µM TB, 1.25 µM B*C, 1 µM T*C*:CR* and 1 µM streptavidin was prepared with reaction buffer. For the blank analysis, reaction buffer was used in place of streptavidin. The reaction mixture was incubated for 30 minutes at 37°C and then all samples were mixed in a 5:1 ratio with loading dye and loaded into a freshly prepared 10 % gel. A voltage of 80 mV was applied to the gel until separation was achieved. After separation, the gel was submerged in a 10000x dilute SYBR Gold solution for 40 minutes and then imaged on a Chemidoc MP.

4.3.8. Electrochemical validation assay

To verify that protein detection could be performed using electrochemical analysis, 10 µL of varying streptavidin concentrations was mixed with 10 µL of 250 nM TB, 10 µL of 250 nM of B*C, 10 µL of 200 nM T*C*:CR* and 60 µL of reaction buffer. A blank solution was prepared by adding 10 µL of reaction buffer in place of streptavidin. The solution was incubated at 37°C for 30 minutes. After incubation the solution was mixed and 3 µL of the reaction solution was deposited onto the prepared sensing electrode and the electrode was placed in a humidity chamber for incubation at 37°C for 45 minutes. The electrode was then washed with washing buffer and SWV was performed from 0 – (-0.5) V in washing buffer. The LOD was calculated using the linear regression equation of the most linear region and the (LOB) which is defined as the highest signal obtained in response to a solution that is void of target analyte. [179] This method of LOD calculation was done to take into consideration the peak current that is produced via non-specific interactions within a blank solution and was used for all subsequent protein quantification. All experiments were done in triplicates.

4.3.9. Electrochemical quantification of PSA

For the detection of PSA in PBS and undiluted human plasma, 10 µL of varying PSA concentrations was mixed with 10 µL of 250 nM antibody conjugated TB, 10 µL of 250 nM antibody conjugated B*C, 10 µL of 200 nM T*C*:CR* and 60 µL of either the reaction buffer or undiluted plasma. A blank solution was also prepared by adding 10 µL of either reaction buffer or undiluted plasma in place of PSA. The solution was incubated at 37°C for 30 minutes followed by depositing 3 µL of the solution onto the prepared sensing electrode and the electrode was then placed in a humidity chamber and incubated at 37°C for 45 minutes. The electrodes were then washed in washing buffer and SWV was performed from 0 – (-0.5) V in washing buffer. All experiments were done in triplicate.

4.3.10. Nanostructuring of the planar electrodes

A 10 mM $HAuCl_4$ solution was prepared by mixing 30 mL of 0.5 M HCl with 207.9 µL of stock $HAuCl_4$, followed by degassing with nitrogen for 20 minutes. Planar electrodes were cleaned by rinsing in isopropanol and DI water. The clean planar electrodes were then held at a potential of -0.7 V for 600 seconds in the degassed 10 mM $HAuCl_4$ solution. The electrodes were then rinsed with DI water and stored for later used at room temperature.

4.3.11. Determining specificity of the bio-barcode assay

For antibody specificity experiments, control recognition probes (TB and B*C) that were not specific for PSA biorecognition were prepared following the previous protocol (4.3.4) using normal goat IgG control in place of anti-PSA. Electrochemical protein detection was done using

10 µL of 250 nM control TB, 10 µL of 250 nM control B*C, 10 µL of 200 nM T*C*:CR*, 10 µL of 10 ng mL^{-1} PSA and 60 µL of reaction buffer.

4.3.12. Studying the effect of poly-A on generated electrochemical signal

To investigate the affect of poly-A on signal generation, the same protocol was followed for preparation of the sensing surface, except deposition of poly-A was omitted. The same steps for electrochemical PSA detection using anti-PSA conjugated recognition probes were followed using 10 µL of 250 nM TB, 10 µL of 250 nM B*C, 10 µL of 200 nM T*C*:CR*, 10 µL of 100 ng mL^{-1} IL-6 or 10 µL of 100 ng mL^{-1} GFAP and 60 µL of reaction buffer. GFAP and IL-6 were prepared using 1X PBS.

4.3.13. Electrochemical experiments

All electrochemical experiments were performed on a CHI 420b using a three-electrode set up with a Au working electrode, a Ag/AgCl reference electrode and a platinum wire counter electrode. Detection experiments were performed using SWV scanning from 0 – (-0.5) V with a step potential of 0.001 V, an amplitude of 0.025 V and a frequency of 60 Hz.

4.4 Results and Discussion

4.4.1 Validation of the Bio-barcode Assay

In order to validate the designed bio-barcode method, we first verified that protein binding triggers the release of a barcode DNA strand *via* a real-time fluorescence assay and using

streptavidin as a model protein target. Streptavidin was captured using the biotin molecules (K_d = 10^{-15})[160] modified at the 5'- and 3'-end of TB and B*C DNA motifs, respectively. TB and B*C were specifically designed to contain a six base pair long complementary region (green domain in Figure 4.1a) that does not form a stable duplex at room temperature. Recognition of the same streptavidin molecule by both sequences forces them to come closer together, hybridize, and form a DNA/protein complex (Figure 4.1a). Hybridization of the toehold region in T*C* (red domain) to the exposed single stranded regions of the TB:B*C duplex allows for strand displacement, resulting in the release of CR*. In the following signal generation step, a fluorophore(CP)- and quencher(D1)-labeled partial DNA duplex probe (CP:D1) was utilized, in which the released reporter CR* displaces the quencher strand, generating a fluorescence signal. Using this assay design, the fluorescent signal was measured in the presence and absence of the target analyte . At 20 minutes, a signal-to-blank ratio of 13.5 was measured (Figure 4.1b), indicating a robust and rapid assay with little interference from unbound biorecognition elements. The successful formation of the designed DNA structure and the release of the barcode were further verified using native polyacrylamide gel electrophoresis PAGE (Chapter 4 Appendix, Figure 4.4).

After demonstrating that the bio-barcode assay is capable of generating the designed products using fluorescence, we integrated it with electrochemical readout. Our electrochemical assay performs protein capture in solution, followed by on-chip hybridization of the released barcode at the electrode surface. This design enables the most critical step of protein capture to occur in solution, circumventing the diffusion and steric hindrance limitations that are encountered in surface-based antibody/protein binding.[180–182]

We re-engineered the assay for electrochemical readout by immobilizing the capture probe (CP:D1 complex) on the electrode surface, eliminating the quencher and fluorophore needed in

the fluorescent assay, and modifying the CR* strand with an electrochemical reporter (methylene blue (MB)). The 3D nanostructured gold electrode used for electrochemical signal transduction was functionalized with three molecular layers designed to capture the desired target (capture probe, CP:D1) and repel the biological background (mercaptohexanol (MCH) and poly-A). The result was an SIAO system where the sample was introduced into a vial containing the reaction mix, followed by adding a drop of that solution to the chip, where the electrochemical measurement was performed (Scheme 4.1a). In the presence of the target analyte, the released barcode CR* is designed to hybridize with the immobilized capture probe and displace D1, which brings the MB moiety close to the electrode surface, thus generating an electrochemical signal (Scheme 4.1a,b). To examine the feasibility of the e-biobarcode assay, we established a baseline system using streptavidin as the target and planar gold as the electrochemical transducer. Increasing the protein concentration increased the current generated by the reduction of MB, demonstrating a signal-on electrochemical sensor (Figure 4.1c). This sensor demonstrates a log-linear response in the 1 pM – 10 nM concentration range and a limit-of-detection (LOD) of 208 fM (Figure 2d). Sensitive detection is vital for biosensors owing to the low abundance of biomarkers in clinical samples. The sub-pM LOD demonstrated here positions the proximity induced bio-barcode assay as a platform for ultrasensitive protein detection.

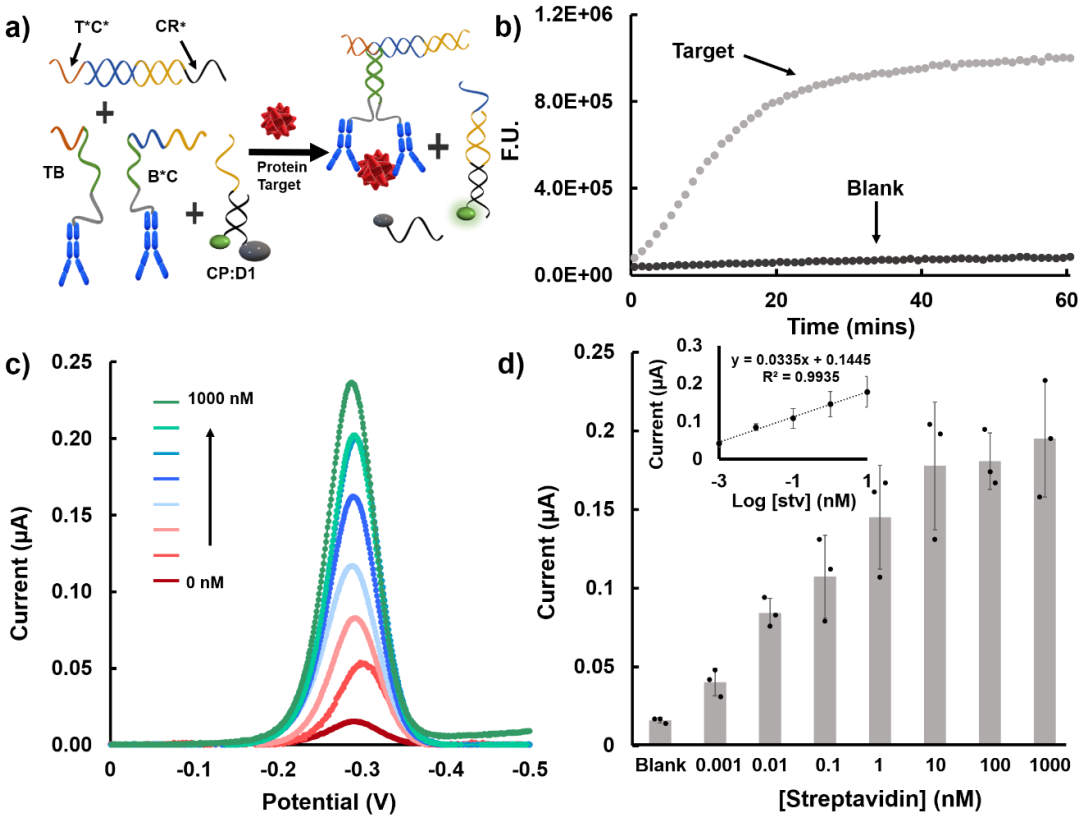

Figure 4.1 Validation of the bio-barcode assay using a model streptavidin/biotin system. a) Schematic representation of the fluorescence bio-barcode validation assay for protein detection. b) Generation of fluorescent signal by the release of the bio-barcode upon recognition of the streptavidin protein target, Target = 10 nM streptavidin, Blank = 0 nM streptavidin. c) Validation of the e-biobarcode assay on planar gold electrodes using methylene blue as the redox reporter. Square wave voltammetry scans recorded for the increasing streptavidin concentrations from 0 nM – 1000 nM with a Ag/AgCl reference electrode. d) The peak electrochemical current extracted from c) in response to the increasing concentrations of streptavidin with linear trend included as an inset. The error bars represent the standard deviation from the mean. Each bar represents average data obtained from the same sample measured using at least 3 electrodes.

4.4.2 Electrochemical Detection of PSA using the Bio-barcode Assay

In order to demonstrate the applicability of the sensor to detecting relevant cancer protein biomarkers, prostate specific antigen (PSA) was employed as the target protein and polyclonal anti-PSA antibodies were conjugated to TB and B*C motifs as biorecognition elements. Upon binding, the DNA-antibody/protein complexes are generated, and the programmed strand displacement reactions are initiated, leading to the release and subsequent on-chip capture of the MB-labelled reporter barcode. As a result, the measured electrochemical current on planar

electrodes is increased with increasing PSA concentration (Figure 4.2a), indicating the successful detection of PSA. Using data gathered from over 30 chips, PSA was analyzed within a log-linear range of 0.5 to 100 ng mL^{-1} ($y = 0.0305x + 0.0508$, $R^2 = 0.97$) with an LOD of 2.08 ng mL^{-1} (Figure 4.2c). We expect this lower LOD compared to the case with streptavidin to be related to the lower binding affinity of anti-PSA and PSA compared to streptavidin and biotin, and the increased steric hindrance caused by larger biorecognition elements used for PSA. In clinical applications, PSA concentrations higher than a threshold level of 4 ng mL^{-1} are indicative of prostate cancer.[45] Although the achieved LOD was below this clinically-relevant threshold, we sought to re-engineer our transducers for further enhancing their LOD for more robust and reliable sensing performance.

Three-dimensional transducers created from the assembly of nanostructured building blocks allow for an increased number of biorecognition probes to be deposited on the electrode surface with a more suitable orientation and spacing for target capture compared to two-dimensional sensing electrodes.[31,32,183,184] Additionally, we expect the bulky biomolecular complexes used in this assay to be accumulated at the electrode surface, making it critical to develop strategies for reducing steric hindrance at the surface.[185] As a result, we hypothesized that performing the e- biobarcode assay on three-dimensional and nanostructured transducers would enhance the efficiency of interfacial DNA strand displacement reactions and assay sensitivity.[186] To validate this hypothesis, we created star-shaped gold electrodes with sharp edges that were designed to result in three-dimensional nanostructured electrodes (3D nano-electrodes) following electrodeposition (Chapter 4 Appendix, Figure 4.6).

We compared the performance of the 3D nano-electrodes with planar electrodes (Figure 4.2c,d) in analysing PSA using the e-biobarcode assay. The 3D nano-electrodes demonstrated PSA detection within the clinically-relevant log-linear range of 0.5 ng mL^{-1} – 200 ng mL^{-1} ($y = 0.1423x + 0.1152$, $R^2 = 0.99$) with a sensitivity of 0.14 µA/ log (ng mL^{-1}) and a LOD of 0.332 ng mL^{-1}. As hypothesized, using the 3D nano-electrodes resulted in a remarkable enhancement in sensitivity (four times) and LOD (six times) compared to the planar electrodes, leading to an assay that is suitable for clinical analysis.

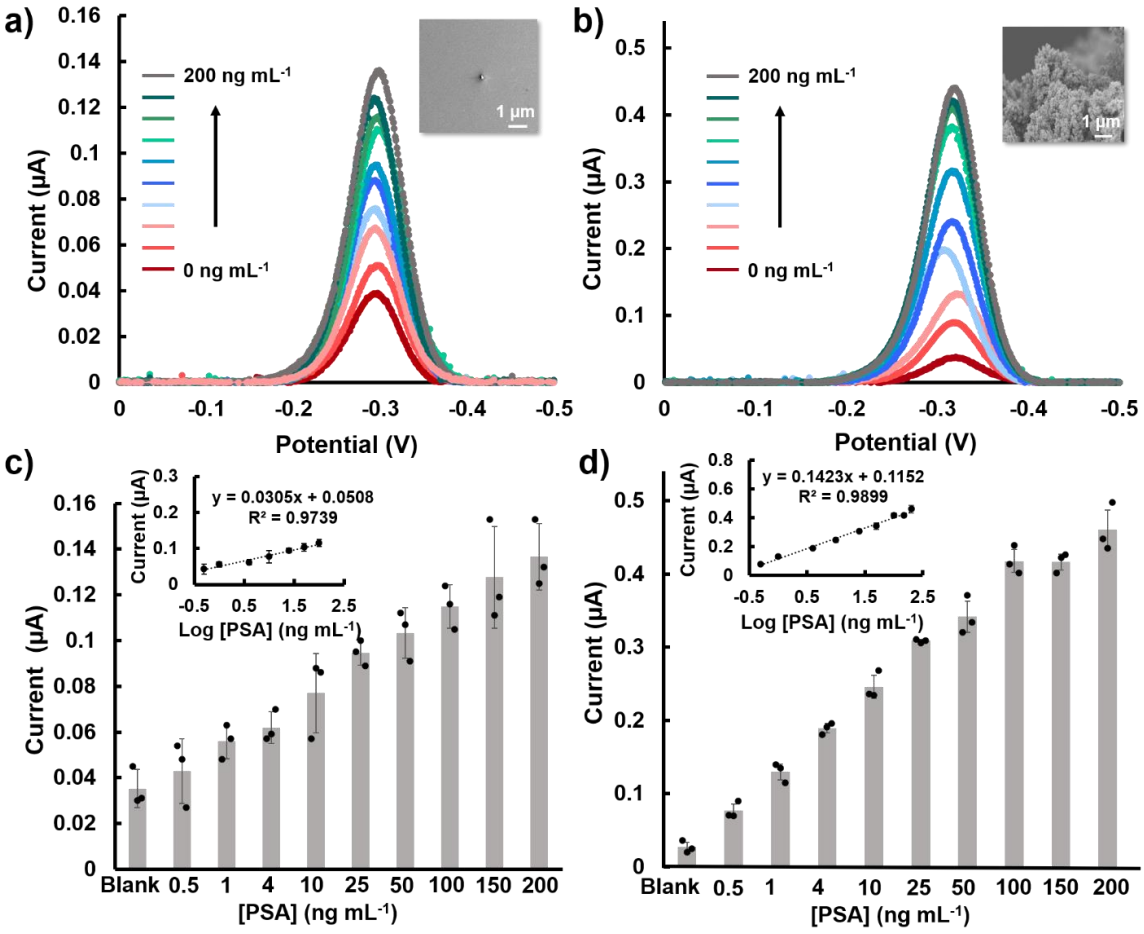

Figure 4.2. Evaluating the performance of the e-biobarcode assay for the electrochemical detection of PSA. a) SWV responses for increasing PSA concentrations from 0 – 200 ng mL^{-1} obtained using planar electrodes with a SEM image of the planar electrode suface as an inset. b) SWV responses for increasing PSA concentrations from 0 – 200 ng mL^{-1} obtained using 3D nano-electrodes with a SEM image of the 3D-nano electrode surface as an inset. All electrochemical potentials are with respect to a Ag/AgCl reference electrode. c) Electrochemical detection of PSA on planar electrodes with peak current extracted from a) with the linear trend in the log concentration as an inset. d) Electrochemical detection of PSA on 3D nano-electrodes with the peak current extracted from b) with the linear trend in the log concentration as an inset. Each bar represents average data obtained from the same sample measured using at least 3 electrodes.

4.4.3. Application and Selectivity of the E-biobarcode Assay

For a biosensor to be used in clinical analysis and decision making, it must perform successfully in complex solutions such as serum, plasma, blood, or urine.[187] These solutions are composed of proteins and other large biomolecules that can degrade assay reagents and/or non-specifically adsorb onto the electrode surface and influence the sensor's performance. To circumvent these effects, surface blockers such as bovine serum albumin (BSA), short chain alkanethiols, poly(ethylene glycol), carbo-free blocking solution, and gelatin have been used.[19,188,189] In our assay, we used poly-A strands to exploit the strong affinity between the adenine bases of DNA and gold[35] to reduce the surface area of the unreacted electrode available for non-specific adsorption of interfering biomolecules. Unlike bulky proteins used as surface blockers, the small size of poly-A strands does not interfere with electron transport or the hybridization of the capture and reporter probes while reducing the negative effects of non-specific adsorption.

To assess whether our bio-barcode assay integrated with poly-A as a surface blocker was suitable for clinical use, we challenged our system with samples that contained PSA spiked in undiluted human plasma. As previously observed with PSA targets suspended in buffer, increasing the target concentration resulted in an increase in the electrochemical current (Figure 4.3a-b). Although the signal magnitudes decreased from the values measured in buffer, the sensitivity remained high, achieving an LOD of 0.385 ng mL^{-1} and a linear range in the log concentration from 1 ng mL^{-1} – 200 ng mL^{-1} ($y = 0.1136x + 0.0883$, $R^2 = 0.99$) (Figure 4.3b). The loss in signal magnitude can be explained by the non-specific adsorption of large proteins and other molecules

present in undiluted plasma. Nevertheless, the poly-A played an instrumental role in maintaining the signal-to-blank ratio and as a result, the assay sensitivity and LOD (Figure 4.3c).

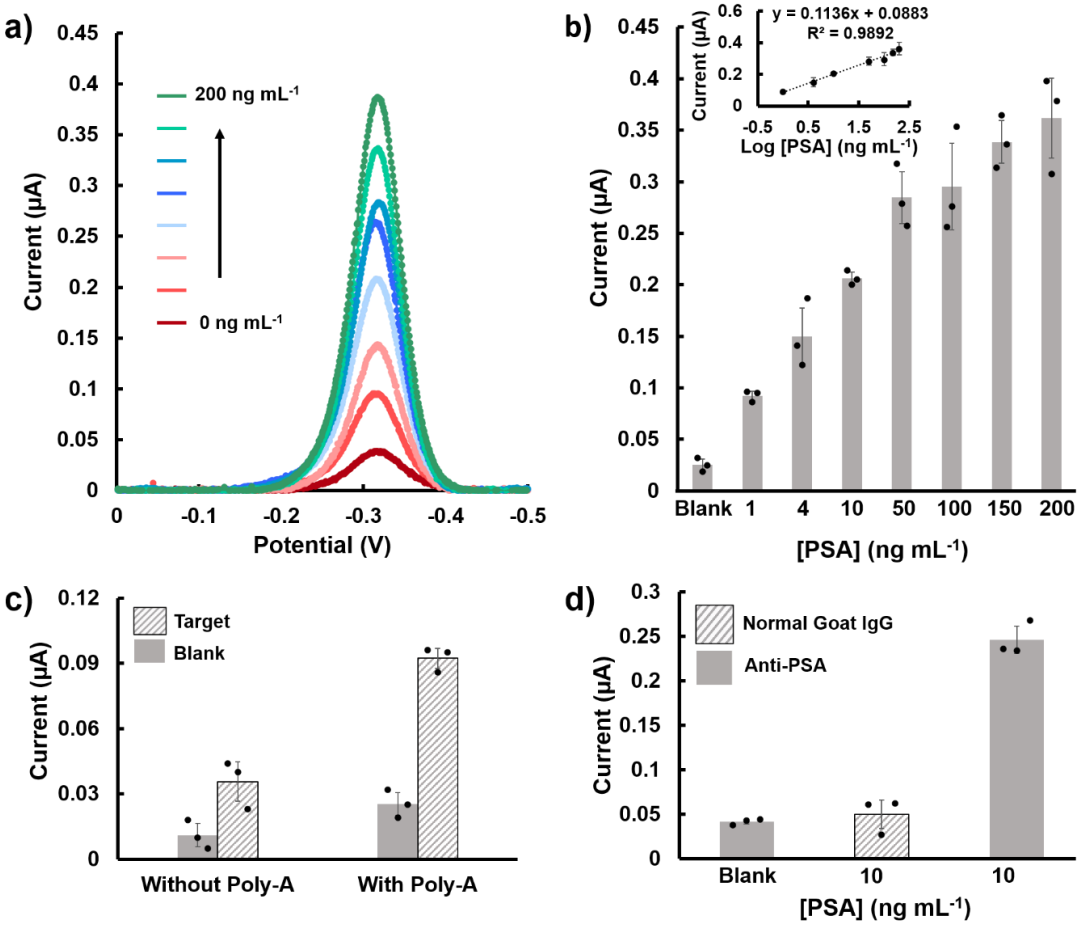

Figure 4.3. Validation of the performance of the e-biobarcode assay in the presence of biological interfering materials. a) SWV responses for increasing PSA concentrations from 0 – 200 ng mL^{-1} obtained using 3D nano-electrodes in undiluted human plasma. All electrochemical potentials are with respect to a Ag/AgCl reference electrode. b) Electrochemical detection of PSA in undiluted human plasma with the linear trend of the log concentration as an inset. The peak currents are extracted from the data presented in a). c) effect of poly-A on electrochemical signal produced in undiluted human plasma using 1 ng mL^{-1} PSA. d) detection of 10 ng mL^{-1} of PSA with specific and non-specific recognition antibodies compared to blank signal obtained using anti-PSA. Each bar represents average data obtained from the same sample measured using at least 3 electrodes

To further demonstrate the specificity of the bio-barcode assay, normal goat IgG control antibodies were used in place of anti-PSA as the detection element. As expected, a much larger current increase was seen with anti-PSA compared to the non-specific normal goat IgG antibodies

(Figure 4.3d). Furthermore, the sensor was challenged with non-specific proteins IL-6 and GFAP, with anti-PSA antibodies as recognition molecules (Chapter 4 Appendix, Figure 4.8). Again, a statistically significant signal increase was only observed when PSA was present in solution with the specific antibody ($p = 0.316$ for IL-6, $p = 0.097$ for GFAP, $p = 0.003$ for PSA). These results confirm that the assay is both specific and sensitive in real human samples and demonstrate the potential use in clinical applications.

4.5 Conclusion

In this chapter, the analytical ability of the bio-barcode assay was evaulted for sensitivity and practicalty for protein detection. The assay was first validated using the steptavidin/biotin binding model that was optimized in chapter 3. Real-time fluorescence was first used to validate that a bio-barcode was released in repsonce to a protein target (streptavidin). The result was an increasing fluorescent signal only when the protein target was in the solution and a SBR of 13.5 was calculated after only 20 minutes. The assay was translated from fluorescent readout to electrochemical readout on planar gold electrodes and the ability of the sensor was investigated using increasing streptavidin concentrations from 1 pM to 1 µM. The results showed increasing electrochemcial current in repsonse to increasing protein concentration yeilding a LOD of 208 fM and a log-linear responce in the concentration range of 1 pM to 10 nM.

The validated assay was then applied to the detection of a cancer protein biomarker, PSA, by conjugating anti-PSA antibodies to the biorecognition motifs. The assay was used to detect increasing protein concentrations from 0.5 to 200 ng mL^{-1}. The results showed increasing generated electrochemical signal corresponding to increasing protein cocnetrations and a log-linear range of 0.5 to 100 ng mL^{-1} was found with a LOD of 2.08 ng mL^{-1}. The sensitivity of the e-biobarcode assay was then further enhanced using 3D-nano electrodes. The electrodes were

fabricated using electrodeposition to build 3D structures on the transducing surface. As expected, the LOD was enhanced (roughly 6 times) from 2.08 ng mL^{-1} to 0.332 ng mL^{-1} and an increase in the log-linear range was also observed (0.5 to 200 ng mL^{-1}).

The practicality of the sensor was then evalutated by applying it towards PSA detection in undiluted and unprocessed human plasma. PSA concentrations from 1 to 200 ng mL^{-1} were used and an increasing trend was observed for the measured current. A LOD of 0.385 ng mL^{-1} was calculated and a log-linear range from 1 to 200 ng mL^{-1} was observed. The instrumental role of poly-A in achieving such high sensitivity in an undiltued biological fluid was demonstrated by performing the e-biobarcode assay with 1 ng mL^{-1} of PSA on electrodes with and without 1 µM of poly-A on the surface. The results showed that the electrodes integrated with poly-A achieved higher signals than those without poly-A (2.6 times higher). This is expected as human plasma is a protein rich solution with many molecules that can non-specifically adsorb to the surface preventing target hybridzation or electron transfer.

Lastly, specificity of the e-biobarcode was investigate using both non-specific biorecognition elements and non-specific proteins. To demonstrate the specificity of the biorecognition motifs we replaced the anti-PSA antibodies with control normal goat IgG antibodies. We used this modified e-biobarcode assay to try and detect 10 ng mL^{-1} of PSA, and the results showed that this could not be done. The electrochemical signal that was obtained was similar to the signal obtained from a blank solution. To demonstrate target specificity, the e-biobarcode with anti-PSA biorecognition elements was used to detect 1 ng mL^{-1} of non-specific protein targets IL-6 and GFAP. The electrochemical signal that was generated in responce to these targets was not signifcantly larger than the signal obtained from a blank solution. Combined, these results demonstrate that the e-biobarcode assay is specific towards a protein target.

The electrochemical bio-barcode assay demonstrated in this chapter allows proteins to be analyzed, in undiluted and unprocessed human plasma, with the analytical sensitivity and specificity that is required for clinical decision making. Importantly, this analysis is performed in a sample-in-answer-out approach without the need for the sequential addition of reagents or multi-step processing, demonstrating a viable option for enabling clinical decision making at the point-of-care.

4.6. Appendix

4.6.1. Native PAGE

In order to verify the formation of the desired DNA structures and the occurrence of the programmed strand displacement reactions, a native PAGE was performed. Biotinylated TB and B*C strands were used as the biorecognition element with 1 µM of streptavidin as the protein target to demonstrate protein capture and bio-barcode release. Lane 1 contained the blank which had 1.25 nM TB, 1.25 nM B*C and 1 µM T*C*:CR; lane 2 contained the target solution with 1.25 nM TB, 1.25 nM B*C, 1 µM T*C*:CR and 1 µM streptavidin; lane 3 contained 1 µM CR*; lane 4 contained 1 µM T*C*:CR*; lane 5 contained 1 µM TB; lane 6 contained 1 µM B*C. The formation of the TWJ can be seen as a wide band with the least migration distance, only forming in lane 2 with the presence of the protein target. Additionally, a less prominent T*C*:CR* band and an increase in the CR* band can also be seen in lane 2, suggesting the formation of the TWJ leads to the release of the bio-barcode. Alternatively, when there is no protein target present (lane 1) the TWJ does not form and there is a prominent T*C*:CR band, indicating that without protein target the bio-barcode cannot be released.

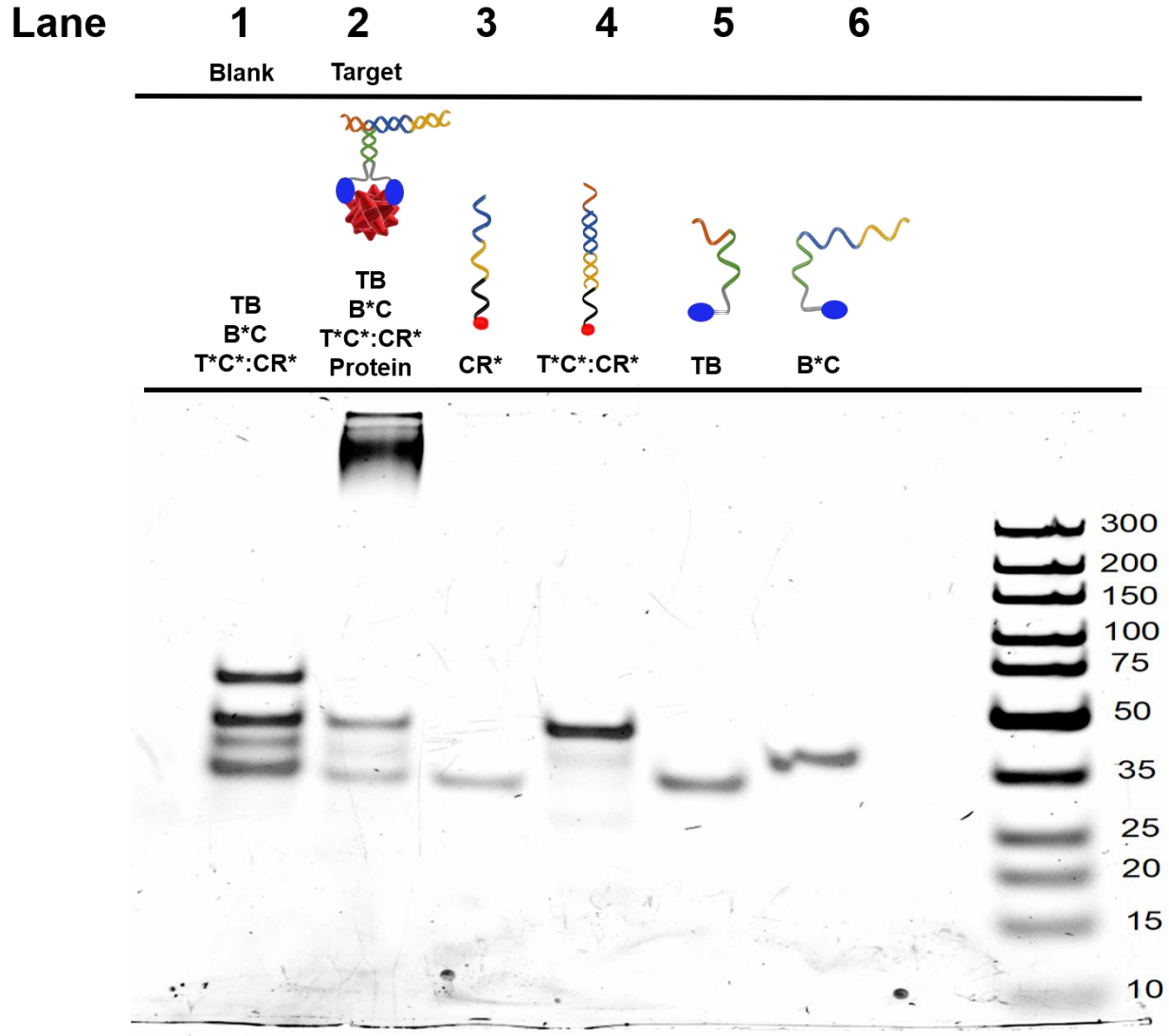

*Figure 4.4 Native PAGE of the bio-barcode assay using 1 µM streptavidin target; lane 1 contained 1.25 nM TB, 1.25 nM B*C, 1 µM T*C*:CR; lane 2 contained 1.25 nM TB, 1.25 nM B*C, 1 µM T*C*:CR, 1 µM streptavidin; lane 3 contained 1 uM CR*; lane 4 contained 1 µM T*C*:CR*; lane 5 contained 1 µM TB; lane 6 contained 1 µM B*C.*

4.6.2. Fluorescent detection of PSA

For further verification that PSA could be detected using the bio-barcode assay, a fluorescence assay was done following the same procedure that was performed for the validation assay using a streptavidin target (4.3.6). The biotinylated TB and B*C motifs were conjugated with anti-PSA to be used as the biorecognition element and 1 µg mL^{-1} PSA was used as the protein target. The fluorescent signal was measured in the presence and absence of PSA and an increase in signal can be seen correlating to the presence of the protein target (Figure 4.5).

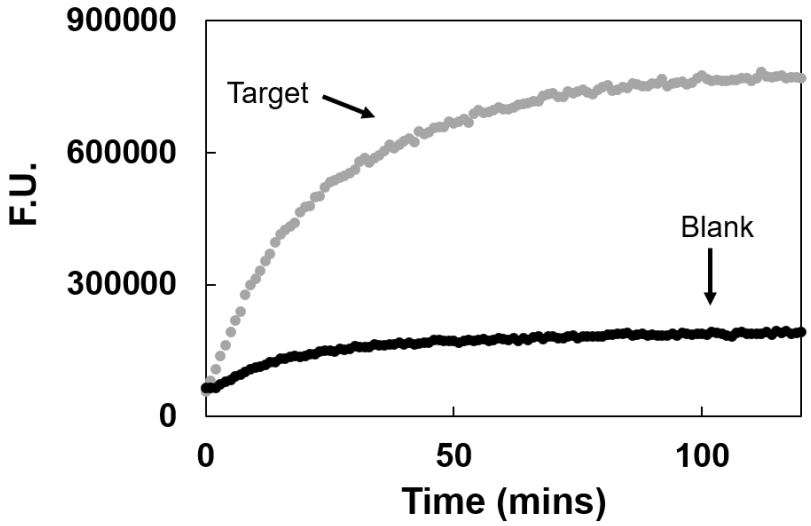

*Figure 4.5. Fluorescent detection of PSA in reaction buffer using 25 nM TB, 25 nM B*C, 20 nM T*C*:CR*, 20 nM FAM/IOWA Black CP:D1 and 1 µg mL^{-1} PSA.*

4.6.3. Determining the electroactive surface area of gold electrodes

The electroactive surface area of a gold electrode can be found using the integration of the gold oxide reduction peak using the following formula: $\Gamma = A / (v \cdot 482\ \mu C\ cm^{-2})$ where Γ is the electrochemical surface area, A is the cathodic peak area in the cyclic voltammogram and v is the scan rate. [190] Substituting in values obtained from the plot by reversibly scanning from 0 – 1.6 V

(against Ag/AgCl) in 0.5 M H_2SO_4 at a scan rate of 0.1 V/s, the surface area of the planar electrodes was found to be 0.26 cm^2 and the surface of the 3D-nano electrodes was found to be 1.13 cm^2, roughly demonstrating a 4.5x enhancement of surface area.

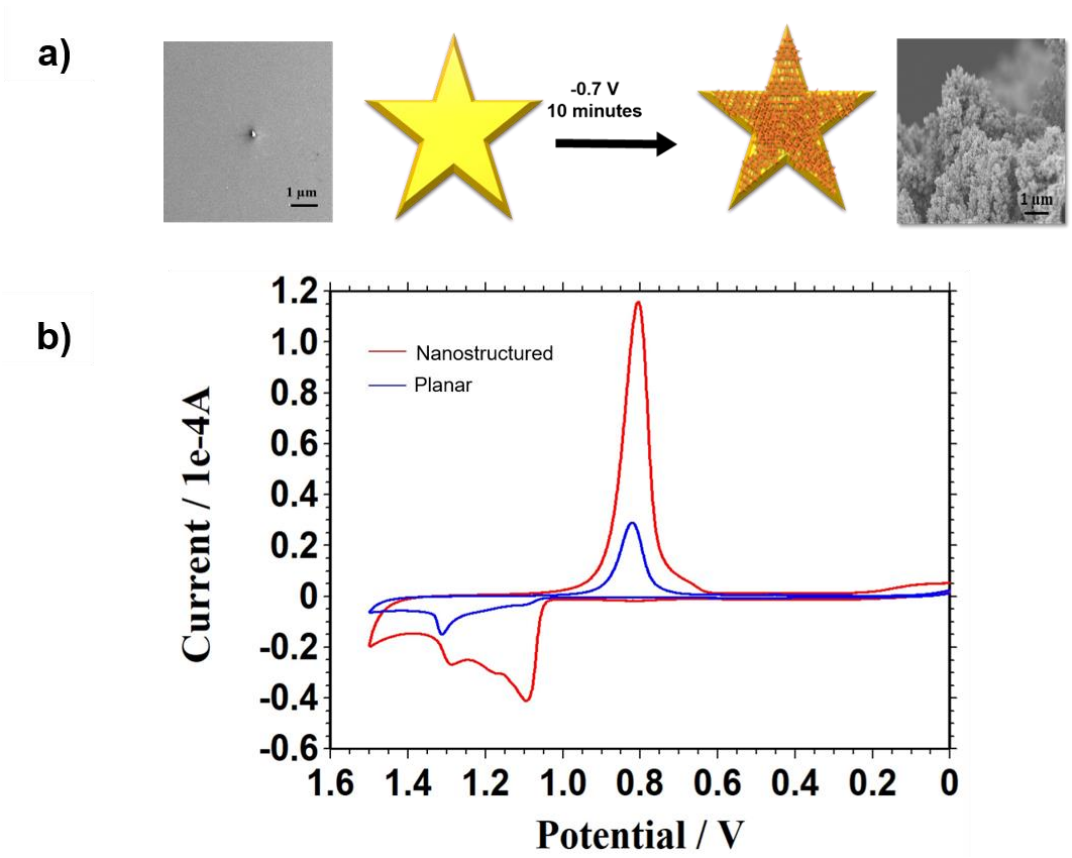

Figure 4.6. a) Schematic of the fabrication of the 3D nano-electrodes with SEM images of the electrode surface before and after electrodeposition. b) Characteristic redox curve for Au in 0.5 M H_2SO_4 produced from reversible cycling from 0 – 1.6 V against Ag/AgCl at a scan rate of 0.1 V/s.

4.6.4. CV scan of gold electrode in 2 mM $[Fe(CN)_6]^{4-}$

Measuring the CV curves of electrodes in $[Fe(CN)_6]^{4-/3-}$ can be used to qualitatively determine the surface passivation of the electrodes by assessing the oxidation and reduction peaks. On bare gold, $[Fe(CN)_6]^{4-}$ can access the surface of the electrode and can be easily oxidized to $[Fe(CN)_6]^{3-}$ followed by reduction back to $[Fe(CN)_6]^{4-}$, producing the characteristic redox curve. When negatively charged DNA is deposited on the surface of the electrodes the anions are repelled hindering the redox activity of the species. The result is a flat curve with no peaks. MCH is used to both remove the non-specifically adsorbed DNA by competing for free gold sites and aligning the DNA probe by filling the self-assembled monolayer and slightly repelling DNA with the hydroxide. [191]

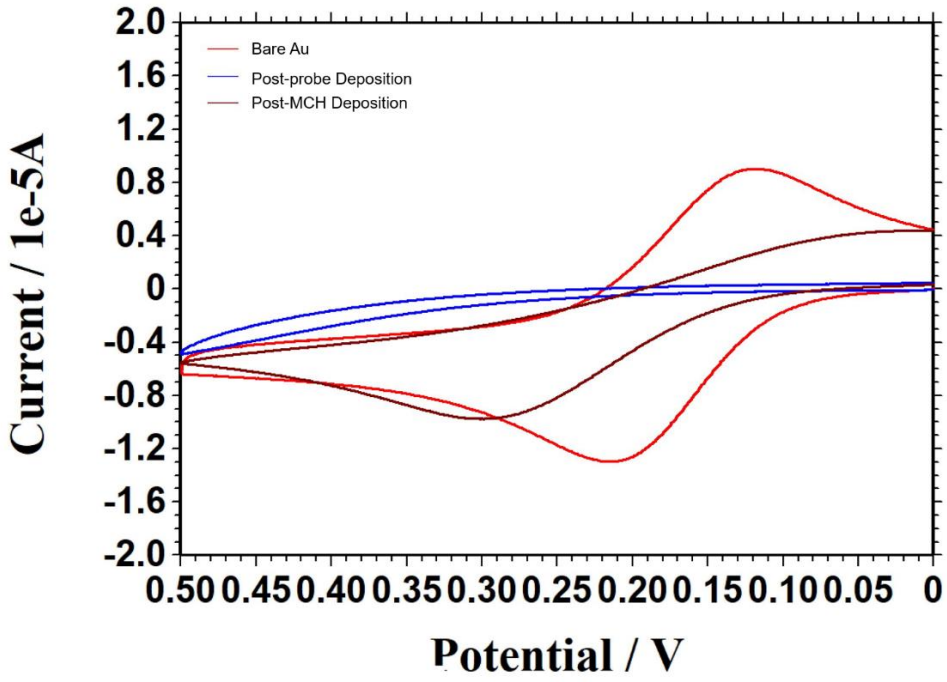

Figure 4.7. Cyclic scanning of the planar gold electrode in 2 mM $[Fe(CN)_6]^{4-}$ for the verification of DNA probe and MCH deposition.

4.6.5. Specificity of the e-biobarcode assay

To demonstrate the specificity of the e-biobarcode assay, it was challenged with IL-6 and GFAP, two non-specific protein biomarkers. A larger current increase can be seen only in response to PSA, demonstrating specificity. Detection of these proteins was performed following the same protocol that was used for detecting PSA.

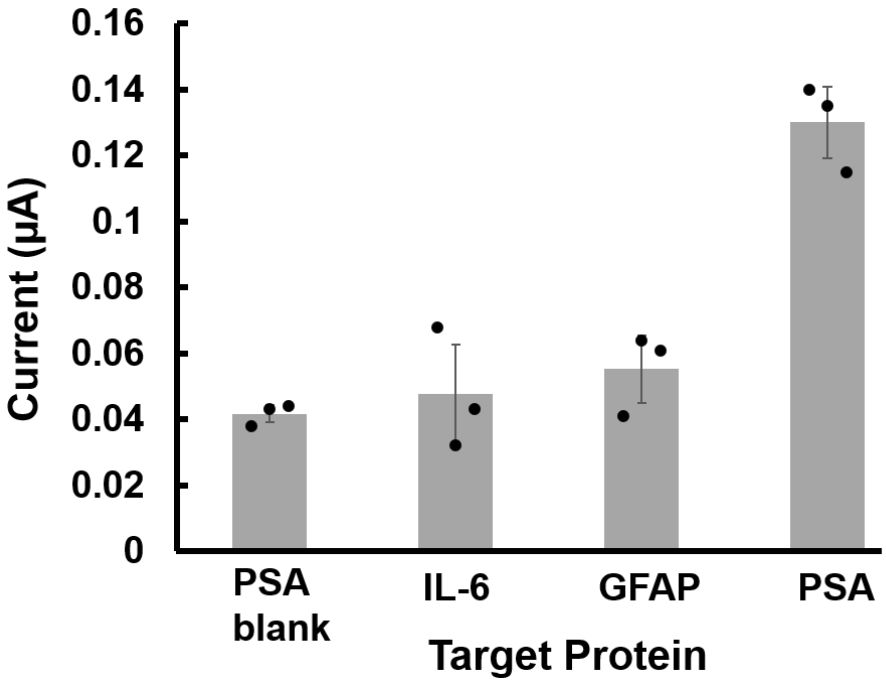

Figure 4.8. The peak electrochemical current in response to various targets: blank solution, 10 ng mL^{-1} IL-6, 10 ng mL^{-1} GFAP and 10 ng mL^{-1} PSA, all in reaction buffer. The error bars represent the standard deviation from the mean. Each bar represents average data obtained from the same sample measured using at least 3 electrodes.

Chapter 5: Conclusion

5.1 Thesis Summary and Key Findings

In chapter 1, a brief background on biosensors was given, highlighting challenges of incorporating them into handheld devices for point-of-care analysis. The motivation of this work was discussed, and an outline of the objectives were presented.

In chapter 2, a literature review on electrochemical detection of prostate specific antigen was done. The relevance of this chapter was to highlight work that has been done in the last 5 years and demonstrate the many classes of detection schemes currently being used. Prostate specific antigen was used as a model cancer protein marker in this research and so the clinical significance of the protein was also discussed.

In chapter 3 optimization of the purposed bio-barcode assay for electrochemical protein detection was done. The parameters that were optimized and the key findings from each experiment were as follows:

1. Studying the effect of probe density on the generated electrochemical signal (section 3.3.1) – Probe density is affected by both the concentration of the capture probe and the length of time given for immobilization. In this section square-wave voltammetry was used to determine the optimal deposition concentration and time of deposition for the capture probe used for on-chip hybridization of the released barcode DNA. The variance of capture probe concentration used was 0.25, 0.5 and 1 µM and the deposition time was 2, 4, 8, 16 and 24 hours. The optimal conditions were characterized by the result that yielded the highest electrochemical signal generated from hybridization of a target strand to the immobilized probe. In this study 300 nM of the MB-labelled bio-barcode was used as the target. Overall,

the trend was an increasing electrochemical signal corresponding to an increasing deposition time with a plateau reached at 16 hours, for all probe concentrations. In addition, 0.5 µM of probe yielded the highest electrochemical signal for all probe deposition times. The results indicated that 0.5 µM of probe left for 16 hours on the working electrode at room temperature achieved the optimal density.

2. Studying the effect of target hybridization time on the generated electrochemical signal (section 3.3.2) – This section again used square-wave voltammetry to determine the time required for optimal target hybridization at 37°C with the immobilized capture probe on the surface of the electrode. The electrochemical signal that was generated from hybridization of 50 nM of the MB-labelled bio-barcode with the capture probe was measured after incubating the sensing electrode with the target for 5, 15, 30, 45, 60 and 120 minutes. The current showed an increasing trend with increasing hybridization time until 60 minutes. At 120 minutes the signal significantly dropped (over 50%). Although this result was not expected, we hypothesize it is a result of the reverse strand displacement reaction. The strand D1 that is displaced from the capture probe by CR* is likely displacing CR* when given excess time. The largest electrochemical signal was achieved after 60 minutes; however, it was determined that the difference in generated signal between 45 and 60 minutes was not enough to increase the total detection time. For this reason, 45 minutes was chosen as the optimal target hybridization time.
3. Studying the effect of the ratio of the T*C* strand to the CR* strand during annealing for preparation of bio-barcode containing duplex on the signal-to-blank ratio (section 3.3.3) – The importance of decreasing background signal through optimal assay intermediate preparation was explored in this section. Square-wave voltammetry was used to investigate

the signal-to-blank ratio obtained from varying the ratio of the T*C* strand to the CR* strand during annealing of the duplex. The target for this study was 50 nM of a strand complementary to T*C* (TCcomp) used to replicate the formation of the three-way junction and the release of the bio-barcode. The ratios used were 1:1, 1.1:1 and 1.2:1, increasing the amount of T*C* relative to the amount of CR*. The trend observed was a decreasing target and blank signal in response to higher amounts of T*C*. A ratio of 1.1:1 (T*C*:CR*) resulted in the highest signal-to-blank ratio of 4.5, indicating this was the optimal ratio for preparing the intermediate duplex.

4. Studying the effect of the assay intermediate concentrations on the signal-to-blank ratio (section 3.3.4) – Within the bio-barcode assay, there were intermediate DNA sequence that had to react together efficiently to release a reporting barcode while minimizing the background signal. In this section, square-wave voltammetry was used to determine the optimal concentration for each intermediate. In previous studies, the ratio of the barcode containing duplex T*C*:CR* to biorecognition motifs TB and B*C was determined to be 1:1.25. This ratio was kept constant throughout this experiment with varying concentrations of each intermediate. The concentrations that were investigated were 1 nM : 1.25 nM, 10 nM : 12.5 nM, 20 nM : 25 nM, 60 nM : 75 nM and 100 nM : 125 nM (T*C*:CR* : TB/B*C). The increase of assay intermediate concentration corresponded to an increasing electrochemical signal for both the target and the blank solution. To compare the effect of the intermediate concentration the signal-to-blank ratio was determined, this time using 10 nM of streptavidin as the protein target. A concentration of 20 nM : 25 nM resulted in the largest signal-to-blank ratio of 4.0 and was determined to be the optimal intermediate concentrations. High intermediate concentrations likely induced spontaneous

formation of the three-way junction, increasing the blank signal and at lower intermediate concentrations there likely was not enough biorecognition probe to generate efficient release of the MB-labelled bio-barcode, decreasing the target signal. In both cases the signal-to-blank ratios were affected.

5. Studying the effect of introducing a 37℃ reaction step on the signal-to-blank ratio (section 3.3.5) – This section examined the protein capture step that was performed in solution to circumvent issues that arise from surface capture of proteins. To ensure that protein capture was successful and efficiently released the MB-labelled bio-barcode, the effect of an incubation step prior to on-chip hybridization was studied. The effect was evaluated by measuring the electrochemical signal that was generated from the bio-barcode assay using 10 nM of streptavidin with and without incubation at 37℃ prior to on-chip hybridization. When a 30-minute incubation step was introduced the signal-to-blank ratio slightly increased from 4.0 to 4.3, indicating that there was improvement. This experiment was done using the streptavidin/biotin model and it was hypothesized that a larger effect on the signal-to-blank ratio would be seen when using this assay with less efficient binding pairs such as antibody/antigen. The decision was made to include this step when validating the assay in chapter 4.
6. Studying the effect of poly-A as a surface blocker (section 3.3.6) – In this section, the effectiveness of poly-A as a surface blocker was explored. The full e-biobarcode assay was performed in buffer with and without poly-A on the surface of the electrode and square-wave voltammetry was used to obtain an electrochemical signal. Using 10 nM of streptavidin as the target in buffer, it was demonstrated that poly-A contributed to slightly decreasing the background signal and minimally increasing the target signal. It was

hypothesized that the effect of poly-A would be much more relevant in a more complex sample. It was determined that it should be a suitable surface blocker for the e-biobarcode assay at a concentration of 1 µM and was used for further experiments in chapter 4.

7. Studying the effect of human plasma dilution on the total electrochemical signal loss (section 3.3.7) – Human plasma was to be used as the complex solution for validating the performance of the e-biobarcode assay. The first step in using a complex matrix is to determine the amount of signal loss with varying degrees of dilution so that the assay can successfully detect the target. Human plasma was diluted 2X, 4X, 6X and 8Xand square-wave voltammetry was used to determine the electrochemical signal obtained from 20 nM of the MB-labelled bio-barcode. All levels of dilution (2-8X) resulted in similar signal loss as undiluted plasma (roughly 20%), suggesting that undiluted plasma could be used for the validation experiments.

In chapter 4 the performance of the bio-barcode assay that was optimized in chapter 3 was demonstrated as follows:

1. Validation of the bio-barcode assay (section 4.4.1) – In this section the bio-barcode assay was assessed for protein detection using both fluorescent and electrochemical signal transduction methods and the model streptavidin/biotin system. Real-time fluorescence was used to demonstrate that in the presence of the protein target a bio-barcode was released generating a signal. The assay was then re-engineered for electrochemical readout and once again was assessed using the streptavidin/biotin system on planar gold electrodes. The optimized conditions were used to test the e-biobarcode assay. A limit-of-detection of 208 fM and a log-linear response from 1 pM – 10 nM was determined. This section revealed the bio-barcode assay as a potential platform for ultrasensitive protein detection.

2. Electrochemical detection of PSA using the bio-barcode assay (section 4.4.2) – In this section the applicability of the purposed e-biobarcode system was explored using a model cancer protein biomarker, prostate specific antigen. With a sub-pM detection limit being reached in the previous section using planar gold electrodes, the assay was directly applied to the detection of prostate specific antigen with minor changes. Biotin was replaced with anti-PSA as the biorecognition element for capture of the protein target, but all other conditions were kept the same. The limit-of-detection was found to be 2.08 ng mL^{-1} and a log-linear range from 0.5 to 100 ng mL^{-1} was demonstrated. This experiment revealed that the e-biobarcode assay was suitable for detection of a cancer protein biomarker, achieving a detection limit lower than the clinical relevancy (4 ng mL^{-1}). While successful protein detection was performed, one of the objectives of this thesis was to demonstrate how material engineering can contribute to increased sensitivity. To do so, the planar electrodes were redesigned, and electrodeposition was performed to create an electrode with a 3-dimensional surface morphology. This presence of the 3D nanostructures on the surface of the electrode was assessed using SEM and cyclic voltammetry, demonstrating an increase in electroactive surface area. The e-biobarcode assay was employed using the 3D-nano electrodes to determine if sensitivity was increased. A limit-of-detection of 0.332 ng mL^{-1} and a log-linear range of 0.5 – 200 ng mL^{-1} was realized. This experiment revealed a four-times enhancement in sensitivity and a six-times enhancement in the limit-of-detection.
3. Application and selectivity of the e-biobarcode assay (section 4.4.3) – In this section, the practical application and selectivity of the e-biobarcode assay were demonstrated and the contribution of poly-A as a surface blocker in human plasma was highlighted. The e-biobarcode assay was challenged with varying levels of prostate specific antigen spiked

into undiluted human plasma using the 3D-nano electrodes and a limit-of-detection of 0.385 ng mL^{-1} was determined with a log-linear range of 1 – 200 ng mL^{-1}. This experiment showed minor (1 times) increase in the limit-of-detection of the purposed sensor in unprocessed biological sample compared to buffer, demonstrating use in a practical matrix. The selectivity was examined by substituting anti-PSA biorecognition elements with non-specific anti-goat IgG control antibodies. Using this non-specific detection mechanism, it was shown that a signal increase was only generated using the specific biorecognition elements. A large contributing factor to the use of the sensor in unprocessed plasma comes from the use of poly-A as a surface blocker. This was demonstrated by performing the assay with and without poly-A in plasma. The result was a large increase in the target signal (2.6 times), indicating that it prevented insulating biomolecules adsorbing to the surface.

5.2 Contributions to the Field

The work described in this thesis contributed to the following fields in the following ways:

Prevention of non-specific adsorption of interfering molecules

The practicality of the sensor was demonstrated using spiked human plasma that did not undergo any processing. The ability of the e-biobarcode assay to be used under such conditions was attributed to both the use of poly-A as a surface blocker and performing protein capture in solution. Non-specific adsorption of poly-A to the surface of the electrode prevented other biomolecules from accessing the electrode surface therefore mitigating the effect of interferents in the solution. Non-specific adsorption is one of the most common challenges faced in biosensing devices. While

many options are available for surface blocking, this aspect of the thesis offers a solution with a molecule whose small size does not interfere with assay components or contribute to increasing steric hindrance.

Increasing sensitivity using 3-dimensional nanostructures

The use of surface modification, especially with regards to nanostructuring, to increase sensitivity has been well documented. This research confirms that 3-dimensional nanostructures can be used in electrochemical bio-barcode assays for increased sensitivity towards protein detection. Probe density was a parameter that was investigated and optimized in chapter 3, with results indicating that adequate spacing is required for optimal target capture. Engineering the electrode surface with 3-dimensional structures promotes optimal spacing and an increase of probe deposition locations.

Rapid analysis of a protein cancer biomarker in a sample-in-answer-out manner

The work described within this thesis focused on developing a biosensor capable of sensitive protein quantification in a manner that would allow for feasible integration into a point-of-care device. The challenges of developing detection platforms that would allow for translation into remote clinical analysis have been thoroughly covered within this thesis. To reiterate the most prominent challenges faced; complexity of the assay, time requirements and sample preparation. The e-biobarcode assay presented here was uniquely translated from real-time fluorescence readout to electrochemical readout, taking the benefits of no-wash solution capture of the protein target and increasing the signal transduction sensitivity. We were able to demonstrate one-pot detection that occurred within 1 hour and 15 minutes with no required sample preparation or wash

steps. This will expedite biosensing research pertaining to integration into point-of-care devices and provides other researcher with a viable design for doing so.

5.3 Future Direction

The future of this work should address three outstanding areas that would further improve the ability and application of the purposed sensor.

The first area is reagent stability and manufacturing costs. Both factors are extremely important in creating a commercially viable product ready for mass production. While the assay components are relatively cheaper than assays with comparable metrics and it does not rely on notoriously unstable reagents such as enzymes, the use of antibodies as the biorecognition element increases cost and can decrease stability if they are not properly processed. With respect to stability, further tests should be done using the e-biobarcode assay to assess whether the results will be reproducible over a prolonged period of time. Work should also be done to develop a method of properly preserving the assay reagents so that they can be shipped dry or easily stored.

The cost and stability of the sensor could potentially be explored using more reliable and cost-effective biorecognition elements. Aptamers and peptides have proven to be a good alternative to antibodies in detection schemes, demonstrating exceptional selectivity and stability. This future work would involve adapting the fundamentals of the e-biobarcode assay (release of the bar-code via three-way junction formation) with alternative biorecognition elements. This may require repeating some of the optimizations that were performed in this work but has the potential to decrease cost and increase stability.

The second area that should be investigated is the ability to detect other protein cancer biomolecules. Prostate specific antigen was chosen due to the high level of validation and comparable metrics in literature, as well as the clinical significance of the protein. The selectivity of the e-biobarcode assay that was demonstrated in this research suggests that translation to another protein biomarker is possible, however, the size of the protein biomarker was not specifically taken into any considerations. Further work should be done to demonstrate how this assay translates to the detection of different protein biomarkers by substituting the anti-prostate specific antigen antibodies with alternative antibodies. This work should begin with studies using similarly sized proteins but should also include both larger and smaller protein targets.

The third area that should be focused on in future work is increasing the accuracy of the detection. The controversial relationship between prostate specific antigen serum levels and benign impairments such as benign prostatic hyperplasia indicates a non-specific nature of the biomarker.[192] In order to ensure the utmost accuracy and minimize the amount of false-positive results obtained through prostate specific antigen quantification, the parallel analysis of multiple analytes is becoming increasingly important. As with many diseases, there are multiple biomarkers that indicate the development and growth of prostate cancer, some that are specific to prostate cancer and others that indicate general tumor growth.[193] Vascular endothelial growth factor is one of the most commonly paired protein biomarkers but other detection schemes containing prostate specific membrane antigen, interleukin-6, and platelet factor-4 have been reported.[194] In addition, nucleic acid is another class of important disease biomarkers that can be used for prostate cancer diagnosis and monitoring since they are circulated at early stages of disease and simple methods of amplification exist that aid in ultra-sensitive detection.[195]

While multiplexing promises an approach to increasing diagnostic accuracy, there have been few reports of successful simultaneous multi-target analysis. For this reason, the future of this purposed biosensor would be to incorporate elements that enable multi-analyte analysis. Due to the nature of the customizable bio-barcode assay, this complex task is feasible by modification of components in the detection scheme. The extreme selectivity of the assay demonstrated suggests that introduction of another protein capture element conjugated with a different protein biomarker antibody has the potential to initiate the release of an alternative bio-barcode labelled with a different redox tag. The ease of immobilization of the on-chip capture probe would allow for the co-deposition of multiple capture probe sequences, suggesting that a one-pot multi-target analysis could be plausible. Another method could potentially include modification to the chip design, by introducing additional working electrodes where alternative capture probes could be immobilized. In this design, multiple redox markers would not be necessary since obtaining a signal from a particular working electrode would indicate the presence of that particular protein biomarker. Another attempt at incorporating various biomarkers could include designing the sequence of the duplex containing the reporting redox-labelled bio-barcode such that a nucleic acid biomarker associated with prostate cancer could initiate the release of the reporting strand, and again modify the on-chip capture probe as necessary. While this design is specific for increasing the accuracy of prostate cancer diagnosis, many diseases can benefit from multi-analyte detection. The development of a universal sensor would be expected to drastically impact the accuracy of not only prostate cancer diagnosis and monitoring, but disease diagnostics as a whole.

Bibliography

(1) Luppa, P. B.; Müller, C.; Schlichtiger, A.; Schlebusch, H. Point-of-Care Testing (POCT): Current Techniques and Future Perspectives. *TrAC*. **2011**, *30*, 887–898. https://doi.org/10.1016/j.trac.2011.01.019.

(2) Scheller, F.; Schubert, F. *Biosensors* ; Elsevier : Amsterdamn, 1992; Vol. 11.

(3) Turner, A. P. F. Biosensors: Sense and Sensibility. *Chem. Soc. Rev.* **2013**, *42*, 3196-3196. https://doi.org/10.1039/c3cs35528d.

(4) Ly Sin, M.; Mach, K. E.; Wong, P. K.; Liao, J. C. Advances and Challenges in Biosensor-Based Diagnosis of Infectious Diseases. *Expert Rev. Mol. Diagn* **2014**, *14*, 225–244. https://doi.org/10.1586/14737159.2014.888313.

(5) Gubala, V.; Harris, L. F.; Ricco, A. J.; Tan, M. X.; Williams, D. E. Point of Care Diagnostics: Status and Future. *Anal. Chem.* **2012**, *84*, 487–515. https://doi.org/10.1021/ac2030199.

(6) Pai, N. P.; Vadnais, C.; Denkinger, C.; Engel, N.; Pai, M. Point-of-Care Testing for Infectious Diseases: Diversity, Complexity, and Barriers in Low-And Middle-Income Countries The Promise of Point-of-Care Testing. *PLoS Med* **2012**, *9*, e10011306. https://doi.org/10.1371/journal.pmed.1001306.

(7) Kim, J.; Campbell, A. S.; Esteban-Fernández Ávila, B.; Wang, J. Wearable Biosensors for Healthcare Monitoring. *Nat. Biotechnol.* **2019**, *37*, 389–406. https://doi.org/10.1038/s41587-019-0045-y.

(8) Yager, P.; Domingo, G. J.; Gerdes, J. Point-of-Care Diagnostics for Global Health. *Annu. Rev. Biomed. Eng.* **2008**, *10*, 107–144. https://doi.org/10.1146/annurev.bioeng.10.061807.160524.

(9) Dai, Y.; Liu, C. C. Recent Advances on Electrochemical Biosensing Strategies toward Universal Point-of-Care Systems. *Angew. Chemie Int. Ed.* **2019**, *58*, 12355-12368. https://doi.org/10.1002/ange.201901879.

(10) Corrie, S. R.; Coffey, J. W.; Islam, J.; Markey, K. A.; Kendall, M. A. F. Blood, Sweat, and Tears: Developing Clinically Relevant Protein Biosensors for Integrated Body Fluid Analysis. *Analyst.* **2015**, *140*, 4364. https://doi.org/10.1039/c5an00464k.

(11) Henry, N. L.; Hayes, D. F. Cancer Biomarkers. *Mol. Oncol.* **2012**, *6*, 140–146. https://doi.org/10.1016/j.molonc.2012.01.010.

(12) Wilson, R. The Use of Gold Nanoparticles in Diagnostics and Detection. *Chem. Soc. Rev.* **2008**, *37*, 2028–2045. https://doi.org/10.1039/b712179m.

(13) Huang, X.; Liu, Y.; Yung, B.; Xiong, Y.; Chen, X. Nanotechnology-Enhanced No-Wash Biosensors for in Vitro Diagnostics of Cancer. *ACS Nano* **2017**, *11*, 5238–5292. https://doi.org/10.1021/acsnano.7b02618.

(14) Leung, V.; Brooks, M.; Emerson, S.; Ali, M.; Filipe, C. D. M. Ready-to-use Thermally

Stable Mastermix Pills for Molecular Biology Applications. *Biotechnol. Prog.* **2019**, *35*, e2764. https://doi.org/10.1002/btpr.2764.

(15) Asghar, W.; Yuksekkaya, M.; Shafiee, H.; Zhang, M.; Ozen, M. O.; Inci, F.; Kocakulak, M.; Demirci, U. Engineering Long Shelf Life Multi-Layer Biologically Active Surfaces on Microfluidic Devices for Point of Care Applications. *Sci. Rep.* **2016**, *6*, 1–10. https://doi.org/10.1038/srep21163.

(16) Kumar Vashist, S.; Luppa, P. B.; Yeo, L. Y.; Ozcan, A.; Luong, J. H. T. Emerging Technologies for Next-Generation Point-of-Care Testing. *Trends Biotechnol.* **2015**, *11*, 692–705. https://doi.org/10.1016/j.tibtech.2015.09.001.

(17) Choi, J. R.; Yong, W.; Tang, R.; Gong, Y.; Wen, T.; Li, F.; Pingguan-Murphy, B.; Bai, D.; Xu, F. Advances and Challenges of Fully Integrated Paper-Based Point-of-Care Nucleic Acid Testing. *Trends Anal. Chem.* **2017**, *93*, 37–50. https://doi.org/10.1016/j.trac.2017.05.007.

(18) Labib, M.; Sargent, E. H.; Kelley, S. O. Electrochemical Methods for the Analysis of Clinically Relevant Biomolecules. *Chem. Rev.* **2016**, *116*, 9001–9090. https://doi.org/10.1021/acs.chemrev.6b00220.

(19) Choi, S.; Chae, J. Methods of Reducing Non-Specific Adsorption in Microfluidic Biosensors. *J. Micromechanics Microengineering* **2010**, *20*. https://doi.org/10.1088/0960-1317/20/7/075015.

(20) Oh, B.-K.; Nam, J.-M.; Lee, S. W.; Mirkin, C. A. A Fluorophore-Based Bio-Barcode Amplification Assay for Proteins. *Small* **2006**, *2*, 103–108. https://doi.org/10.1002/smll.200500260.

(21) Nam, J. M.; Thaxton, C. S.; Mirkin, C. A. Nanoparticle-Based Bio-Bar Codes for the Ultrasensitive Detection of Proteins. *Science.* **2003**, *301*, 1884–1886. https://doi.org/10.1126/science.1088755.

(22) Dutta, G.; Nagarajan, S.; Lapidus, L. J.; Lillehoj, P. B. Enzyme-Free Electrochemical Immunosensor Based on Methylene Blue and the Electro-Oxidation of Hydrazine on Pt Nanoparticles. *Biosens. Bioelectron.* **2017**, *92*, 372–377. https://doi.org/10.1016/j.bios.2016.10.094.

(23) Lubin, A. A.; Plaxco, K. W. Folding-Based Electrochemical Biosensors: The Case for Responsive Nucleic Acid Architectures. *Acc. Chem. Res.* **2010**, *43*, 496–505. https://doi.org/10.1021/ar900165x.

(24) Craw, P.; Balachandran, W. Isothermal Nucleic Acid Amplification Technologies for Point-of-Care Diagnostics: A Critical Review. *Lab on a Chip*. **2012**, *14*, 2469–2486. https://doi.org/10.1039/c2lc40100b.

(25) Qureshi, A.; Gurbuz, Y.; Niazi, J. H. Biosensors for Cardiac Biomarkers Detection: A Review. *Sensors and Actuators, B: Chemical*. **2012**, *171*, 62–76. https://doi.org/10.1016/j.snb.2012.05.077.

(26) Drummond, T. G.; Hill, M. G.; Barton, J. K. Electrochemical DNA Sensors. *Nat.*

Biotechnol. **2003**, *21*, 1192–1199. https://doi.org/10.1038/nbt873.

(27) Huh, S. Y.; Chung, J. A.; Erickson, D. Surface Enhanced Raman Spectroscopy and Its Application to Molecular and Cellular Analysis. *Microfluid Nanofluid.* **2009**, *6*, 285–297. https://doi.org/10.1007/s10404-008-0392-3.

(28) Wang, J. Electrochemical Glucose Biosensors. *Chem. Rev.* **2008**, *108*, 814–825. https://doi.org/10.1021/cr068123a.

(29) Drummond, T. G.; Hill, M. G.; Barton, J. K. Electrochemical DNA Sensors. *Nat. Biotechnol*. **2003**, 1192–1199. https://doi.org/10.1038/nbt873.

(30) Nam, J.-M.; Wise, A. R.; Groves, J. T. Colorimetric Bio-Barcode Amplification Assay for Cytokines. *Anal. Chem.* **2005**, *77*, 6985–6988. https://doi.org/10.1021/ac0513764.

(31) Soleymani, L.; Fang, Z.; Sargent, E. H.; Kelley, S. O. Programming the Detection Limits of Biosensors through Controlled Nanostructuring. *Nat. Nanotechnol.* **2009**, *4*, 844–848. https://doi.org/10.1038/nnano.2009.276.

(32) Soleymani, L.; Fang, Z.; Sun, X.; Yang, H.; Taft, B. J.; Sargent, E. H.; Kelley, S. O. Nanostructuring of Patterned Microelectrodes To Enhance the Sensitivity of Electrochemical Nucleic Acids Detection. *Angew. Chemie Int. Ed.* **2009**, *48*, 8457–8460. https://doi.org/10.1002/anie.200902439.

(33) Banerjee, I.; Pangule, R. C.; Kane, R. S. Antifouling Coatings: Recent Developments in the Design of Surfaces That Prevent Fouling by Proteins, Bacteria, and Marine Organisms. *Adv. Mater.* **2011**, *23*, 690–718. https://doi.org/10.1002/adma.201001215.

(34) Jeyachandran, Y. L.; Mielczarski, J. A.; Mielczarski, E.; Rai, B. Efficiency of Blocking of Non-Specific Interaction of Different Proteins by BSA Adsorbed on Hydrophobic and Hydrophilic Surfaces. *J. Colloid Interface Sci.* **2010**, *341*, 136–142. https://doi.org/10.1016/j.jcis.2009.09.007.

(35) Kundu, J.; Neumann, O.; Janesko, B. G.; Zhang, D.; Lal, S.; Barhoumi, A.; Scuseria, G. E.; Halas, N. J. Adenine− and Adenosine Monophosphate (AMP)−Gold Binding Interactions Studied by Surface-Enhanced Raman and Infrared Spectroscopies. *J. Phys. Chem.* **2009**, *113*, 14390–14397. https://doi.org/10.1021/jp903126f.

(36) Giese, B. Electron Transfer in DNA . *Curr. Opin. Chem. Biol.* **2002**, *6*, 612–618.

(37) Wulfkuhle, J. D.; Liotta, L. A.; Petricoin, E. F. Proteomic Applications for the Early Detection of Cancer. *Nat. Rev. Cancer* **2003**, *3* (4), 267–275. https://doi.org/10.1038/nrc1043.

(38) Karley, D.; Gupta, D.; Tiwari, A. Press Biomarker for Cancer: A Great Promise for Future. *World J Oncol.* **2011**, *2*, 151–157. https://doi.org/10.4021/wjon352w.

(39) Swierczewska, M.; Liu, G.; Lee, S.; Chen, X. High-Sensitivity Nanosensors for Biomarker Detection. *Chem. Soc. Rev.* **2012**, *41*, 2641–2655. https://doi.org/10.1039/c1cs15238f.

(40) Siegel, R.; Miller, K.; Jemal, A. Cancer Statistics, 2018. *CA. Cancer J. Clin.* **2018**, *68*, 7–

30. https://doi.org/10.3322/caac.21442.

(41) Oesterling, J. E. Prostate Specific Antigen: A Critical Assessment of the Most Useful Tumor Marker for Adenocarcinoma of the Prostate. *J. Urol.* **1991**, *145*, 907–923. https://doi.org/10.1016/S0022-5347(17)38491-4.

(42) Wang, M. C.; Valenzuela, L. A.; Murphy, G. P.; Chu, T. M. Purification of a Human Prostate Specific Antigen. *Invest. Urol.* **1979**, *17*, 159–163.

(43) Papsidero, L. D.; Wang, M. C.; Valenzuela, L. A.; Murphy, G. P.; Chu, T. M. A Prostate Antigen in Sera of Prostatic Cancer Patients. *Cancer Res.* **1980**, *40*, 2428–2432.

(44) Stamey, Thomas A, MD; Yang, Norman, PhD; Hay, Alan R, MD; McNeal, John E, MD; Freiha, Fuad S, MD; Redwine, Elise, B. Prostate-Specific Antigen as a Serum Marker for Adenocarcinoma of the Prostate. *Massachusetts Med. Soc.* **1987**, *317*, 909–916.

(45) Thompson, I. M.; Pauler, D. K.; Goodman, P. J.; Tangen, C. M.; Scott Lucia, M.; Parnes, H. L.; Minasian, L. M.; Ford, L. G.; Lippman, S. M.; David Crawford, E.; Crowley, J. J.; Coltman, C. A. Prevalence of Prostate Cancer among Men with a Prostate-Specific Antigen Level ≤4.0 Ng per Milliliter. *N. Engl. J Med.* **2004**, *22*, 2239-2246. https://doi.org/10.1056/nejmoa031918.

(46) Jung, K.; Elgeti, U.; Lein, M.; Brux, B.; Sinha, P.; Rudolph, B.; Hauptmann, S.; Schnorr, D.; Loening, S. A. Ratio of Free or Complexed Prostate-Specific Antigen (PSA) to Total PSA: Which Ratio Improves Differentiation between Benign Prostatic Hyperplasia and Prostate Cancer? *Clin. Chem.* **2000**, *46*, 55-62. https://doi.org/10.1093/clinchem/46.1.55.

(47) Prensner, J. R.; Rubin, M. A.; Wei, J. T.; Chinnaiyan, A. M. Beyond PSA: The next Generation of Prostate Cancer Biomarkers. *Sci. Transl. Med.* **2012**, *4*, 127rv3. https://doi.org/10.1126/scitranslmed.3003180.

(48) Healy, D. A.; Hayes, C. J.; Leonard, P.; McKenna, L.; O'Kennedy, R. Biosensor Developments: Application to Prostate-Specific Antigen Detection. *Trends Biotechnol.* **2007**, *25*, 125–131. https://doi.org/10.1016/j.tibtech.2007.01.004.

(49) Warsinke, A. Point-of-Care Testing of Proteins. *Anal. Bioanal. Chem.* **2009**, *393*, 1393–1405. https://doi.org/10.1007/s00216-008-2572-0.

(50) Soleymani, L.; Li, F. Mechanistic Challenges and Advantages of Biosensor Miniaturization into the Nanoscale. *ACS Sensors*. **2017**, *2*, 458–467. https://doi.org/10.1021/acssensors.7b00069.

(51) Oh, S. W.; Kim, Y. M.; Kim, H. J.; Kim, S. J.; Cho, J.-S.; Choi, E. Y. Point-of-Care Fluorescence Immunoassay for Prostate Specific Antigen. *Clin. Chim. Acta*. **2009**, *406*, 18–22. https://doi.org/10.1016/j.cca.2009.04.013.

(52) Gao, Z.; Xu, M.; Hou, L.; Chen, G.; Tang, D. Magnetic Bead-Based Reverse Colorimetric Immunoassay Strategy for Sensing Biomolecules. *Anal. Chem.* **2013**, *85*, 6945–6952. https://doi.org/10.1021/ac401433p.

(53) Homola, J. Surface Plasmon Resonance Sensors for Detection of Chemical and Biological Species. *Chem. Rev.* **2008**, *108*, 462-493. https://doi.org/10.1021/CR068107D.

(54) Grubisha, D. S.; Lipert, R. J.; Park, H.-Y.; Driskell, J.; Porter, M. D. Femtomolar Detection of Prostate-Specific Antigen: An Immunoassay Based on Surface-Enhanced Raman Scattering and Immunogold Labels. *Anal. Chem.* **2003**, *75*, 5936–5943. https://doi.org/10.1021/ac034356f.

(55) Xu, L.; Wen, Y.; Pandit, S.; Mokkapati, V. R. S. S.; Mijakovic, I.; Li, Y.; Ding, M.; Ren, S.; Li, W.; Liu, G. Graphene-Based Biosensors for the Detection of Prostate Cancer Protein Biomarkers: A Review. *BMC Chem.* **2019**, *13*, 112. https://doi.org/10.1186/s13065-019-0611-x.

(56) Singh, S.; Gill, A. A. S.; Nlooto, M.; Karpoormath, R. Prostate Cancer Biomarkers Detection Using Nanoparticles Based Electrochemical Biosensors. *Biosens. Bioelectron.* **2019**, *137*, 213–221. https://doi.org/10.1016/J.BIOS.2019.03.065.

(57) Ghorbani, F.; Abbaszadeh, H.; Dolatabadi, J. E. N.; Aghebati-Maleki, L.; Yousefi, M. Application of Various Optical and Electrochemical Aptasensors for Detection of Human Prostate Specific Antigen: A Review. *Biosens. Bioelectron.* **2019**, *142*, 111484. https://doi.org/10.1016/J.BIOS.2019.111484.

(58) Wujcik, E. K.; Wei, H.; Zhang, X.; Guo, J.; Yan, X.; Sutrave, N.; Wei, S.; Guo, Z. Antibody Nanosensors: A Detailed Review. *RSC Adv.* **2014**, *4*, 43725–43745. https://doi.org/10.1039/c4ra07119k.

(59) Yadav, S. K.; Chandra, P.; Goyal, R. N.; Shim, Y. B. A Review on Determination of Steroids in Biological Samples Exploiting Nanobio-Electroanalytical Methods. *Anal. Chim. Acta.* **2013**, *762*, 14–24. https://doi.org/10.1016/j.aca.2012.11.037.

(60) Guo, S.; Wang, E. Noble Metal Nanomaterials: Controllable Synthesis and Application in Fuel Cells and Analytical Sensors. *Nano Today* **2011**, *6*, 240–264. https://doi.org/10.1016/j.nantod.2011.04.007.

(61) Niina J. Ronkainen, a H. B. H. and W. R. H. Electrochemical Biosensors. *Chem. Soc. Rev.* **2014**, *39*, 1747–1763. https://doi.org/10.1039/b714449k.

(62) Chen, X.; Zhou, G.; Song, P.; Wang, J.; Gao, J.; Lu, J.; Fan, C.; Zuo, X. Ultrasensitive Electrochemical Detection of Prostate-Specific Antigen by Using Antibodies Anchored on a DNA Nanostructural Scaffold. *Anal. Chem.* **2014**, *86*, 7337–7342. https://doi.org/10.1021/ac500054x.

(63) Vural, T.; Yaman, Y. T.; Ozturk, S.; Abaci, S.; Denkbas, E. B. Electrochemical Immunoassay for Detection of Prostate Specific Antigen Based on Peptide Nanotube-Gold Nanoparticle-Polyaniline Immobilized Pencil Graphite Electrode. *J. Colloid Interface Sci.* **2018**, *510*, 318–326. https://doi.org/10.1016/j.jcis.2017.09.079.

(64) Kavosi, B.; Salimi, A.; Hallaj, R.; Amani, K. A Highly Sensitive Prostate-Specific Antigen Immunosensor Based on Gold Nanoparticles/PAMAM Dendrimer Loaded on MWCNTS/Chitosan/Ionic Liquid Nanocomposite. *Biosens. Bioelectron.* **2014**, *52*, 20–28. https://doi.org/10.1016/j.bios.2013.08.012.

(65) Dong, Y. X.; Cao, J. T.; Liu, Y. M.; Ma, S. H. A Novel Immunosensing Platform for Highly Sensitive Prostate Specific Antigen Detection Based on Dual-Quenching of

Photocurrent from CdSe Sensitized TiO2 Electrode by Gold Nanoparticles Decorated Polydopamine Nanospheres. *Biosens. Bioelectron.* **2017**, *91*, 246–252. https://doi.org/10.1016/j.bios.2016.12.043.

(66) Miao, P.; Jiang, Y.; Wang, Y.; Yin, J.; Tang, Y. An Electrochemical Approach Capable of Prostate Specific Antigen Assay in Human Serum Based on Exonuclease-Aided Target Recycling Amplification. *Sensors Actuators B.* **2018**, *257*, 1021–1026. https://doi.org/10.1016/j.snb.2017.11.064.

(67) Barman, S. C.; Hossain, M. F.; Yoon, H.; Park, J. Y. Trimetallic Pd@Au@Pt Nanocomposites Platform on -COOH Terminated Reduced Graphene Oxide for Highly Sensitive CEA and PSA Biomarkers Detection. *Biosens. Bioelectron.* **2018**, *100*, 16–22. https://doi.org/10.1016/j.bios.2017.08.045.

(68) Tang, Z.; Fu, Y.; Ma, Z. Bovine Serum Albumin as an Effective Sensitivity Enhancer for Peptide-Based Amperometric Biosensor for Ultrasensitive Detection of Prostate Specific Antigen. *Biosens. Bioelectron.* **2017**, *94*, 394–399. https://doi.org/10.1016/j.bios.2017.03.030.

(69) Heydari-Bafrooei, E.; Sadat Shamszadeh, N. Electrochemical Bioassay Development for Ultrasensitive Aptasensing of Prostate Specific Antigen. **2017**. *91*, 284. https://doi.org/10.1016/j.bios.2016.12.048.

(70) Li, H.; Li, S.; Xia, F. Electrochemical Sandwich Assays for Protein Detection. *Biosens. Based on Sandwich Assays*. **2018**, 47–68. https://doi.org/10.1007/978-981-10-7835-4_4.

(71) Bard, A. J.; Faulkner, L. R. *ELECTROCHEMICAL METHODS Fundamentals and Applications*; Kluwer Academic Publishers-Plenum Publishers, 2000; Vol. 38. https://doi.org/10.1023/A:1021637209564.

(72) Kounaves, S. P. Voltammetric Techniques. In *Handbook of Instrumental Techniques for Analytical Chemistry*; 1997; 709–726.

(73) Paleček, E.; Tkáč, J.; Bartošík, M.; Bertók, T.; Ostatná, V.; Paleček, J. Electrochemistry of Nonconjugated Proteins and Glycoproteins. Toward Sensors for Biomedicine and Glycomics. *Chem. Rev.* **2015**, *115*, 2045–2108. https://doi.org/10.1021/cr500279h.

(74) Hushegyi, A.; Bertok, T.; Damborsky, P.; Katrlik, J.; Tkac, J. An Ultrasensitive Impedimetric Glycan Biosensor with Controlled Glycan Density for Detection of Lectins and Influenza Hemagglutinins. *Chem. Commun.* **2015**, *51*, 7474–7477. https://doi.org/10.1039/c5cc00922g.

(75) Prasad, S.; Selvam, A. P.; Reddy, R. K.; Love, A. Silicon Nanosensor for Diagnosis of Cardiovascular Proteomic Markers. *J. Lab. Autom.* **2013**, *18*, 143–151. https://doi.org/10.1177/2211068212460038.

(76) Randviir, E. P.; Banks, C. E. Electrochemical Impedance Spectroscopy: An Overview of Bioanalytical Applications. *Anal. Methods* **2013**, *5*, 1098–1115. https://doi.org/10.1039/c3ay26476a.

(77) Chang, B.-Y.; Su-Moon Park. Electrochemical Impedance Spectroscopy. *Annu. Rev. Anal.*

Chem. **2010**, *3*, 207–229. https://doi.org/10.1146/annurev.anchem.012809.102211.

(78) Grossi, M.; Riccò, B. Electrical Impedance Spectroscopy (EIS) for Biological Analysis and Food Characterization: A Review. *J. Sensors Sens. Syst.* **2017**, *6*, 303–325. https://doi.org/10.5194/jsss-6-303-2017.

(79) Chornokur, G.; Arya, S. K.; Phelan, C.; Tanner, R.; Bhansali, S. Impedance-Based Miniaturized Biosensor for Ultrasensitive and Fast Prostate-Specific Antigen Detection. *J. Sensors* **2011**, *2011*, 7. https://doi.org/10.1155/2011/983752.

(80) Ohno, R.; Ohnuki, H.; Wang, H.; Yokoyama, T.; Endo, H.; Tsuya, D.; Izumi, M. Biosensors and Bioelectronics Electrochemical Impedance Spectroscopy Biosensor with Interdigitated Electrode for Detection of Human Immunoglobulin A. *Biosens. Bioelectron.* **2013**, *40*, 422–426. https://doi.org/10.1016/j.bios.2012.07.052.

(81) Johnson, E. D.; Kotowski, T. M. Detection of Prostate Specific Antigen by ELISA. *J. Forensic Sci.* **1993**, *38*, 13403J. https://doi.org/10.1520/JFS13403J.

(82) Chen, S.; Wang, Z.; Cui, X.; Jiang, L.; Zhi, Y.; Ding, X.; Nie, Z.; Zhou, P.; Cui, D. Microfluidic Device Directly Fabricated on Screen-Printed Electrodes for Ultrasensitive Electrochemical Sensing of PSA. *Nanoscale Res. Lett.* **2019**, *14*, 71. https://doi.org/10.1186/s11671-019-2857-6.

(83) Zani, A.; Laschi, S.; Mascini , M.; Marrazza, G. A New Electrochemical Multiplexed Assay for PSA Cancer Marker Detection. *Electroanalysis* **2011**, *23*, 91–99. https://doi.org/10.1002/elan.201000486.

(84) Niu, X.; Cheng, N.; Ruan, X.; Du, D.; Lin, Y. Review—Nanozyme-Based Immunosensors and Immunoassays: Recent Developments and Future Trends. *J. Electrochem. Soc.* **2020**, *167*, 037508. https://doi.org/10.1149/2.0082003JES.

(85) Tang, S.; Hewlett, I. Nanoparticle-Based Immunoassays for Sensitive and Early Detection of HIV-1 Capsid (P24) Antigen. *J. Infect. Dis.* **2010**, *201 Suppl*, S59-64. https://doi.org/10.1086/650386.

(86) Hong, W.; Lee, S.; Cho, Y. Dual-Responsive Immunosensor That Combines Colorimetric Recognition and Electrochemical Response for Ultrasensitive Detection of Cancer Biomarkers. *Biosens. Bioelectron.* **2016**, *86*, 920–926. https://doi.org/10.1016/J.BIOS.2016.07.014.

(87) Zhou, X.; Yang, L.; Tan, X.; Zhao, G.; Xie, X.; Du, G. A Robust Electrochemical Immunosensor Based on Hydroxyl Pillar[5]Arene@ AuNPs@g-C 3 N 4 Hybrid Nanomaterial for Ultrasensitive Detection of Prostate Specific Antigen. *Biosens. Bioelectron.* **2018**, *112*, 31-39. https://doi.org/10.1016/j.bios.2018.04.036.

(88) Hwang, H.; Choi, E.; Han, S.; Lee, Y.; Choi, T.; Kim, M.; Shin, H.; Kim, J.; Choi, J. MESIA: Magnetic Force-Assisted Electrochemical Sandwich Immunoassays for Quantification of Prostate-Specific Antigen in Human Serum. *Anal. Chemi. Acta.* **2019**. *1061*, 92-100. https://doi.org/10.1016/j.aca.2019.02.018.

(89) Zhao, L.; Ma, Z. New Immunoprobes Based on Bovine Serum Albumin-Stabilized

Copper Nanoclusters with Triple Signal Amplification for Ultrasensitive Electrochemical Immunosensing for Tumor Marker. *Sens. Act. B.* **2017**, 849–854. https://doi.org/10.1016/j.snb.2016.11.012.

(90) Jiang, L.; Li, Y.; Gao, Z.; Wang, P.; Li, D.; Dong, Y. Sensitive Detection of Prostate Specific Antigen Based on Copper Ions Doped Ag-Au Nanospheres Labeled Immunosensor. *J. Electrochem. Soc.* **2019**, *166*, B1637–B1643. https://doi.org/10.1149/2.1341915jes.

(91) Zhang, D.; Li, W.; Ma, Z. Improved Sandwich-Format Electrochemical Immunosensor Based on "Smart" SiO 2 @polydopamine Nanocarrier. *Biosens. Bioelectron.* **2018**. *109*, 171-176. https://doi.org/10.1016/j.bios.2018.03.027.

(92) Fan, D.; Li, N.; Ma, H.; Li, Y.; Hu, L.; Wei, Q. Electrochemical Immunosensor for Detection of Prostate Specific Antigen Based on an Acid Cleavable Linker into MSN-Based Controlled Release System. *Biosens. Bioelectron.* **2016**. *85*, 580-586. https://doi.org/10.1016/j.bios.2016.05.063.

(93) Chu, Y.; Wang, H.; Ma, H.; Wu, D.; Du, B.; Wei, Q. Sandwich-Type Electrochemical Immunosensor for Ultrasensitive Detection of Prostate-Specific Antigen Using Palladium-Doped Cuprous Oxide Nanoparticles. *RSC Adv.* **2016**, *6*, 84698–84704. https://doi.org/10.1039/C6RA13841A.

(94) Feng, J.; Li, Y.; Li, M.; Li, F.; Han, J.; Dong, Y.; Chen, Z.; Wang, P.; Liu, H.; Wei, Q. A Novel Sandwich-Type Electrochemical Immunosensor for PSA Detection Based on PtCu Bimetallic Hybrid (2D/2D) RGO/g-C3N4. *Biosens. Bioelectron.* **2017**, *91*, 441–448. https://doi.org/10.1016/j.bios.2016.12.070.

(95) Tang, C. K.; Vaze, A.; Shen, M.; Rusling, J. F. High-Throughput Electrochemical Microfluidic Immunoarray for Multiplexed Detection of Cancer Biomarker Proteins. *ACS Sensors.* **2016**, *1*, 1036–1043. https://doi.org/10.1021/acssensors.6b00256.

(96) Muyldermans, S. Nanobodies: Natural Single-Domain Antibodies. *Annu. Rev. Biochem.* **2013**, *82*, 775–797. https://doi.org/10.1146/annurev-biochem-063011-092449.

(97) Liu, X.; Wang, D.; Chu, J.; Xu, Y.; Wang, W. Sandwich Pair Nanobodies, a Potential Tool for Electrochemical Immunosensing Serum Prostate-Specific Antigen with Preferable Specificity. *J. Pharm. Biomed. Anal.* **2018**, *158*, 361–369. https://doi.org/10.1016/j.jpba.2018.06.021.

(98) Ellington, A. D.; Szostak, J. W. Selection in Vitro of Single-Stranded DNA Molecules That Fold into Specific Ligand-Binding Structures. *Nature* **1992**, *355*, 850–852. https://doi.org/10.1038/355850a0.

(99) Olsen, T. R.; Tapia-Alveal, C.; Yang, K. A.; Zhang, X.; Pereira, L. J.; Farmakidis, N.; Pei, R.; Stojanovic, M. N.; Lin, Q. Integrated Microfluidic Selex Using Free Solution Electrokinetics. *J. Electrochem. Soc.* **2017**, *164*, B3122–B3129. https://doi.org/10.1149/2.0191705jes.

(100) Savory, N.; Abe, K.; Sode, K.; Ikebukuro, K. Selection of DNA Aptamer against Prostate Specific Antigen Using a Genetic Algorithm and Application to Sensing. *Biosens.*

Bioelectron. **2010**, *26*, 184–8588. https://doi.org/10.1016/j.bios.2010.07.057.

(101) Meng, W.; Zhang, W.; Zhang, J.; Chen, X.; Zhang, Y. An Electrochemical Immunosensor for Prostate Specific Antigen Using Nitrogen-Doped Graphene as a Sensing Platform. *Anal. Methods.* **2019**. *11*, 2183-2189. https://doi.org/10.1039/c9ay00064j.

(102) Meyerhoff, M. E.; Duan, C.; Meusel, M. Novel Nonseparation Sandwich-Type Electrochemical Enzyme Immunoassay System for Detecting Marker Proteins in Undiluted Blood. *Clin. Chem.* **1995**, *41*, 1378.

(103) Urban, G. *Label-Free Biosensing*; 2018; Vol. 16. https://doi.org/10.1007/978-3-319-75220-4.

(104) Kumar, N.; Kumar, S.; Kumar, J.; Panda, S. Investigation of Mechanisms Involved in the Enhanced Label Free Detection of Prostate Cancer Biomarkers Using Field Effect Devices. *J. Electrochem. Soc.* **2017**, *164*, B409–B416. https://doi.org/10.1149/2.0541709jes.

(105) E B Randles, B. J.; Physicochim, A. KINETICS OF RAPID ELECTRODE REACTIONS. A Few Investigations. *Ann. Reports Chem.* **1938**, *169*.

(106) Lien, T. T. N.; Takamura, Y.; Tamiya, E.; Vestergaard, M. C. Modified Screen Printed Electrode for Development of a Highly Sensitive Label-Free Impedimetric Immunosensor to Detect Amyloid Beta Peptides. *Anal. Chim. Acta* **2015**, *892*, 69–76. https://doi.org/10.1016/j.aca.2015.08.036.

(107) Assari, P.; Amir, &; Rafati, A.; Feizollahi, A.; Joghani, R. A. An Electrochemical Immunosensor for the Prostate Specific Antigen Based on the Use of Reduced Graphene Oxide Decorated with Gold Nanoparticles. *Microchim. Acta.* **2019**, *186*, 484. https://doi.org/10.1007/s00604-019-3565-8.

(108) Pihikova, D.; Kasak, P.; Kubanikova, P.; Sokol, R.; Tkac, J. Aberrant Sialylation of a Prostate-Specific Antigen: Electrochemical Label-Free Glycoprofiling in Prostate Cancer Serum Samples. *Anal. Chim. Acta* **2016**, *934*, 72–79. https://doi.org/10.1016/j.aca.2016.06.043.

(109) Jolly, P.; Formisano, N.; Tkáč, J.; Kasák, P.; Frost, C. G.; Estrela, P. Label-Free Impedimetric Aptasensor with Antifouling Surface Chemistry: A Prostate Specific Antigen Case Study. *Sensors Actuators, B Chem.* **2015**, *209*, 306–312. https://doi.org/10.1016/j.snb.2014.11.083.

(110) Srivastava, M.; Nirala, N. R.; Srivastava, S. K.; Prakash, R. A Comparative Study of Aptasensor Vs Immunosensor for Label-Free PSA Cancer Detection on GQDs-AuNRs Modified Screen-Printed Electrodes. *Sci. Rep.* **2018**, *8*, 1923. https://doi.org/10.1038/s41598-018-19733-z.

(111) Mavrikou, S.; Moschopoulou, G.; Zafeirakis, A.; Kalogeropoulou, K.; Giannakos, G.; Skevis, A.; Kintzios, S. An Ultra-Rapid Biosensory Point-of-Care (POC) Assay for Prostate-Specific Antigen (PSA) Detection in Human Serum. *Sensors* **2018**, *18*, 3834. https://doi.org/10.3390/s18113834.

(112) Bogomolova, A.; Komarova, E.; Reber, K.; Gerasimov, T.; Yavuz, O.; Bhatt, S.; Aldissi, M. Challenges of Electrochemical Impedance Spectroscopy in Protein Biosensing. *Anal. Chem.* **2009**, *81*, 3944–3949. https://doi.org/10.1021/ac9002358.

(113) Heydari-Bafrooei, E.; Shamszadeh, N. S. Electrochemical Bioassay Development for Ultrasensitive Aptasensing of Prostate Specific Antigen. *Biosens. Bioelectron.* **2017**, *91*, 284–292. https://doi.org/10.1016/j.bios.2016.12.048.

(114) Bockaj, M.; Fung, B.; Tsoulis, M.; Foster, W. G.; Soleymani, L. Method for Electrochemical Detection of Brain Derived Neurotrophic Factor (BDNF) in Plasma. *Anal. Chem.* **2018**, *90*, 8561–8566. https://doi.org/10.1021/acs.analchem.8b01642.

(115) Kumar, V.; Srivastava, S.; Umrao, S.; Kumar, R.; Nath, G.; Sumana, G.; Saxena, P. S.; Srivastava, A. Nanostructured Palladium-Reduced Graphene Oxide Platform for High Sensitive, Label Free Detection of a Cancer Biomarker. *RSC Adv.* **2014**, *4*, 2267–2273. https://doi.org/10.1039/C3RA41986J.

(116) Argoubi, W.; Sánchez, A.; Parrado, C.; Raouafi, N.; Villalonga, R. Label-Free Electrochemical Aptasensing Platform Based on Mesoporous Silica Thin Film for the Detection of Prostate Specific Antigen. *Sensors Actuators B* **2018**, *255*, 309–315. https://doi.org/10.1016/j.snb.2017.08.045.

(117) Deng, H.; Li, J.; Zhang, Y.; Pan, H.; Xu, G. A New Strategy for Label-Free Electrochemical Immunoassay Based on ``gate-Effect'' of β-Cyclodextrin Modified Electrode. *Anal. Chim. Acta.* **2016**. *926*, 48-54. https://doi.org/10.1016/j.aca.2016.04.035.

(118) Barman, S. C.; Hossain, M. F.; Park, J. Y. Gold Nanoparticles Assembled Chemically Functionalized Reduced Graphene Oxide Supported Electrochemical Immunosensor for Ultra-Sensitive Prostate Cancer Detection. *J. Electrochem. Soc.* **2017**, *164*, B234–B239. https://doi.org/10.1149/2.1461706jes.

(119) Sharifuzzaman, M.; Barman, S. C.; Rahman, M. T.; Zahed, M. A.; Xuan, X.; Park, J. Y. Green Synthesis and Layer-by-Layer Assembly of Amino-Functionalized Graphene Oxide/Carboxylic Surface Modified Trimetallic Nanoparticles Nanocomposite for Label-Free Electrochemical Biosensing. *J. Electrochem. Soc.* **2019**, *166*, B983–B993. https://doi.org/10.1149/2.0821912jes.

(120) Jeong, S.; Barman, S. C.; Yoon, H.; Park, J. Y. A Prostate Cancer Detection Immunosensor Based on Nafion/Reduced Graphene Oxide/Aldehyde Functionalized Methyl Pyridine Composite Electrode. *J. Electrochem. Soc.* **2019**, *166* , B920–B926. https://doi.org/10.1149/2.0361912jes.

(121) Li, Y.; Khan, M. S.; Tian, L.; Liu, L.; Hu, L.; Fan, D.; Cao, W.; Wei, Q. An Ultrasensitive Electrochemical Immunosensor for the Detection of Prostate-Specific Antigen Based on Conductivity Nanocomposite with Halloysite Nanotubes. *Anal. Bioanal. Chem.* **2017**, *409*, 3245–3251. https://doi.org/10.1007/s00216-017-0266-1.

(122) Wei, B.; Mao, K.; Liu, N.; Zhang, M.; Yang, Z. Graphene Nanocomposites Modified Electrochemical Aptamer Sensor for Rapid and Highly Sensitive Detection of Prostate Specific Antigen. *Biosens. Bioelectron.* **2018**. *121*, 41-46.

https://doi.org/10.1016/j.bios.2018.08.067.

(123) Wang, Y.; Qu, Y.; Liu, G.; Hou, & X.; Huang, Y.; Wu, W.; Wu, K.; Li, C. Electrochemical Immunoassay for the Prostate Specific Antigen Using a Reduced Graphene Oxide Functionalized with a High Molecular-Weight Silk Peptide. *Microchim. Acta.* **2015**, *182*, 2061-2067. https://doi.org/10.1007/s00604-015-1552-2.

(124) Barman, S. C.; Hossain, M. F.; Yoon, H.; Park, J. Y. Trimetallic Pd@Au@Pt Nanocomposites Platform on -COOH Terminated Reduced Graphene Oxide for Highly Sensitive CEA and PSA Biomarkers Detection. *Biosens. Bioelectron.* **2017**. *100*, 16-22. https://doi.org/10.1016/j.bios.2017.08.045.

(125) Talamini, L.; Zanato, N.; Zapp, E.; Brondani, D.; Westphal, E.; Gallardo, H.; Vieira, I. C. Heparin-Gold Nanoparticles and Liquid Crystal Applied in Label-Free Electrochemical Immunosensor for Prostate-Specific Antigen. *Electroanalysis* **2018**, *30*, 353–360. https://doi.org/10.1002/elan.201700651.

(126) Li, Z.; Yin, J.; Gao, C.; Qiu, G.; Meng, A.; Li, Q. The Construction of Electrochemical Aptasensor Based on Coral-like Poly-Aniline and Au Nano-Particles for the Sensitive Detection of Prostate Specific Antigen. *Sensors Act. B Chem.* **2019**. *295*, 93-100. https://doi.org/10.1016/j.snb.2019.05.070.

(127) Chen, Y.; Yuan, P.-X.; Wang, A.-J.; Luo, X.; Xue, Y.; Zhang, L.; Feng, J.-J. A Novel Electrochemical Immunosensor for Highly Sensitive Detection of Prostate-Specific Antigen Using 3D Open-Structured PtCu Nanoframes for Signal Amplification. *Biosens. Bioelectron.* **2019**. *126*, 197-192. https://doi.org/10.1016/j.bios.2018.10.057.

(128) Çevik, E.; Bahar, Ö.; Şenel, M.; Fatih Abasıyanık, M. Construction of Novel Electrochemical Immunosensor for Detection of Prostate Specific Antigen Using Ferrocene-PAMAM Dendrimers. *Biosens. Bioelectron.* **2016**. *86*, 1074-1079. https://doi.org/10.1016/j.bios.2016.07.064.

(129) Zhang, G.; Liu, Z.; Fan, L.; Guo, Y. Electrochemical Prostate Specific Antigen Aptasensor Based on Hemin Functionalized Graphene-Conjugated Palladium Nanocomposites. *Microchim. Acta.* **2018**, *185*, 159. https://doi.org/10.1007/s00604-018-2686-9.

(130) Li, F.; Li, Y.; Feng, J.; Dong, Y.; Wang, P.; Chen, L.; Chen, Z.; Liu, H.; Wei, Q. Ultrasensitive Amperometric Immunosensor for PSA Detection Based on Cu2O@CeO2-Au Nanocomposites as Integrated Triple Signal Amplification Strategy. *Biosens. Bioelectron.* **2017**, *87*, 630–637. https://doi.org/10.1016/j.bios.2016.09.018.

(131) Tuite, E.; Norden, B. Sequence-Specific Interactions of Methylene Blue with Polynucleotides and DNA: A Spectroscopic Study. *J. Am. Chem. Soc.* **1994**, *116*, 7548–7556. https://doi.org/10.1021/ja00096a011.

(132) and, S. O. K.; Barton, J. K.; and, N. M. J.; Hill, M. G. Electrochemistry of Methylene Blue Bound to a DNA-Modified Electrode. *Bioconjugate Chem.* **1997**. *8*, 31-37. https://doi.org/10.1021/BC960070O.

(133) Tahmasebi, F.; Noorbakhsh, A. Sensitive Electrochemical Prostate Specific Antigen

Aptasensor: Effect of Carboxylic Acid Functionalized Carbon Nanotube and Glutaraldehyde Linker. *Electroanalysis* **2016**, *28*, 1134–1145. https://doi.org/10.1002/elan.201501014.

(134) Raouafi, A.; Sánchez, A.; Raouafi, N.; Villalonga, R. Electrochemical Aptamer-Based Bioplatform for Ultrasensitive Detection of Prostate Specific Antigen. *Sens. Actuators B Chem.* **2019**, *297*, 126762. https://doi.org/10.1016/j.snb.2019.126762.

(135) Rahi, A.; Sattarahmady, N.; Heli, H. Label-Free Electrochemical Aptasensing of the Human Prostate-Specific Antigen Using Gold Nanospears. *Talanta* **2016**, *156*, 281-224. https://doi.org/10.1016/j.talanta.2016.05.029.

(136) Sattarahmady, N.; Rahi, A.; Heli, H. A Signal-on Built in-Marker Electrochemical Aptasensor for Human Prostate-Specific Antigen Based on a Hairbrush-like Gold Nanostructure. *Sci. Rep.* **2017**, *7*, 11238. https://doi.org/10.1038/s41598-017-11680-5.

(137) Zhao, Y.; Cui, L.; Sun, Y.; Zheng, F.; Ke, W. Ag/CdO NP-Engineered Magnetic Electrochemical Aptasensor for Prostatic Specific Antigen Detection. *ACS Appl. Mater. Interfaces* **2018**, *11*, 3474-3481. https://doi.org/10.1021/acsami.8b18887.

(138) He, Y.; Xie, S.; Yang, X.; Yuan, R.; Chai, Y. Electrochemical Peptide Biosensor Based on in Situ Silver Deposition for Detection of Prostate Specific Antigen. *ACS Appl. Mater. Interfaces* **2015**, *7*, 13360–13366. https://doi.org/10.1021/acsami.5b01827.

(139) Ren, K.; Wu, J.; Yan, F.; Ju, H. Ratiometric Electrochemical Proximity Assay for Sensitive One-Step Protein Detection. *Sci. Rep.* **2015**, *4*, 4360. https://doi.org/10.1038/srep04360.

(140) Zhao, J.; Ma, Z. Ultrasensitive Detection of Prostate Specific Antigen by Electrochemical Aptasensor Using Enzyme-Free Recycling Amplification via Target-Induced Catalytic Hairpin Assembly. **2018**. *102*, 316-320. https://doi.org/10.1016/j.bios.2017.11.044.

(141) Zhu, Y.; Wang, H.; Wang, L.; Zhu, J.; Jiang, W. Cascade Signal Amplification Based on Copper Nanoparticle-Reported Rolling Circle Amplification for Ultrasensitive Electrochemical Detection of the Prostate Cancer Biomarker. *ACS Appl. Mater. Interfaces* **2016**, *8*, 37. https://doi.org/10.1021/acsami.5b10285.

(142) Pan, L.-H.; Kuo, S.-H.; Lin, T.-Y.; Lin, C.-W.; Fang, P.-Y.; Yang, H.-W. An Electrochemical Biosensor to Simultaneously Detect VEGF and PSA for Early Prostate Cancer Diagnosis Based on Graphene Oxide/SsDNA/ PLLA Nanoparticles. *Biosens. Bioelectron.* **2016**. *89*, 598-605. https://doi.org/10.1016/j.bios.2016.01.077.

(143) Xie, S.; Zhang, J.; Yuan, Y.; Chai, Y.; Yuan, R. An Electrochemical Peptide Cleavage-Based Biosensor for Prostate Specific Antigen Detection via Host-Guest Interaction between Ferrocene and b-Cyclodextrin. *Chem. Commun* **2015**, *51*, 3387. https://doi.org/10.1039/c4cc10363g.

(144) Xia, N.; Cheng, C.; Liu, L.; Peng, P.; Liu, C.; Chen, J. Electrochemical Glycoprotein Aptasensors Based on the In-Situ Aggregation of Silver Nanoparticles Induced by 4-Mercaptophenylboronic Acid. *Microchim. Acta.* **2017**, *184*, 4393-4400. https://doi.org/10.1007/s00604-017-2488-5.

(145) Liu, Q.; Wang, J.; Boyd, B. J. Peptide-Based Biosensors. *Talanta* **2015**, *136*, 114–127. https://doi.org/10.1016/j.talanta.2014.12.020.

(146) Parnsubsakul, A.; Safitri, R. E.; Rijiravanich, P.; Surareungchai, W. Electrochemical Assay of Proteolytically Active Prostate Specific Antigen Based on Anodic Stripping Voltammetry of Silver Enhanced Gold Nanoparticle Labels. *J. Electroanal. Chem.* **2017**, *785*, 125–130. https://doi.org/10.1016/j.jelechem.2016.12.010.

(147) Tang, Z.; Wang, L.; Ma, Z. Triple Sensitivity Amplification for Ultrasensitive Electrochemical Detection of Prostate Specific Antigen. *Biosens. Bioelectron.* **2017**. *92*, 577-582. https://doi.org/10.1016/j.bios.2016.10.057.

(148) Cumming, A. P.; Hopmans, S. N.; Vukmirović-Popović, S.; Duivenvoorden, W. C. PSA Affects Prostate Cancer Cell Invasion in Vitro and Induces an Osteoblastic Phenotype in Bone in Vivo. *Prostate Cancer Prostatic Dis.* **2011**, *14*, 286–294. https://doi.org/10.1038/pcan.2011.34.

(149) Jaffrezic-Renault, N.; Martelet, C.; Chevolot, Y.; Cloarec, J.-P. Biosensors and Bio-Bar Code Assays Based on Biofunctionalized Magnetic Microbeads. *Sensors* **2007**, *7*, 589–614. https://doi.org/10.3390/s7040589.

(150) Goluch, E. D.; Nam, J.-M.; Georganopoulou, D. G.; Chiesl, T. N.; Shaikh, K. A.; Ryu, K. S.; Barron, A. E.; Mirkin, C. A.; Liu, C. A Bio-Barcode Assay for on-Chip Attomolar-Sensitivity Protein Detection. *Lab Chip* **2006**, *6*, 1293–1299. https://doi.org/10.1039/b606294f.

(151) Li, F.; Lin, Y.; Le, X. C. Binding-Induced Formation of DNA Three-Way Junctions and Its Application to Protein Detection and DNA Strand Displacement Scheme 1. Schematic Showing the Principle of the Binding-Induced Formation of DNA Three-Way Junction (TWJ) A. *Anal. Chem* **2013**, *85*, 10835-10841. https://doi.org/10.1021/ac402179a.

(152) Song, S.; Qin, Y.; He, Y.; Huang, Q.; Fan, C.; Chen, H.-Y. Functional Nanoprobes for Ultrasensitive Detection of Biomolecules. *Chem. Soc. Rev* **2010**, *39*, 4234–4243. https://doi.org/10.1039/c000682n.

(153) Li, D.; Song, S.; Fan, C. Target-Responsive Structural Switching for Nucleic Acid-Based Sensors. *Acc. Chem. Res.* **2010**, *43*, 631–641. https://doi.org/10.1021/ar900245u.

(154) Yang, M.; Yau, H. C. M.; Chan, H. L. Adsorption Kinetics and Ligand-Binding Properties of Thiol-Modified Double-Stranded DNA on a Gold Surface. *Langmuir* **1998**, *14*, 6121–6129. https://doi.org/10.1021/la980577i.

(155) Mourougou-Candoni, N.; Naud, C.; Thibaudau, F. Adsorption of Thiolated Oligonucleotides on Gold Surfaces: An Atomic Force Microscopy Study. *Langmuir* **2003**, *19*, 682–686. https://doi.org/10.1021/la026021j.

(156) Keighley, S. D.; Li, P.; Estrela, P.; Migliorato, P. Optimization of DNA Immobilization on Gold Electrodes for Label-Free Detection by Electrochemical Impedance Spectroscopy. *Biosens. Bioelectron.* **2008**, *23*, 1291–1297. https://doi.org/10.1016/j.bios.2007.11.012.

(157) Ricci, F.; Lai, R. Y.; Heeger, A. J.; Plaxco, K. W.; Sumner, J. J. Effect of Molecular

Crowding on the Response of an Electrochemical DNA Sensor. *Langmuir* **2007**, *23*, 6827–6834. https://doi.org/10.1021/la700328r.

(158) Gao, Y.; Wolf, L. K.; Georgiadis, R. M. Secondary Structure Effects on DNA Hybridization Kinetics: A Solution versus Surface Comparison. *Nucliec Acids Research* **2006**, *34*, 3370–3377. https://doi.org/10.1093/nar/gkl422.

(159) Weber, P. C.; Ohlendorf, D. H.; Wendoloski, J. J.; Salemme, F. R. Structural Origins of High-Affinity Biotin Binding to Streptavidin. *Science.* **1989**, *243*, 85–88. https://doi.org/10.1126/science.2911722.

(160) Hosseini, A.; Villegas, M.; Yang, J.; Badv, M.; Weitz, J. I.; Soleymani, L.; Didar, T. F. Conductive Electrochemically Active Lubricant-Infused Nanostructured Surfaces Attenuate Coagulation and Enable Friction-Less Droplet Manipulation. *Adv. Mater. Interfaces* **2018**, *5*, 1800617. https://doi.org/10.1002/admi.201800617.

(161) Wang, J.; Rivas, G.; Fernandes, J. R.; Luis Lopez Paz, J.; Jiang, M.; Waymire, R. Indicator-Free Electrochemical DNA Hybridization Biosensor. *Sensors* **1998**, *11*, 5616-5629. https://dx.doi.org/10.3390%2Fs110605616

(162) Hui, N.; Sun, X.; Niu, S.; Luo, X. PEGylated Polyaniline Nanofibers: Antifouling and Conducting Biomaterial for Electrochemical DNA Sensing. *ACS Appl. Mater. Interfaces* **2016**. *9*, 2914-2923. https://doi.org/10.1021/acsami.6b11682.

(163) Wu, L.; Qu, X. Cancer Biomarker Detection: Recent Achievements and Challenges. *Chem. Soc. Rev.* **2015**, *44*, 2963–2997. https://doi.org/10.1039/c4cs00370e.

(164) Zhang, J.; Lan, T.; Lu, Y. Translating in Vitro Diagnostics from Centralized Laboratories to Point-of-Care Locations Using Commercially-Available Handheld Meters. *Trends Anal. Chem.* **2020**, *124*, 115782. https://doi.org/10.1016/j.trac.2019.115782.

(165) Vestergaard, delanji; Kerman, K.; Tamiya, E. An Overview of Label-Free Electrochemical Protein Sensors. *Sensors* **2007**, *7*, 3442–3458. https://doi.org/10.3390/s7123442

(166) Bonham, A. J.; Paden, N. G.; Ricci, F.; Plaxco, K. W. Detection of IP-10 Protein Marker in Undiluted Blood Serum via an Electrochemical E-DNA Scaffold Sensor. *Anal.* **2013**, *138*, 5580–5583. https://doi.org/10.1039/c3an01079a.

(167) Traynor, S. M.; Pandey, R.; Maclachlan, R.; Hosseini, A.; Didar, T. F.; Li, F.; Soleymani, L. Review—Recent Advances in Electrochemical Detection of Prostate Specific Antigen (PSA) in Clinically-Relevant Samples. *J. Electrochem. Soc.* **2020**, *167*, 037551. https://doi.org/10.1149/1945-7111/ab69fd.

(168) Lin, J.; Ju, H. Electrochemical and Chemiluminescent Immunosensors for Tumor Markers. *Biosens. Bioelectron.* **2005**, *20*, 1461–1470. https://doi.org/10.1016/j.bios.2004.05.008.

(169) Lu, Y.; Liu, J. Functional DNA Nanotechnology: Emerging Applications of DNAzymes and Aptamers. *Curr. Opin. Biotechnol.* **2006**, *17*, 580–588. https://doi.org/10.1016/j.copbio.2006.10.004.

(170) Yang, J.; Dou, B.; Yuan, R.; Xiang, Y. Aptamer/Protein Proximity Binding-Triggered Molecular Machine for Amplified Electrochemical Sensing of Thrombin. *Anal. Chem.* **2017**, *89*, 5138–5143. https://doi.org/10.1021/acs.analchem.7b00827.

(171) Zhang, Y. L.; Huang, Y.; Jiang, J. H.; Shen, G. L.; Yu, R. Q. Electrochemical Aptasensor Based on Proximity-Dependent Surface Hybridization Assay for Single-Step, Reusable, Sensitive Protein Detection. *J. Am. Chem. Soc.* **2007**, *129*, 15448–15449. https://doi.org/10.1021/ja0773047.

(172) Hu, J.; Wang, T.; Kim, J.; Shannon, C.; Easley, C. J. Quantitation of Femtomolar Protein Levels via Direct Readout with the Electrochemical Proximity Assay. *J. Am. Chem. Soc.* **2012**, *134*, 7066–7072. https://doi.org/10.1021/ja3000485.

(173) Greenwood, C.; Ruff, D.; Kirvell, S.; Johnson, G.; Dhillon, H. S.; Bustin, S. A. Proximity Assays for Sensitive Quantification of Proteins. *Biomol. Detect. Quantif.* **2015**, *4*, 10–16. https://doi.org/10.1016/j.bdq.2015.04.002.

(174) Labaer, J.; Ramachandran, N. Protein Microarrays as Tools for Functional Proteomics. *Curr. Opin. Chem. Biol.* **2005**, *9*, 14–19. https://doi.org/10.1016/j.cbpa.2004.12.006.

(175) Thaxton, S.; Elghanian, R.; Thomas, A. D.; Stoeva, S. I.; Lee, J.-S.; Smith, N. D.; Schaeffer, A. J.; Klocker, H.; Horninger, W.; Bartsch, G.; Mirkin, C. A. Nanoparticle-Based Bio-Barcode Assay Redefines "'undetectable'" PSA and Biochemical Recurrence after Radical Prostatectomy. *Proc. Natl. Acad. Sci.* **2009**, *106*, 18437-18442. https://doi.org/10.1073/pnas.0904719106.

(176) Lau, I. P. M.; Ngan, E. K. S.; Loo, J. F. C.; Suen, Y. K.; Ho, H. P.; Kong, S. K. Aptamer-Based Bio-Barcode Assay for the Detection of Cytochrome-c Released from Apoptotic Cells. *Biochem. Biophys. Res. Commun.* **2010**, *395*, 560–564. https://doi.org/10.1016/j.bbrc.2010.04.066.

(177) Vijayendran, R. A.; Motsegood, K. M.; Beebe, D. J.; Leckband, D. E. Evaluation of a Three-Dimensional Micromixer in a Surface-Based Biosensor. *Langmuir* **2003**, *19*, 1824–1828. https://doi.org/10.1021/la0262250.

(178) Shrivastava, A.; Gupta, V. Methods for the Determination of Limit of Detection and Limit of Quantitation of the Analytical Methods. *Chronicles Young Sci.* **2011**, *2*, 21. https://doi.org/10.4103/2229-5186.79345.

(179) Stenberg, M.; Nygren, H. Kinetics of Antigen-Antibody Reactions at Solid-Liquid Interfaces. *J. Immunol. Methods* **1988**, *113*, 3–15.

(180) Gaster, R. S.; Xu, L.; Han, S. J.; Wilson, R. J.; Hall, D. A.; Osterfeld, S. J.; Yu, H.; Wang, S. X. Quantification of Protein Interactions and Solution Transport Using High-Density GMR Sensor Arrays. *Nat. Nanotechnol.* **2011**, *6*, 314–320. https://doi.org/10.1038/nnano.2011.45.

(181) Mahshid, S. S.; Sébastien, S.; Camiré, C.; Ricci, F.; Valleé-Beíisle, A. A Highly Selective Electrochemical DNA-Based Sensor That Employs Steric Hindrance Effects to Detect Proteins Directly in Whole Blood. *J. Am. Chem. Soc.* **2015**, *137*, 15596–15599. https://doi.org/10.1021/jacs.5b04942.

(182) Bockaj, M.; Fung, B.; Tsoulis, M.; Foster, W. G.; Soleymani, L. Method for Electrochemical Detection of Brain Derived Neurotrophic Factor (BDNF) in Plasma. *Anal. Chem.* **2018**, *90*, 8561–8566. https://doi.org/10.1021/acs.analchem.8b01642.

(183) Soleymani, L.; Fang, Z.; Lam, B.; Bin, X.; Vasilyeva, E.; Ross, A. J.; Sargent, E. H.; Kelley, S. O. Hierarchical Nanotextured Microelectrodes Overcome the Molecular Transport Barrier to Achieve Rapid, Direct Bacterial Detection. *ACS Nano* **2011**, *5*, 3360–3366. https://doi.org/10.1021/nn200586s.

(184) Nakano, S.; Miyoshi, D.; Sugimoto, N. Effects of Molecular Crowding on the Structures, Interactions, and Functions of Nucleic Acids. *Chemical Reviews*. **2014**, *12*, 2733–2758. https://doi.org/10.1021/cr400113m.

(185) Lin, M.; Wang, J.; Zhou, G.; Wang, J.; Wu, N.; Lu, J.; Gao, J.; Chen, X.; Shi, J.; Zuo, X.; Fan, C. Programmable Engineering of a Biosensing Interface with Tetrahedral DNA Nanostructures for Ultrasensitive DNA Detection. *Angew. Chemie - Int. Ed.* **2015**, *54*, 2151–2155. https://doi.org/10.1002/anie.201410720.

(186) Plaxco, K. W.; Soh, H. T. Switch-Based Biosensors: A New Approach towards Real-Time, in Vivo Molecular Detection. *Trends Biotechnol.* **2011**, *29*, 1–5. https://doi.org/10.1016/j.tibtech.2010.10.005.

(187) Wang, F.; Anderson, M.; Bernards, M. T.; Hunt, H. K.; Holler, S. PEG Functionalization of Whispering Gallery Mode Optical Microresonator Biosensors to Minimize Non-Specific Adsorption during Targeted, Label-Free Sensing. *Sensors* **2015**, *15*, 18040–18060. https://doi.org/10.3390/s150818040.

(188) Pihikova, D.; Kasak, P.; Kubanikova, P.; Sokol, R.; Tkac, J. Aberrant Sialylation of a Prostate-Specific Antigen: Electrochemical Label-Free Glycoprofiling in Prostate Cancer Serum Samples. *Anal. Chim. Acta.* **2016**, *934*, 72-79. https://doi.org/10.1016/j.aca.2016.06.043.

(189) Nikolaev, K.; Ermakov, S.; Ermolenko, Y.; Averyaskina, E.; Offenhäusser, A.; Mourzina, Y. A Novel Bioelectrochemical Interface Based on in Situ Synthesis of Gold Nanostructures on Electrode Surfaces and Surface Activation by Meerwein's Salt. A Bioelectrochemical Sensor for Glucose Determination. *Bioelectrochemistry* **2015**, *105*, 34–43. https://doi.org/10.1016/j.bioelechem.2015.05.004.

(190) Levicky, R.; Herne, T. M.; Tarlov, M. J.; Satija, S. K. Using Self-Assembly To Control the Structure of DNA Monolayers on Gold: A Neutron Reflectivity Study. *J. Am. Chem. Soc.* **1998**, *120*, 9787-9792. https://doi.org/10.1021/ja981897r.

(191) Catalona, W. J.; Smith, D. S.; Ratliff, T. L.; Dodds, K. M.; Coplen, D. E.; Yuan, J. J. J.; Petros, J. A.; Andriole, G. L. Measurement of Prostate-Specific Antigen in Serum as a Screening Test for Prostate Cancer. *N. Engl. J. Med.* **1991**, *324*, 1156–1161. https://doi.org/10.1056/NEJM199104253241702.

(192) Zheng, G.; Patolsky, F.; Cui, Y.; Wang, W. U.; Lieber, C. M. Multiplexed Electrical Detection of Cancer Markers with Nanowire Sensor Arrays. *Nat. Biotechnol.* **2005**, *23*, 1294–1301. https://doi.org/10.1038/nbt1138.

(193) Munge, B. S.; Stracensky, T.; Gamez, K.; DiBiase, D.; Rusling, J. F. Multiplex Immunosensor Arrays for Electrochemical Detection of Cancer Biomarker Proteins. *Electroanalysis* **2016**, *28*, 2644–2658. https://doi.org/10.1002/elan.201600183.

(194) Metcalf, G. A. D.; Shibakawa, A.; Patel, H.; Sita-Lumsden, A.; Zivi, A.; Rama, N.; Bevan, C. L.; Ladame, S. Amplification-Free Detection of Circulating MicroRNA Biomarkers from Body Fluids Based on Fluorogenic Oligonucleotide-Templated Reaction between Engineered Peptide Nucleic Acid Probes: Application to Prostate Cancer Diagnosis. *Anal. Chem.* **2016**, *88*, 8091–8098. https://doi.org/10.1021/acs.analchem.6b01594.